Mathematical Modelling mTOR-NMT Signalling Pathway

by Yang Zhang

A Thesis submitted to the Faculty of Graduate Studies of
the University of Manitoba in partial fulfilment of the requirements of the degree of

MASTER OF SCIENCE

Department of Mathematics
University of Manitoba
Winnipeg, MB

Abstract

Since mammalian target of rapamycin (mTOR) and N-myristoltransferase (NMT) have been shown to be potentially related to breast cancer, mTOR-NMT signalling pathway is taken into specific consideration. In this thesis, mathematical models are developed to not only describe the mTOR-NMT signalling pathways, but also to analyze and predict the response to a treatment. Based on different biological hypotheses, candidate models are obtained by using an ordinary differential equation formalism. An optimization method called the Differential Evolution algorithm is applied to find the best parameter sets for our candidates. Doing so, will give the smallest distance between experimental data and simulated results. The experimental data are provided by Dr Shrivastav's laboratory, Department of Biology, University of Winnipeg. Furthermore, the mathematical analysis for our candidate models has been found to show their asymptotic behaviours. To determine which candidate model is most likely to be the "best" among the subgroup of models, model selection is used. Ultimately, the collaboration with Dr Shrivastav's laboratory let us understand the simplified mTOR-NMT signalling pathway.

Acknowledgements

First, I would like to thank my supervisor Dr. Stephanie Portet for her understanding, patience and support during my academic career. Thanks to her, I was able to develop the work ethic required to succeed in my program.

Second, I would like to thank Dr. Anuraag Shrivastav and Dr. Vasma Shrivastav for their collaboration.

Third, I would like to thank the Faculty of Science and Faculty of Graduate Studies at the University of Manitoba, and also my sponsors for their financial support.

Finally, I would like to thank all my friends, family and girlfriend for their endless love and support.

Dedication

To

my father, MinZhong Zhang,

my mother, JunCun Fang,

and

my loving girlfriend XueJing Jiang,

for their love and support.

Contents

List of Tables

List of Figures

Abbreviation

PI-3 Kinase	Phosphatidy1 Innositol-3 Kinase
Ark	Protein kinase B
mTOR	Mammalian Target of Rapamycin
IRS	Insulin Receptor Substrate
eNOS	Endothelial nitric oxide synthase
NO	Nitric oxide
Ras	Retrovirus-associated DNA sequences
MAPK	Mitogen activated protein kinase
pmTOR	Phosphorylated Mammalian Target of Rapamycin
NMT	N-MyristolTransferase
pNMT	Phosphorylated N-MyristolTransferase
ODEs	Ordinary Differential Equations
DE	Differential Evolution
GAs	Genetic Algorithms
AIC	Akaike Information Criterion
IVP	Initial Value Problem
LAS	Locally Asymptotically Stable
GAS	Globally Asymptotically Stable

Chapter 1

Introduction

1.1 Motivation

In 2015, breast cancer was one of the most diagnosed cancer among Canadian women over the age of 20 and was the second most lethal cancer [3]. During the last few decades, some kinases (enzymes that catalyze the phosphorylation of substrates) have been shown to promote tumorigenesis through the coordinated phosphorylation of proteins that directly regulates cell-cycle progression and metabolism, as well as transcription factors that regulate the expression of genes involved in oncogenic processes [6]. The importance of these kinases in oncology is widely accepted to be related to mutation of cells [6]. Signalling events that activate these kinases are important to understand the mechanism of tumorigenesis and to develop effective therapies against cancer. For instance, phosphatidylinnositol-3 kinase/protein kinase B/mammalian target of Rapamycin (PI-3 Kinase/Akt/mTOR) pathway is a specific signalling event that has been shown to be dysregulated in cancers [31]. Mutations of PI-3 Kinase/Akt /mTOR pathway proteins are common in breast cancers and their activations have been known as one of the potential mechanisms responsible for the resistance to drugs used in breast cancer treatment among patients [31]. Therefore, inhibitors of PI-3 kinase, Akt, or mTOR in this pathway are of particular interest. The aim of our study is to develop mathematical models that can predict the response of cells to treatment protocols in breast cancer therapy. Doing so, individual tailor-made treatments for breast cancer patients can be determined.

1.2 Signal pathways

1.2.1 Signal transduction

There are a large number of intracellular signalling pathways responsible for transmitting information within the same cell or between different cells to regulate their corresponding proteins' activations; this information transmitting process is called signal transduction. Signal transduction is a process of signal relay which occurs when, for instance, either an extracellular signalling molecule binds to its specific transmembranar receptors on the cell membrane, or pass through cell membranes to activate a specific receptor within the cell. In turn, this receptor triggers a chain of biochemical events inside the cell, creating a response. Depending on the cells' type, the response can be the change in metabolism, gene expression, or cell proliferation.

For example, as described in Figure 1.1, when insulin binds to insulin receptors present on the cell membrane, it triggers a conformational change of the receptor and activates its intrinsic tyrosine kinase activities. The receptor undergoes autophosphorylation and subsequently activates other downstream target molecules, including insulin receptor substrate (IRS), phosphatidylinnositol-3 kinase (PI3-Kinase), protein kinase B (Akt), endothelial nitric oxide synthase (eNOS), nitric oxide (NO), retrovirus-associated DNA sequences (Ras) and mitogen activated protein kinase (MAPK) through a series of phosphorylation events. Target molecules are mainly involved in two sorts of activation of insulin signalling pathways with the first being Ras/ MAPK which results in cell proliferation; the second is PI-3K/Akt/ eNOS/NO, resulting in metabolic modulation [32].

1.2.2 mTOR-NMT signalling pathway

In the 1970s, in Easter Island, scientists found a special soil sample that contains a bacterial strain, streptomycin hygroscopicus, which produces an anti-fungal metabolite [38]. This metabolite happened to be a macrocyclic lactone and was named Rapamycin. Subsequently, it was shown to have immunosuppressive effects and to be able to suppress cell proliferation [38]. That stimulated further research on its properties and its target protein. In the 1990s, the target was identified as a protein, and named TOR (target of Rapamycin) [25, 39].

The molecule "mammalian target of Rapamycin" (mTOR) belongs to the series of Akt-activated molecules mentioned in Figure 1.1 [32]. This signalling pathway senses and integrates a variety of environmental stimuli to regulate major cellular processes, organismal growth and homeostasis

Figure 1.1: Insulin signalling pathways. Insulin binds to the insulin receptor, causing mainly two sorts of activations; the activation of Ras/MAPK signalling pathway and/or the activation of PI-3K/ Akt/ eNOS/NO signalling pathway [32].

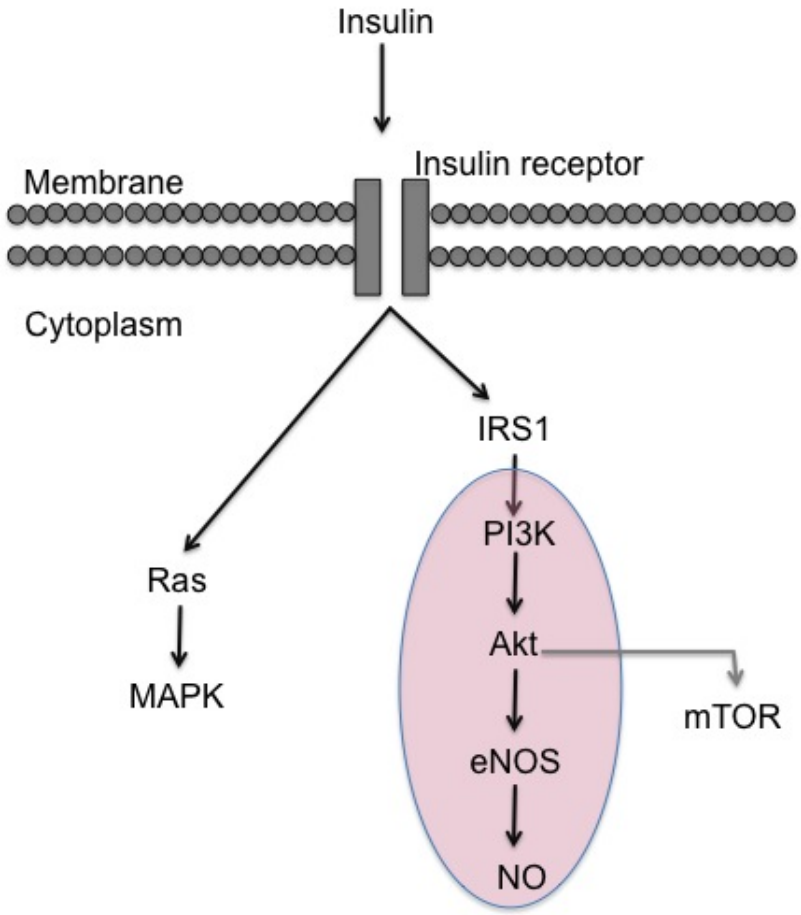

[18]. Recent research indicate that the immunoreactivity of phosphorylated mTOR (pmTOR) on tissue sections is present in 63.5% of hepatocellular carcinoma cases, and a significant association was found between pmTOR expression and tumour size/metastasis [7].

The mTOR pathway have shown a critical effector in apoptosis/programmed cell-death which is associated with the recent cancer research. Genetic showing, the mutations in the PTEN (phosphatase and tensin homolog deleted on chromosome 10) gene impinging upon mTOR signalling are commonly found in human cancer [36]. PTEN mutations are related to the cancers, including breast, lung, bladder, brain, and so on, making it one of the most frequently mutated in tumour-related genes [8]. PTEN affects the signalling activities in the mTOR signalling pathway, and causes the mTOR pathway dysregulation [8]. As the dysregulation of the mTOR pathway is commonly found in different cancers, the inhibitor of mTOR, Rapamycin is widely used as a drug in effective therapies and cancer study [25].

N-myristoltransferase (NMT) is an enzyme that catalyses the addition of the myristic acid group to N-terminal glycine residue of its target proteins, allowing proper functioning and localization [28]. Many proteins involved in a variety of signal cascades are myristoylated such as several G-proteins, kinases and phosphates.

1.3 Objectives

1.3.1 mTOR-NMT signalling pathway: a simplified version

Research at Dr Shrivastav's laboratory, Department of Biology, University of Winnipeg have identified that the mTOR pathway member Akt/PKB regulates NMT1 activity, establishing a connection between mTOR signalling pathway and NMT signalling pathway [30], i.e., mTOR "indirectly" phosphorylates N-myristoltransferase (NMT). Collaboration with Dr Shrivastav's laboratory allowed us to investigate the interactions between the target molecules of mTOR-NMT signalling pathway. As the mTOR pathway is a complex system, a simplified version is considered. Figure 1.2 represents the partial mTOR-NMT signalling pathway studied in this work. The simplified mTOR-NMT signalling pathway involves the following events:

- Binding of Rapamycin to mTOR prevents the phosphorylation of mTOR. Rapamycin represses the activation of mTOR by binding to it and "occupies" the phosphate site of mTOR, inhibiting the phosphorylation/activation of mTOR [40].
- Phosphorylation of mTOR by some kinase. The phosphorylated mTOR (pmTOR) induces the activation of mTOR.
- Dephosphorylation of pmTOR by some phosphatase.
- Phosphorylation of NMT by pmTOR.
- Degradation of pNMT.
- Dephosphorylation of pNMT by some phosphatase.

Figure 1.2 presents the biological events considered in this work.

1.3.2 Modelling the mTOR-NMT signalling pathway

Mathematical models are developed to describe and analyze the signalling pathways. Our goal in this thesis is to develop mathematical models to not only describe the reactions in simplified

Figure 1.2: Simplified mTOR-NMT pathway. Four target molecules are considered: mammalian target of rapamycin (mTOR), phosphorylated mTOR (pmTOR), N-myristoltransferase (NMT) and phosphorylated NMT (pNMT). Rapamycin inhibits the phosphorylation of mTOR. Active enzyme pmTOR plays the role of catalyst that deactivates NMT by phosphorylation.

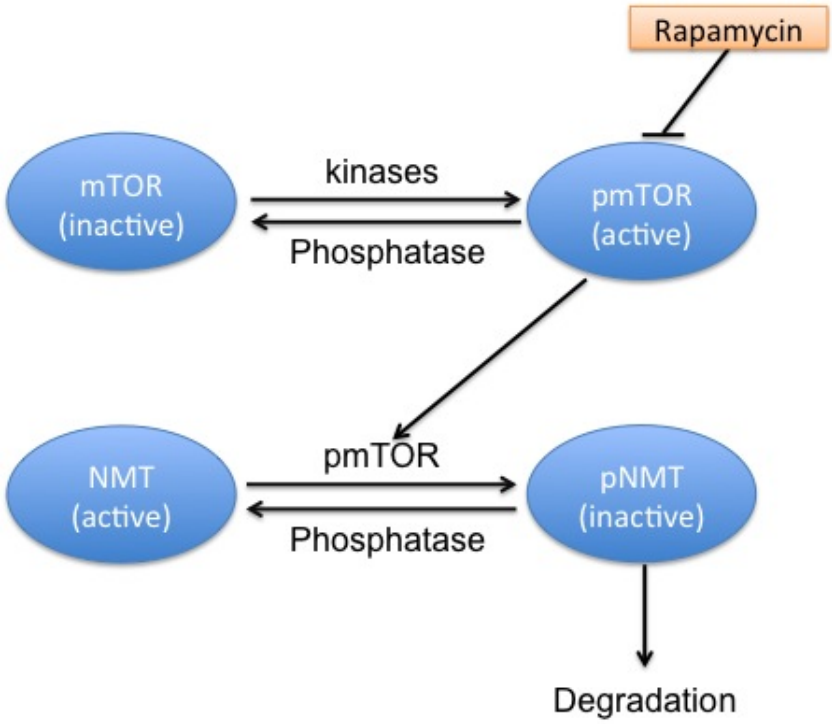

mTOR-NMT signalling pathway presented in Figure 1.2, but also to analyze the response to the treatment (Rapamycin). Some well-known methods can be applied to develop the mathematical models of signalling pathways, such as ordinary differential equations (ODEs), stochastic processes [1], game theory [21], and Boolean logic [12].

In this work, we consider time to be continuous and the observed kinetic dynamics to be deterministic. That is why the ODE formalism is used. The models that we develop are based on the law of Mass Action and Michaelis-Menten kinetics. Additionally, a collection of models were designed to follow the different biological hypotheses.

1.3.3 Structure of the manuscript

Chapter 2 presents the methods for developing mathematical models, fitting mathematical models to experimental data to estimate the parameters, and to finally determine the "best" model among the group of candidate models that we have selected. In Chapter 3, based on different hypotheses, candidate models are introduced. Furthermore, in Chapter 4, mathematical analysis and results

are introduced. In Chapter 5, numerical analysis and results are presented. Lastly, in Chapter 6, we briefly discuss some interesting conclusions from the previous analyses.

Chapter 2

Methods

Several methods used in this project are introduced in this chapter. Specifically, in Section 2.1, we describe how to translate the signalling pathways into mathematical models using the ODE formalism. In Section 2.2, in order to calibrate the models to the experimental data, it is explained how parameters are estimated by Differential Evolution (DE) algorithm. In Section 2.3, to determine which hypothesis is the most likely to occur, model selection is finally presented.

2.1 Modelling Approaches

2.1.1 Modelling a reversible chemical reaction

Consider a general reversible chemical reaction in the signalling pathway:

$$mA + nB \underset{k^-}{\overset{k^+}{\rightleftharpoons}} pA + sC,$$

where A, B, C are reactants involved in the reaction. Rates constant k^+ and k^- are the proportionality constants for a given reaction. The numbers $m,\ n,\ p$ and s describe the participation of reactants in reactions. Identically, the reversible chemical reaction can be separated into two subreactions R_1 and R_2:

Forward reaction R_1:

$$mA + nB \xrightarrow{k^+} pA + sC.$$

Backward reaction R_2:

$$pA + sC \xrightarrow{k^-} mA + nB.$$

Taking the reactant A as an example, the evolution equation of reactant is derived by using the Mass Action Law [16]. The evolution equation describes the rate of change of the reactant amount or its change with respect to the time, which is written as follows:

$$Rate\ of\ change\ of\ the\ reactant = Stoichiometric\ Number \times Reaction\ Speed.$$

The stoichiometric numbers and reaction speeds are now introduced for each reaction.

- **Stoichiometric number** is the net number of the amount of a reactant consumed or produced in the reaction. For reactions R_i, the stoichiometric number is denoted n_i.

Forward reaction R_1:

$$n_1 = p - m.$$

Backward reaction R_2:

$$n_2 = m - p.$$

- **Reaction speed** reflects how fast the chemical species react. For a reaction R_i, the reaction speed is denoted v_i.

Forward reaction R_1:

$$v_1 = k^+ A^m B^n.$$

Backward reaction R_2:

$$v_2 = k^- A^p C^s.$$

Thus, the evolution equation for reactant A is:

$$\frac{dA}{dt} = (p - m)k^+ A^m B^n + (m - p)k^- A^p C^s.$$

Similarly, the differential equations for all reactants present in the reversible reaction are:

$$\begin{aligned}
\frac{dA}{dt} &= (p - m)k^+ A^m B^n + (m - p)k^- A^p C^s, \\
\frac{dB}{dt} &= -nk^+ A^m B^n + nk^- A^p C^s, \\
\frac{dC}{dt} &= sk^+ A^m B^n - sk^- A^p C^s.
\end{aligned}$$

2.1.2 Michaelis-Menten dynamics

The biochemical reactions considered for the simplified mTOR-NMT signalling pathway are shown in Figure (1.2). Some reactants of this pathway are enzymes and it is assumed that the enzymatic reactions follow the Michaelis-Menten kinetics [24].

Consider the following enzymatic reaction, in which E is the enzyme, S is the substrate and P is the product. The reaction is noted as

$$S \xrightarrow{E} P.$$

It can be decomposed as follows,

$$E + S \underset{\tilde{k}}{\overset{Binding(k)}{\rightleftharpoons}} N_1 \xrightarrow{Catalysis(\mathrm{k}^*)} P + E,$$

where N_1 is the complex formed by the binding of the enzyme E to the substrate S. Using the previous derivation, the enzymatic kinetics is described by the following differential equations:

$$\frac{dE}{dt} = -kES + \tilde{k}N_1 + k^*N_1, \tag{2.1a}$$
$$\frac{dS}{dt} = -kES + \tilde{k}N_1, \tag{2.1b}$$
$$\frac{dN_1}{dt} = kES - \tilde{k}N_1 - k^*N_1, \tag{2.1c}$$
$$\frac{dP}{dt} = k^*N_1. \tag{2.1d}$$

Adding (2.1a) and (2.1c) reveals a common feature of enzymatic reactions:

$$\frac{dE}{dt} + \frac{dN_1}{dt} = 0.$$

This implies that the total number of enzyme is conserved over time and stays constant, $E(t) + N_1(t) = c$, $\forall t \geq 0$, where c is the initial concentration of enzyme. Hence, $E(t) = c - N_1(t)$, $\forall t \geq 0$. That allows us to reduce the dimension of System (2.1) by ignoring the equation for $E(t)$. Moreover, as System (2.1) does not depend explicitly on concentration $P(t)$, Equation (2.1d) can be

decoupled from the system. Hence, System (2.1) can be analyzed as a 2-dimensional system:

$$\frac{dS}{dt} = -kES + \tilde{k}N_1 = -k(c - N_1)S + \tilde{k}N_1 = -kcS + (\tilde{k} + kS)N_1, \tag{2.2}$$

$$\frac{dN_1}{dt} = kES - \tilde{k}N_1 - k^*N_1 = k(c - N_1)S - \tilde{k}N_1 - k^*N_1 = kcS - (\tilde{k} + k^*)N_1. \tag{2.3}$$

In enzymatic reactions, the concentration of enzyme is much less than the concentration of substrate. Here, it yields that the concentration of $E(t)$ is less than $S(t)$; the enzyme is always working at its maximal capacity (also known as saturation rate), so that the concentration of complex N_1 is virtually constant, which means that

$$\frac{dN_1}{dt} = 0$$

or equivalently from (2.3),

$$N_1 = \frac{kcS}{\tilde{k} + k^* + kS}. \tag{2.4}$$

Substitute (2.4) into (2.2), giving

$$\begin{aligned}
\frac{dS}{dt} &= -kcS + \frac{(\tilde{k} + kS)kcS}{\tilde{k} + k^* + kS} \\
&= -\frac{kk^*cS}{\tilde{k} + k^* + kS} \\
&= -\frac{k^*cS}{\frac{\tilde{k}+k^*}{k} + S} \\
&= -\frac{K_mcS}{K_n + S},
\end{aligned} \tag{2.5}$$

where is $K_m = k^*$ and $K_n = (\tilde{k} + k^*)/k$.

Substituting (2.4) into (2.1d) gives

$$\frac{dP}{dt} = k^*N_1 = \frac{kk^*cS}{\tilde{k} + k^* + kS} = \frac{k^*cS}{\frac{\tilde{k}+k^*}{k} + S} = \frac{K_mcS}{K_n + S} = -\frac{dS}{dt}. \tag{2.6}$$

Thus, Michaelis-Menten dynamics can be described by Equation (2.6), where K_mc is the maximum consumption rate of substrate or the maximum production rate of product achieved by the system parameter K_n (often known as the half saturation constant) corresponds to a substrate concentration. When the concentration of S reaches K_n, the reaction rate of substrate S is half of the maximum rate K_mc.

Note that c is related to the total concentration of active enzyme $E(t)$; hence, $E(t)$ can be introduced in the Equation (2.6) instead of c:

$$\frac{dS}{dt} = -\frac{dP}{dt} = -\frac{K_m E S}{K_n + S}.$$

Mass Action Law and Michaelis-Menten kinetics will be applied to design the collection of models that are based on the biochemical reactions introduced in Figure 1.2.

2.2 Parameter Estimation & Differential Evolution Algorithm

Based on different biological hypotheses, four candidate models will be obtained; for each model, two versions will be considered. These models will be presented in the next chapter and are summarized in Table 3.1. Here, we explain how parameters of these models will be obtained.

Each model contains a different number of parameters that represent the different chemical reactions considered. To obtain the smallest distance between simulated results and experimental data, the parameter set P is acquired in a cost function $C(P)$ which is defined as follows:

$$C(P) = \sum_{i=1}^{N} \sum_{j=1}^{H} (M_j(P, t_i) - D_j(t_i))^2. \tag{2.7}$$

Here P represents the parameters for a given model. N is the number of time points. H is the number of observations at given time points. $M_j(P, t_i)$ is the model response corresponding to the observation j obtained with the parameters P at time t_i. $D_j(t_i)$ are the experimental concentrations of the observation j at time t_i.

As mentioned previously, the goal is to obtain the smallest distance between the simulations and the data. Thus, the best parameter set P^* satisfies the following condition,

$$C(P^*) = \min_{P} \{C(P)\}. \tag{2.8}$$

Cost function (2.7) is minimized by varying values in parameter set P. The optimal values of parameters can be obtained by using the Differential Evolution (DE) algorithm running on a Matlab platform.

The DE algorithm is a simple and efficient heuristic method for global optimization over continuous spaces. It minimizes the cost function by iteratively updating its candidate solutions (parameters in this work) space. Similarly, other well-known optimization methods under genetic

algorithms (GAs) work as well as DE, where both GAs and DE are examples of evolutionary computation [23]. However, there exists some difference between them. Generally, GAs solutions are represented in binary as strings of 0s and 1s, resulting in the application in discrete problems (e.g. the application in Markov chain). However, the solutions of DE are ranging over the real number field, where it is more commonly used in continuous optimization problems. Another difference between these two algorithms are mentioned previously that in DE, the candidate solutions space is iteratively updated, where in GAs it is not. Recent research has shown that in many single-objective and multi-objective optimization cases, the Differential Evolution algorithm performs better than the Genetic algorithms [26, 34]. For that reason, the DE algorithm is preferred in this work.

The Differential Evolution algorithm is based on the greedy criterion [33], which means that the new parameter values are accepted by the algorithm if and only if the value of the cost function is reduced.

The DE algorithm includes intrinsic parameters which are:

- G the maximum generation;
- NP the maximum running times in one generation;
- CR the crossover constant, which is to increase the diversity of the parameter values and it is determined by the user;
- F the differential weight, which is to control the enlargement of the variation of the target parameter set.
- D the dimension of the parameter set.

The DE algorithm uses variables T_l, x and $C_l(P)$ that are initialized to random values at the beginning.

- T_l the current best value of parameter set in l loop. The size of T is equal to $1\times$ D;
- x the varying candidate parameters space for each generation. The size of x is equal to NP $\times$ D, where D depends on the parameter set P from Equation (2.7).
- $C_l(P)$ cost function defined in Equation (2.7) and used in l loop with parameter set P.
- P^* the best parameter set defined by Equation (2.8).

We assume a uniform distribution for all random integer numbers chosen unless otherwise stated. The running time NP does not change during the process of DE.

Procedures followed by the DE are

1. Initialize G, NP ≥ 4, CR $\in [0, 1]$, F $\in [0, 2]$, D and T_0 randomly. The entries of x are all random numbers and $C_0(T)$ is chosen a large real number.

2. Start **loop** **For** $i \in [1, G]$ **do**.

   Start **loop** **For** $l \in [1, NP]$ **do**.

   Pick up three integer numbers a, b and c from $[1, NP]$ at random, and $a \neq b \neq c$.

   Pick up another integer number $j \in [1, D]$ randomly.

   i. Start **loop** **For** $k \in [1, D]$ **do**.

   If a random number $< CR$ **then**

   Do the mutation $T_l(j) = x_l(c, j) + F * (x_l(a, j) - x_l(b, j))$

   Otherwise

   $T_l(j) = x(l, j)$

   End if

   End for k

   ii. Calculate the cost function $C_l(P)$.

   If $C_l(T_l) < C_{l-1}(T_{l-1})$ **then**

   $T_{l+1} = T_l$ and $C_{l+1}(T_{l+1}) = C_l(T_l)$.

   Update the ith row of x by T_l.

   Otherwise

   $T_{l+1} = T_{l-1}$ and $C_{l+1}(T_{l+1}) = C_{l-1}(T_{l-1})$.

   End if

   End for l

   End for i

3. Save the best parameter set $P^* = T$.

The general implementation of DE algorithm is given as MATLAB code in the Appendix A.

2.3 Model Selection

The goal of model selection is to find the best model among all candidate models to support the corresponding hypothesis [15]. In order to determine which model has the highest likelihood to be the ”best” model, the method of Akaike Information Criterion (AIC) will be taken into consideration.

AIC is based on Kullback-Leibler information theory, developed by Akaike. It shows that the information lost between the observations (data) and the representations (models) can be calculated by the Kullback-Leibler divergence [29]. The method of AIC combines the goodness of fit and the complexity of models [13]. Model complexity refers to the number of parameters for the given model.

The general form of AIC [2] is defined as

$$\text{AIC} = -2 \times \ln(\text{likelihood}) + 2 \times Q,$$

where **ln** is the logarithm function, **likelihood** is the maximum value of the likelihood function of the specified model and **Q** is the number of the estimated parameters of the model. Assuming that the residuals (deviation between the data and model responses) of the candidate models follow a normal distribution, we have:

$$\ln(\text{likelihood}) = -\frac{N}{2} \times \ln(\text{RSS/N}),$$

where **N** is the number of data points and **RSS** is the sum of squared residuals or **RSS** is the cost function (2.8) evaluated at the best parameter values, $RSS = C(P^*)$. Hence, AIC for each model can be calculated as follows:

$$\text{AIC} = N \times \ln(RSS/N) + 2 \times Q_e,$$

where Q_e is the number of estimated parameters. As **RSS/N** is considered as the estimate of the variance [15], $Q_e = Q + 1$ where Q is the number of model parameter estimated. Moreover, the smallest value of AIC indicates the ”best” model. To evaluate the likelihood of each model, the difference between the AIC value of each model and the AIC of the best model is first calculated

as

$$\Delta_i = AIC_i - \min AIC. \tag{2.9}$$

Then, the likelihoods of the models are equal to

$$\exp(-0.5 \times \Delta_i).$$

Ultimately, in order to compare the candidate models, the likelihoods are normalized. The normalized likelihoods are called the Akaike information weights W_i. The definition of the Akaike information weight W_i is as follows:

$$W_i = \frac{\exp(-0.5 \times \Delta_i)}{\sum_{i=1}^{R} \exp(-0.5 \times \Delta_i)}, \tag{2.10}$$

where **R** is the total number of candidate models.

The Akaike information weight W_i is the conditional probability of the candidate model i being the "best" model. A larger value of W_i reflects a larger possibility for the candidate model i among all the candidate models to occur.

Chapter 3

Candidate Models & Preliminary Results

Based on the discussions with Dr. Anuraag Shrivastav and Dr. Varma Shrivastav [1], we designed multiple models of mTOR-NMT signalling pathway resulting from different assumptions.

3.1 Candidate Models

Some candidate models are developed to represent the different effects or actions of the drug Rapamycin on the cell machinery, others are considered without drug. For each model, there exist two versions, Version (a) and Version (b); each scenario is studied with and without the dephosphorylation of pNMT. The list of models is given in Table 3.1. Furthermore, each candidate model can be separated into mTOR and NMT components. The mTOR component contains reactants mTOR, Rapamycin-mTOR (if the reactions involves the drug), and pmTOR. The NMT component contains reactants NMT and pNMT.

In Model I, only NMT component is considered. In this case, the underlying assumption is that the reactions related to mTOR components are much faster than those related to NMT components. In contrast, in other models, reactions involving mTOR and NMT components are assumed to occur in the same time scale. More specifically, in Model II, coupled mTOR-NMT components are taken into account. We assume that there is no Rapamycin involved in Model II. In Model III, mTOR and NMT components are both considered and an irreversible drug reaction is assumed to

[1] Department of Biology, University of Winnipeg.

occur. In Model IV, we also consider the coupled mTOR-NMT components and a reversible drug reaction.

Table 3.1: Table of models

Name	Assumption
Model I (a)	NMT component with dephosphorylation of pNMT
Model I (b)	NMT component without dephosphorylation of pNMT
Model II (a)	coupled mTOR-NMT components with dephosphorylation of pNMT
Model II (b)	coupled mTOR-NMT components without dephosphorylation of pNMT
Model III (a)	coupled mTOR-NMT components with irreversible drug reaction with dephosphorylation of pNMT
Model III (b)	coupled mTOR-NMT components with irreversible drug reaction without dephosphorylation of pNMT
Model IV (a)	coupled mTOR-NMT components with reversible drug reaction with dephosphorylation of pNMT
Model IV (b)	coupled mTOR-NMT components with reversible drug reaction without dephosphorylation of pNMT

The state variables used in models are:

- $M(t)$, the concentration of mTOR at time t,
- $P_1(t)$, the concentration of Rapamycin-mTOR at time t,
- $P_2(t)$, the concentration of pmTOR at time t,
- $P_3(t)$, the concentration of NMT at time t,
- $P_4(t)$, the concentration of pNMT at time t.

Table 3.2: Table of parameters

Name	Definition	Model	Unit
k_1	drug reaction rate	III IV	$\mu M^{-1}\ s^{-1}$
k	unbinding rate of Rapamycin-mTOR	IV	s^{-1}
$\tilde{K_m}$	maximum rate of consumption of mTOR	II III IV	μM s^{-1}
$\tilde{K_n}$	Michaelis constant of mTOR	II III IV	μM
K_m^+	maximum rate of consumption of pmTOR	II III IV	μM s^{-1}
K_n^+	Michaelis constant of pmTOR	II III IV	μM
K_m	maximum rate of consumption of NMT	I II III IV	μM s^{-1}
K_n	Michaelis constant of NMT	I II III IV	μM
K_m^*	maximum rate of consumption of pNMT	I II III IV	μM s^{-1}
K_n^*	Michaelis constant of pNMT	I II III IV	μM
Π	rate in producing NMT reactions	I II III IV	μM s^{-1}
r	degradation rate of pNMT	I II III IV	s^{-1}
R	concentration of drug Rapamycin	III IV	μM

All the values of the parameters are nonnegative.

Figure 1.2 (page 4) shows the simplified reactions studied in this work. More specifically, reactions considered for each model are now detailed and the corresponding equations are given. All models are formulated using the ODE formalism. The red part in the following systems highlights the difference between our candidate models, and the blue part highlights the difference between Version (a) and (b) of each model. In Version (a), the dephosphorylation of pNMT is assumed to be present, whereas in (b), the dephosphorylation of pNMT does not occur.

Model I (NMT Component):

Chemical reactions:

Model I (a)

$$P_3 \xrightarrow{P_2} P_4$$

$$P_4 \xrightarrow{\textit{phosphatase}} P_3$$

$$P_4 \xrightarrow{\mathrm{r}} \oslash$$

$$\oslash \xrightarrow{\pi} P_3$$

Model I (b)

$$P_3 \xrightarrow{P_2} P_4$$

$$P_4 \xrightarrow{\mathrm{r}} \oslash$$

$$\oslash \xrightarrow{\pi} P_3.$$

Governing equations:

Model I (a)

$$\frac{dP_3}{dt} = -\frac{K_m P_3}{K_n + P_3} + \frac{K_m^* P_4}{K_n^* + P_4} + \Pi$$
$$\frac{dP_4}{dt} = \frac{K_m P_3}{K_n + P_3} - \frac{K_m^* P_4}{K_n^* + P_4} - rP_4$$

Model I (b)

$$\frac{dP_3}{dt} = -\frac{K_m P_3}{K_n + P_3} + \Pi$$
$$\frac{dP_4}{dt} = \frac{K_m P_3}{K_n + P_3} - rP_4.$$

Model II (mTOR-NMT components-no drug reaction):

Chemical reactions:

Model II (a)

$$M \underset{\textit{phosphatase}}{\overset{\textit{kinase}}{\rightleftharpoons}} P_2$$

$$P_3 \xrightarrow{P_2} P_4$$

$$P_4 \xrightarrow{\textit{phosphatase}} P_3$$

$$P_4 \xrightarrow{\mathrm{r}} \oslash$$

$$\oslash \xrightarrow{\pi} P_3$$

Model II (b)

$$M \underset{\textit{phosphatase}}{\overset{\textit{kinase}}{\rightleftharpoons}} P_2$$

$$P_3 \xrightarrow{P_2} P_4$$

$$P_4 \xrightarrow{\mathrm{r}} \oslash$$

$$\oslash \xrightarrow{\pi} P_3.$$

Governing equations:

Model II (a)

$$\frac{dM}{dt} = -\frac{\tilde{K_m} M}{\tilde{K_n} + M} + \frac{K_m^+ P_2}{K_n^+ + P_2}$$
$$\frac{dP_2}{dt} = \frac{\tilde{K_m} M}{\tilde{K_n} + M} - \frac{K_m^+ P_2}{K_n^+ + P_2}$$
$$\frac{dP_3}{dt} = -\frac{K_m P_2 P_3}{K_n + P_3} + \frac{K_m^* P_4}{K_n^* + P_4} + \Pi$$
$$\frac{dP_4}{dt} = \frac{K_m P_2 P_3}{K_n + P_3} - \frac{K_m^* P_4}{K_n^* + P_4} - rP_4$$

Model II (b)

$$\frac{dM}{dt} = -\frac{\tilde{K_m} M}{\tilde{K_n} + M} + \frac{K_m^+ P_2}{K_n^+ + P_2}$$
$$\frac{dP_2}{dt} = \frac{\tilde{K_m} M}{\tilde{K_n} + M} - \frac{K_m^+ P_2}{K_n^+ + P_2}$$
$$\frac{dP_3}{dt} = -\frac{K_m P_2 P_3}{K_n + P_3} + \Pi$$
$$\frac{dP_4}{dt} = \frac{K_m P_2 P_3}{K_n + P_3} - rP_4.$$

Model III (mTOR-NMT components-irreversible drug reaction):

Chemical reactions:

Model III (a)

$$R\,(constant) + M \xrightarrow{k_1} P_1$$

$$M \underset{phosphatase}{\overset{kinase}{\rightleftharpoons}} P_2$$

$$P_3 \xrightarrow{P_2} P_4$$

$$P_4 \xrightarrow{phosphatase} P_3$$

$$P_4 \xrightarrow{r} \oslash$$

$$\oslash \xrightarrow{\pi} P_3$$

Model III (b)

$$R\,(constant) + M \xrightarrow{k_1} P_1$$

$$M \underset{phosphatase}{\overset{kinase}{\rightleftharpoons}} P_2$$

$$P_3 \xrightarrow{P_2} P_4$$

$$P_4 \xrightarrow{r} \oslash$$

$$\oslash \xrightarrow{\pi} P_3.$$

Governing equations:

Model III (a)

$$\frac{dM}{dt} = -k_1 RM - \frac{\tilde{K_m} M}{\tilde{K_n} + M} + \frac{K_m^+ P_2}{K_n^+ + P_2}$$
$$\frac{dP_1}{dt} = k_1 RM$$
$$\frac{dP_2}{dt} = \frac{\tilde{K_m} M}{\tilde{K_n} + M} - \frac{K_m^+ P_2}{K_n^+ + P_2}$$
$$\frac{dP_3}{dt} = -\frac{K_m P_2 P_3}{K_n + P_3} + \frac{K_m^* P_4}{K_n^* + P_4} + \Pi$$
$$\frac{dP_4}{dt} = \frac{K_m P_2 P_3}{K_n + P_3} - \frac{K_m^* P_4}{K_n^* + P_4} - rP_4$$

Model III (b)

$$\frac{dM}{dt} = -k_1 RM - \frac{\tilde{K_m} M}{\tilde{K_n} + M} + \frac{K_m^+ P_2}{K_n^+ + P_2}$$
$$\frac{dP_1}{dt} = k_1 RM$$
$$\frac{dP_2}{dt} = \frac{\tilde{K_m} M}{\tilde{K_n} + M} - \frac{K_m^+ P_2}{K_n^+ + P_2}$$
$$\frac{dP_3}{dt} = -\frac{K_m P_2 P_3}{K_n + P_3} + \Pi$$
$$\frac{dP_4}{dt} = \frac{K_m P_2 P_3}{K_n + P_3} - rP_4.$$

Model IV (mTOR-NMT components-reversible drug reaction):

Chemical reactions:

Model IV (a)

$$R\,(constant) + M \underset{k}{\overset{k_1}{\rightleftharpoons}} P_1$$

$$M \underset{phosphatase}{\overset{kinase}{\rightleftharpoons}} P_2$$

$$P_3 \xrightarrow{P_2} P_4$$

$$P_4 \xrightarrow{phosphatase} P_3$$

$$P_4 \xrightarrow{r} \oslash$$

$$\oslash \xrightarrow{\pi} P_3$$

Model IV (b)

$$R\,(constant) + M \underset{k}{\overset{k_1}{\rightleftharpoons}} P_1$$

$$M \underset{phosphatase}{\overset{kinase}{\rightleftharpoons}} P_2$$

$$P_3 \xrightarrow{P_2} P_4$$

$$P_4 \xrightarrow{r} \oslash$$

$$\oslash \xrightarrow{\pi} P_3.$$

Governing equations:

Model IV (a)

$$\begin{aligned}
\frac{dM}{dt} &= -k_1 RM - \frac{\tilde{K_m} M}{\tilde{K_n} + M} + \frac{K_m^+ P_2}{K_n^+ + P_2} + kP_1 \\
\frac{dP_1}{dt} &= k_1 RM - kP_1 \\
\frac{dP_2}{dt} &= \frac{\tilde{K_m} M}{\tilde{K_n} + M} - \frac{K_m^+ P_2}{K_n^+ + P_2} \\
\frac{dP_3}{dt} &= -\frac{K_m P_2 P_3}{K_n + P_3} + \frac{K_m^* P_4}{K_n^* + P_4} + \Pi \\
\frac{dP_4}{dt} &= \frac{K_m P_2 P_3}{K_n + P_3} - \frac{K_m^* P_4}{K_n^* + P_4} - rP_4
\end{aligned}$$

Model IV (b)

$$\begin{aligned}
\frac{dM}{dt} &= -k_1 RM - \frac{\tilde{K_m} M}{\tilde{K_n} + M} + \frac{K_m^+ P_2}{K_n^+ + P_2} + kP_1 \\
\frac{dP_1}{dt} &= k_1 RM - kP_1 \\
\frac{dP_2}{dt} &= \frac{\tilde{K_m} M}{\tilde{K_n} + M} - \frac{K_m^+ P_2}{K_n^+ + P_2} \\
\frac{dP_3}{dt} &= -\frac{K_m P_2 P_3}{K_n + P_3} + \Pi \\
\frac{dP_4}{dt} &= \frac{K_m P_2 P_3}{K_n + P_3} - rP_4.
\end{aligned}$$

Now, we generalize the systems as follows:

$$\begin{aligned}
\frac{dM}{dt} &= -F_1(M) + F_2(P_2) - D(\cdot), \\
\frac{dP_1}{dt} &= D(\cdot), \\
\frac{dP_2}{dt} &= F_1(M) - F_2(P_2), \\
\frac{dP_3}{dt} &= -F_3(P_3, P_2) + F_4(P_4) + F_5(\cdot), \\
\frac{dP_4}{dt} &= F_3(P_3, P_2) - F_4(P_4) - F_6(P_4),
\end{aligned} \tag{3.1}$$

$$F_1(M) = \begin{cases} \frac{\tilde{K_m} M}{\tilde{K_n} + M} & \text{Model II III IV} \\ 0 & \text{Model I} \end{cases} \qquad F_2(P_2) = \begin{cases} \frac{K_m^+ P_2}{K_n^+ + P_2} & \text{Model II III IV} \\ 0 & \text{Model I} \end{cases}$$

$$F_3(P_3, P_2) = \begin{cases} \frac{K_m P_2 P_3}{K_n + P_3} & \text{Model II III IV} \\ \frac{K_m P_3}{K_n + P_3} & \text{Model I} \end{cases} \qquad F_4(P_4) = \begin{cases} \frac{K_m^* P_4}{K_n^* + P_4} & \text{Version (a)} \\ 0 & \text{Version (b)} \end{cases}$$

$F_5(\cdot) = \Pi$ and $F_6(P_4) = rP_4$ for all models

All parameters are nonnegative constants listed in Table 3.2.

Finally, $D(\cdot)$ depends on the properties of the drug; the different expressions used for $D(\cdot)$ are listed in Table 3.3.

Table 3.3: The expression of D in different models

Expression of D(·)	Assumption	Model
0	No drug reaction	I II
k_1RM	Irreversible drug reaction	III
$k_1RM - kP_1$	Reversible drug reaction	IV

Chapter 4

Mathematical Analysis & Results

4.1 Preliminary results

4.1.1 Existence and uniqueness of solutions

Set System (3.1) as follows

$$\begin{aligned}
\frac{dM}{dt} &= E_1(M, P_1, P_2, P_3, P_4),\\
\frac{dP_1}{dt} &= E_2(M, P_1, P_2, P_3, P_4),\\
\frac{dP_2}{dt} &= E_3(M, P_1, P_2, P_3, P_4),\\
\frac{dP_3}{dt} &= E_4(M, P_1, P_2, P_3, P_4),\\
\frac{dP_4}{dt} &= E_5(M, P_1, P_2, P_3, P_4).
\end{aligned} \tag{4.1}$$

System (4.1) can be also considered as

$$X'(t) = E(X(t)) \text{ with } E : \mathbb{R}^5 \to \mathbb{R}^5,$$

where $t \in [t_0, \infty), X(t) = (M(t), P_1(t), P_2(t), P_3(t), P_4(t))$ and $X(t_0) \geq 0$.

We set a is Lipschitz constant, b is the radius of the closed ball in $\mathbb{R}^5$ around X_0, C is the least upper bound of $|E(X)|$.

Theorem 4.1. *With an initial condition $X(t_0) \geq 0$, System (4.1) has a unique solution that exists on interval $I : [t_0 - \tau, t_0 + \tau]$, where $0 < \tau < min\{a, b/C\}$, a is Lipschitz constant, $|X - X_0| < b$, $C = sup|E(X)|$.*

Proof. System (4.1) is an autonomous system with the initial conditions

$$X(t_0) = (M(t_0), P_1(t_0), P_2(t_0), P_3(t_0), P_4(t_0)) \text{ and } X(t_0) \geq 0; \forall\, t \in [t_0, \infty).$$

Functions E are the well-defined rational functions which are the continuous functions of (M, P_1, P_2, P_3, P_4). dE/dX are also continuous functions of (M, P_1, P_2, P_3, P_4). Thus, by the Picard-Lindelof Theorem [14], for some values $\tau \in (0, min\{a, b/C\})$, there exists a unique solution of System (4.1) on the interval $I : [t_0 - \tau, t_0 + \tau]$ [4], where a is Lipschitz constant, b is the radius of the closed ball in $\mathbb{R}^5$ around X_0, $C = sup|E(X)|$. □

4.1.2 Nonnegativity of solutions

Now we prove the nonnegativity of solution of System (3.1).

Theorem 4.2. *System* (3.1) *has nonnegative solutions, when considered with an initial condition* $X(t_0) \geq 0$.

Proof. Assume $X(t_0) \geq 0$ When M is 0,

$$\frac{dM}{dt} = F_2(P_2) - D(\cdot) = \frac{K_m^+ P_2}{K_n^+ + P_2} - D(\cdot).$$

Recall from Table 3.3, $D(\cdot)|_{M=0} \leq 0$. It implies the derivative of M is nonnegative for any $P_2 \geq 0$. Therefore, M is increasing at $M = 0$ and M stays nonnegative.

When P_1 is 0,

$$\frac{dP_1}{dt} = D(\cdot).$$

Recall from Table 3.3, $D(\cdot)|_{P_1=0} \geq 0$. It implies the derivative of P_1 is nonnegative for any $M \geq 0$. Therefore P_1 is increasing at $P_1 = 0$ and P_1 stays nonnegative.

When P_2 is 0,

$$\frac{dP_2}{dt} = F_1(M) = \frac{\tilde{K_m} M}{\tilde{K_n} + M},$$

which implies the derivative of P_2 is nonnegative for any $M \geq 0$. Therefore P_2 is increasing at $P_2 = 0$ and P_2 stays nonnegative.

When P_3 is 0,

$$\frac{dP_3}{dt} = F_4(P_4) + F_5(P_5) = \frac{K_m^* P_4}{K_n^* + P_4} + \Pi,$$

which implies the derivative of P_3 is nonnegative for any $P_4 \geq 0$. Therefore P_3 is increasing at $P_3 = 0$ and P_3 stays nonnegative. Note that if $\Pi > 0$, then $P_3(t) > 0 \; \forall t > t_0$.

When P_4 is 0,

$$\frac{dP_4}{dt} = F_3(P_3, P_2) = \frac{K_m P_2 P_3}{K_n + P_3},$$

which implies the derivative of P_4 is nonnegative for any $P_2, P_3 \geq 0$. Therefore P_4 is increasing at $P_4 = 0$ and P_4 stays nonnegative. □

Now, the mathematical analysis of each model is discussed. Recall that the difference between Version (a) and Version (b) of the models is the reaction of dephosphorylation of pNMT. By substituting $K_m^* = K_n^* = 0$ in Version (a), results of the Version (b) are obtained. Therefore, only the models in Version (a) are discussed in detail.

4.2 Model I–NMT Component

Model I is expressed as follows,

$$\begin{aligned} \frac{dP_3}{dt} &= -\frac{K_m P_3}{K_n + P_3} + \frac{K_m^* P_4}{K_n^* + P_4} + \Pi, \\ \frac{dP_4}{dt} &= \frac{K_m P_3}{K_n + P_3} - \frac{K_m^* P_4}{K_n^* + P_4} - r P_4. \end{aligned} \tag{4.2}$$

Parameters are listed in Table 3.2.

Theorem 4.3. *When* $K_m > \Pi + \frac{\Pi K_m^*}{\Pi + K_n^* r}$, *System* (4.2) *has a unique equilibrium point*

$$(P_3^*, P_4^*) = \left(\frac{K_m^* \Pi K_n + K_n^* \Pi r K_n + \Pi^2 K_n}{K_n^* K_m r + \Pi K_m - K_m^* \Pi - K_n^* \Pi r - \Pi^2}, \frac{\Pi}{r} \right)$$

that is locally asymptotically stable.

Proof. In order to find the equilibrium point, we solve the system:

$$-\frac{K_m P_3}{K_n + P_3} + \frac{K_m^* P_4}{K_n^* + P_4} + \Pi = 0, \tag{4.3a}$$

$$\frac{K_m P_3}{K_n + P_3} - \frac{K_m^* P_4}{K_n^* + P_4} - r P_4 = 0. \tag{4.3b}$$

Adding (4.3a)-(4.3b), we have $\Pi + rP_4 = 0$, which gives $P_4^* = \Pi/r$.

Substituting P_4^* into (4.3b), we get

$$\frac{K_m P_3^*}{K_n + P_3^*} - \frac{K_m^* \Pi}{rK_n^* + \Pi} - \Pi = 0 \quad \Longleftrightarrow \frac{K_m P_3^*}{K_n + P_3^*} = \frac{K_m^* \Pi}{rK_n^* + \Pi} + \Pi.$$

Solving the above equation for P_3^*, we obtain

$$P_3^* = \frac{K_m^* \Pi K_n + K_n^* \Pi r K_n + \Pi^2 K_n}{K_n^* K_m r + \Pi K_m - K_m^* \Pi - K_n^* \Pi r - \Pi^2}$$

.

In order to have P_3^* positive, the denominator is required to be:

$$K_n^* K_m r + \Pi K_m - K_m^* \Pi - K_n^* \Pi r - \Pi^2 > 0 \Longleftrightarrow K_m > \Pi + \frac{\Pi K_m^*}{\Pi + K_n^* r}.$$

Therefore, the unique equilibrium $(P_3^*, P_4^*) = \left(\frac{K_m^* \Pi K_n + K_n^* \Pi r K_n + \Pi^2 K_n}{K_n^* K_m r + \Pi K_m - K_m^* \Pi - K_n^* \Pi r - \Pi^2}, \frac{\Pi}{r} \right)$ exists, when $K_m > \Pi + \frac{\Pi K_m^*}{\Pi + K_n^* r}$.

The Jacobian matrix J_1 of System (4.2) is

$$J_1 = \begin{pmatrix} \frac{-K_m K_n}{(K_n + P_3)^2} & \frac{K_m^* K_n^*}{(K_n^* + P_4)^2} \\ \frac{K_m K_n}{(K_n + P_3)^2} & \frac{-K_m^* K_n^*}{(K_n^* + P_4)^2} - r \end{pmatrix}.$$

For any values of (P_3^*, P_4^*), tr(J_1)=$\frac{-K_m K_n}{(K_n + P_3^*)^2} - \frac{K_m^* K_n^*}{(K_n^* + P_4^*)^2} - r < 0$, and det($J_1$)=$\frac{rK_m K_n}{(K_n + P_3^*)^2} > 0$.

Hence, by the Routh-Hurwitz criterion [5], we know that the real parts of eigenvalues of J_1 evaluated at any equilibria are all negative, so that the equilibrium point

$$(P_3^*, P_4^*) = \left(\frac{K_m^* \Pi K_n + K_n^* \Pi r K_n + \Pi^2 K_n}{K_n^* K_m r + \Pi K_m - K_m^* \Pi - K_n^* \Pi r - \Pi^2}, \frac{\Pi}{r} \right)$$

is locally asymptotical stability (LAS) when it exists.

Note that the condition is only specific in the existence of equilibrium; when the equilibrium exists, it is always LAS. □

The global stability of the equilibrium is now investigated.

Theorem 4.4. *For positive initial conditions and when $K_m > K_m^* + \Pi$, the unique equilibrium (P_3^*, P_4^*) of System* (4.2) *is global asymptotic stable.*

Proof. Recalling System (4.2), we set:

$$\begin{aligned}\frac{dP_3}{dt} =& -\frac{K_m P_3}{K_n + P_3} + \frac{K_m^* P_4}{K_n^* + P_4} + \Pi =: F_1(P_3, P_4),\\ \frac{dP_4}{dt} =& \frac{K_m P_3}{K_n + P_3} - \frac{K_m^* P_4}{K_n^* + P_4} - rP_4 =: F_2(P_3, P_4).\end{aligned}$$

As proved previously in Theorem 4.2, the solutions of System (4.2) stay nonnegative for nonnegative initial conditions. Moreover, for positive initial conditions $P_3(t_0) > 0$ and $P_4(t_0) > 0$, $\frac{dP_3}{dt} > 0$ and $\frac{dP_4}{dt} > 0$, which implies that for any positive initial conditions, P_3 and P_4 stay positive. Then, we define a simply connected open set $S_1 = \{(P_3(t), P_4(t)) \mid P_3 > 0,\ P_4 > 0\}$ for the later proof.

System (4.2) can be bounded as follows:

$$\frac{dP_3}{dt} = -\frac{K_m P_3}{K_n + P_3} + \frac{K_m^* P_4}{K_n^* + P_4} + \Pi \le -\frac{K_m P_3}{K_n + P_3} + K_m^* + \Pi, \tag{4.4}$$

$$\frac{dP_4}{dt} = \frac{K_m P_3}{K_n + P_3} - \frac{K_m^* P_4}{K_n^* + P_4} - rP_4 \le K_m - rP_4. \tag{4.5}$$

As System (4.2) is continuous and C^1, it is monotone dynamic. If we prove that the solutions of $\frac{d\tilde{P}_3}{dt} = f(\tilde{P}_3) = -\frac{K_m \tilde{P}_3}{K_n + \tilde{P}_3} + K_m^* + \Pi$ are bounded, then the solution of the differential equation $\frac{dP_3}{dt}$ in (4.2) cannot be unbounded by comparison theorem [20]. To find the equilibrium for $\tilde{P}_3$, we set $-\frac{K_m \tilde{P}_3}{K_n + \tilde{P}_3} + K_m^* + \Pi$=0, which gives us the equilibrium point $\tilde{P}_3^* = \frac{K_n(K_m^* + \Pi)}{K_m - K_m^* - \Pi}$ that exists, when $K_m > K_m^* + \Pi$. Recall that to have a positive equilibrium in System (4.2), the condition $K_m > \Pi + \frac{\Pi K_m^*}{\Pi + K_n^* r}$ is required. Combining the above two conditions, we have $K_m > \max\{\Pi + K_m^*, \Pi + \frac{\Pi K_m^*}{\Pi + K_n^* r}\} = \Pi + K_m^*$.
When considering $\frac{d\tilde{P}_3}{dt} = f(\tilde{P}_3) = -\frac{K_m \tilde{P}_3}{K_n + \tilde{P}_3} + K_m^* + \Pi$,

$$\begin{aligned}&\tilde{P}_3 \in (0, \tilde{P}_3^*),\ f(\tilde{P}_3) = -\frac{K_m P_3}{K_n + P_3} + K_m^* + \Pi > 0,\\ &\tilde{P}_3 \in (\tilde{P}_3^*, \infty),\ f(\tilde{P}_3) = -\frac{K_m P_3}{K_n + P_3} + K_m^* + \Pi < 0.\end{aligned}$$

By phase line analysis, we can conclude that the equilibrium $\tilde{P}_3^*$ is globally asymptotically stable. Moreover, $0 < \limsup\{\tilde{P}_3(t)\} \le m = \max\{\frac{K_n(K_m^* + \Pi)}{K_m - K_m^* - \Pi}, \tilde{P}_3(t_0)\}$. Thus, we conclude that the solution of $P_3(t)$ in System (4.2) is also bounded on S_1 and $0 < \limsup\{P_3(t)\} < \limsup\{\tilde{P}_3(t)\} \le m$.

From Inequation (4.5), we have $\frac{dP_4}{dt} \leq K_m - rP_4$. Integrating with respect to time,

$$P_4(t) \leq \frac{K_m}{r} + \tilde{c}e^{-rt} \text{ with } \tilde{c} = \left[P_4(t_0) - \frac{K_m}{r}\right] e^{rt_0}.$$

As previously proved, we have the positivity of P_4 when $P_4(t_0) > 0$; therefore,

$$0 < P_4(t) \leq \frac{K_m}{r} + \tilde{c}e^{-rt}$$

and

$$0 < \limsup\{P_4(t)\} \leq \max\left\{\frac{K_m}{r}; P_4(t_0)\right\}.$$

Hence, the solution P_4 is bounded in the domain S_1.

System (4.2) has bounded solutions in domain S_1. By Poincaré-Bendixson Trichotomy, the locally asymptotically stable (LAS) unique equilibrium point is globally asymptotically stable (GAS) or periodic solutions exist. Next, Bendixson's negative Criterion [19] is applied to rule out the existence of periodic solutions in S_1. For this, we compute the divergence,

$$\begin{aligned} div(F_1, F_2) &= \frac{dF_1}{dP_3} + \frac{dF_2}{dP_4} \\ &= -\frac{K_m K_n}{(K_n + P_3)^2} - \frac{K_m^* K_n^*}{(K_n^* + P_4)^2} - r \\ &< 0 \text{ in } S_1. \end{aligned}$$

The sign of $div(F_1, F_2)$ does not change in S_1. By Bendixson's negative Criterion, there does not exist periodic solutions of System (4.2). Therefore, the equilibrium point (P_3^*, P_4^*) is GAS when $K_m > K_m^* + \Pi$. □

In summary, the equilibrium point exists in both cases, it is the stability that varies. Specifically, for System (4.2) the following conclusions hold.

1. If $K_m > \frac{\Pi K_m^*}{\Pi + K_n^* r} + \Pi$, there exists a unique equilibrium point

$$(P_3^*, P_4^*) = \left(\frac{K_m^* \Pi K_n + K_n^* \Pi r K_n + \Pi^2 K_n}{K_n^* K_m r + \Pi K_m - K_m^* \Pi - K_n^* \Pi r - \Pi^2}, \frac{\Pi}{r}\right),$$

which is LAS.

2. If $K_m > K_m^* + \Pi$, there exists a unique equilibrium point

$$(P_3^*, P_4^*) = \left(\frac{K_m^* \Pi K_n + K_n^* \Pi r K_n + \Pi^2 K_n}{K_n^* K_m r + \Pi K_m - K_m^* \Pi - K_n^* \Pi r - \Pi^2}, \frac{\Pi}{r} \right)$$

that is GAS.

Remark that the condition for the global stability is more conservative, since $K_m > K_m^* + \Pi > \frac{\Pi K_m^*}{\Pi + K_n^* r} + \Pi$.

Theorems (4.3) and (4.4) all hold for Version (b) of Model I. However, both conditions for local and global stability simplify to $K_m > \Pi$. For Version (b) of Model I, when $K_m > \Pi$, there exists a unique equilibrium that is globally asymptotic stable.

Biological Interpretation

In Model I, we only consider the NMT component. When the rate of phosphorylation of NMT is large enough, the NMT concentration stabilizes. The critical value for the rate of phosphorylation depends on the "production rate" of NMT.

4.3 Model II–Coupled mTOR-NMT Components–No drug reaction

Recall Model II (a):

$$\begin{aligned} \frac{dM}{dt} &= -\frac{\tilde{K_m} M}{\tilde{K_n} + M} + \frac{K_m^+ P_2}{K_n^+ + P_2}, \\ \frac{dP_2}{dt} &= \frac{\tilde{K_m} M}{\tilde{K_n} + M} - \frac{K_m^+ P_2}{K_n^+ + P_2}, \\ \frac{dP_3}{dt} &= -\frac{K_m P_2 P_3}{K_n + P_3} + \frac{K_m^* P_4}{K_n^* + P_4} + \Pi, \\ \frac{dP_4}{dt} &= \frac{K_m P_2 P_3}{K_n + P_3} - \frac{K_m^* P_4}{K_n^* + P_4} - r P_4. \end{aligned} \tag{4.6}$$

Parameters are listed in Table 3.2.

In System (4.6), adding the differential equations for M and P_2 gives,

$$\frac{dM}{dt} + \frac{dP_2}{dt} = 0 \iff \exists\, c \in \mathbb{R},\ M(t) + P_2(t) = c,\ \forall t \geq 0,$$

since $M(t) + P_2(t) = c, \forall t \geq 0$, where $c = M(0) + P_2(0)$.

In order to reduce the dimension of System (4.6), we substitute $M(t)$ in System (4.6) with $c - P_2(t)$, and we have:

$$\begin{aligned}
\frac{dP_2}{dt} =& \frac{\tilde{K_m}(c - P_2)}{\tilde{K_n} + c - P_2} - \frac{K_m^+ P_2}{K_n^+ + P_2}, \\
\frac{dP_3}{dt} =& - \frac{K_m P_2 P_3}{K_n + P_3} + \frac{K_m^* P_4}{K_n^* + P_4} + \Pi, \\
\frac{dP_4}{dt} =& \frac{K_m P_2 P_3}{K_n + P_3} - \frac{K_m^* P_4}{K_n^* + P_4} - r P_4.
\end{aligned} \tag{4.7}$$

We define the following:

$$\begin{aligned}
A &= K_m^+ - \tilde{K_m}, \\
B &= -\tilde{K_m} K_n^+ - K_m^+ \tilde{K_n} - (K_m^+ - \tilde{K_m})c, \\
C &= \tilde{K_m} K_n^+ c, \\
D &= \frac{K_m^* \Pi}{r K_n^* + \Pi} + \Pi.
\end{aligned} \tag{4.8}$$

Theorem 4.5. *System* (4.7) *has a unique equilibrium* $(P_2^*, P_3^*, P_4^*) = \left(P_2^*, \frac{DK_n}{K_m P_2^* - D}, \frac{\Pi}{r}\right)$ *when* $P_2^* > \frac{D}{K_m} = \frac{K_m^* \Pi + r K_n^* \Pi + \Pi^2}{r K_n^* + \Pi K_m}$,

where

$$0 < P_2^* = \begin{cases} \frac{-B - \sqrt{B^2 - 4AC}}{2A}, & \text{when } A \neq 0. \\ -\frac{C}{B}, & \text{when } A = 0. \end{cases}$$

When the equilibrium exists, it is locally asymptotically stable.

Note that the condition is only a condition for the existence of equilibrium; when the equilibrium exists, it is always LAS. The proof is given in Appendix B.

Theorem 4.6. *If, additionally to the conditions in Theorem 4.5, there holds that* $K_m \epsilon > K_m^* + \Pi$ *with* $\epsilon = \min P_2(t) > 0$, *then the equilibrium* (P_2^*, P_3^*, P_4^*) *in Theorem 4.5 is globally asymptotically stable.*

Proof. Observe that System (4.7) can be considered as a hierarchical system, by writing it as follows:

$$\text{mTOR subsystem:} \quad \frac{dP_2}{dt} = \frac{\tilde{K_m}(c - P_2)}{\tilde{K_n} + c - P_2} - \frac{K_m^+ P_2}{K_n^+ + P_2} = F_1(P_2). \tag{4.9}$$

$$\text{NMT subsystem:} \quad \begin{cases} \frac{dP_3}{dt} = & - \frac{K_m P_2 P_3}{K_n + P_3} + \frac{K_m^* P_4}{K_n^* + P_4} + \Pi, \\ \frac{dP_4}{dt} = & \frac{K_m P_2 P_3}{K_n + P_3} - \frac{K_m^* P_4}{K_n^* + P_4} - r P_4. \end{cases} \tag{4.10}$$

First, we investigate the asymptotic behaviour of mTOR subsystem.

To find the equilibrium point of the mTOR subsystem, we set $F_1(P_2) = \frac{\tilde{K_m}(c-P_2)}{\tilde{K_n}+c-P_2} - \frac{K_m^+ P_2}{K_n^+ + P_2} = 0$. That is the same as $f(P_2) = AP_2^2 + BP_2 + C = 0$ defined in polynomial equation (B.2) with notations defined in (4.8).

We are using the same cases I, II, III as in the proof of Theorem 4.5. Recalling that there is a unique P_2^* value in $(0, c]$

1. In case I, when $A > 0$, based on the Figure B.1,

   if $P_2 \in (0, P_2^*)$, $\frac{dP_2}{dt} > 0$,

   if $P_2 \in (P_2^*, c]$, $\frac{dP_2}{dt} < 0$,

   by phase line analysis, P_2^* is GAS in case I.

2. In case II, when $A < 0$, based on the Figure B.2,

   if $P_2 \in (0, P_2^*)$, $\frac{dP_2}{dt} > 0$,

   if $P_2 \in (P_2^*, c]$, $\frac{dP_2}{dt} < 0$,

   by phase line analysis, P_2^* is GAS in case II.

3. In case III, when $A = 0$, based on the Figure B.3,

   if $P_2 \in (0, P_2^*)$, $\frac{dP_2}{dt} > 0$,

   if $P_2 \in (P_2^*, c]$, $\frac{dP_2}{dt} < 0$,

   by phase line analysis, P_2^* is GAS in case III.

Thus, for the mTOR subsystem, there exists a unique interior equilibrium that is always GAS.

Finally, we investigate the stability of the NMT subsystem. For any positive initial condition $P_2(t_0) > 0$, we have $dP_2/dt > 0$. Moreover, since, as previously mentioned, $M(t) + P_2(t) = c$ from System (4.6), we have $P_2(t) < c$, $\forall\, t > t_0$. Thus, we define the domain $S_2 = \{P_2 \,|\, 0 < P_2 < c\}$. Domain S_2 is invariant under the flow of System (4.9), so $\exists\ \epsilon > 0$ such as $P_2(t) > \epsilon$, $\forall t \geq 0$. Consequently, the following inequations can be considered:

$$\begin{aligned}
\frac{dP_3}{dt} &= -\frac{K_m P_2 P_3}{K_n + P_3} + \frac{K_m^* P_4}{K_n^* + P_4} + \Pi < -\frac{K_m \epsilon P_3}{K_n + P_3} + K_m^* + \Pi, \\
\frac{dP_4}{dt} &= \frac{K_m P_2 P_3}{K_n + P_3} - \frac{K_m^* P_4}{K_n^* + P_4} - rP_4 \leq K_m - rP_4.
\end{aligned}$$

Similarly to the proof of Model I (NMT component), if we prove that the solutions of

$$\frac{d\tilde{P}_3}{dt} = f(\tilde{P}_3) = -\frac{K_m\epsilon\tilde{P}_3}{K_n + \tilde{P}_3} + K_m^* + \Pi$$

are bounded, then the solution of the differential equation $\frac{dP_3}{dt}$ in (4.10) cannot be unbounded. To find the equilibrium for $\tilde{P}_3$, we set $-\frac{K_m\epsilon\tilde{P}_3}{K_n+\tilde{P}_3} + K_m^* + \Pi = 0$, which gives us the equilibrium point $\tilde{P}_3^*(t) = \frac{K_n(K_m^*+\Pi)}{K_m\epsilon - K_m^* - \Pi}$ that exists when $K_m\epsilon > K_m^* + \Pi$.

Remark that the P_3-components of the equilibrium for systems (4.7) and (4.10) are the same, and all the analysis done on the existence and expression of equilibrium for (4.7) holds for (4.10). Recall that to have a positive equilibrium P_3^* in Equation (B.3), the following conditions are required: $P_2^* > \frac{D}{K_m} = \frac{K_m^*\Pi + rK_n^*\Pi + \Pi^2}{(rK_n^*+\Pi)K_m}$ and $D = \frac{K_m^*\Pi}{rK_n^*+\Pi} + \Pi$. As shown previously, the condition $K_m\epsilon > K_m^* + \Pi$ is required to the existence of $\tilde{P}_3^*(t)$. Combining the above conditions, we know that $P_2^* > \epsilon$ and $K_m^* > \frac{K_m^*\Pi}{rK_n^*+\Pi}$. Then, $K_mP_2^* > K_m\epsilon > K_m^* + \Pi > D$. Thus, when $K_m\epsilon > K_m^* + \Pi$, P_3^* is positive and the interior equilibrium of System (4.10) exists and so the same is true for (4.7).

Similarly to the proof of Theorem (4.4),

$$\text{when } \tilde{P}_3 \in (0, \tilde{P}_3^*),\ f(\tilde{P}_3) = -\frac{K_m\epsilon\tilde{P}_3}{K_n + \tilde{P}_3} + K_m^* + \Pi > 0,$$
$$\text{when } \tilde{P}_3 \in (\tilde{P}_3^*, \infty),\ f(\tilde{P}_3) = -\frac{K_m\epsilon\tilde{P}_3}{K_n + \tilde{P}_3} + K_m^* + \Pi < 0.$$

Therefore, by phase line analysis the equilibrium $\tilde{P}_3^*$ is GAS when it exists. Moreover,

$$\limsup\left\{\tilde{P}_3(t)\right\} \leq m = \max\{\frac{K_n(K_m^*+\Pi)}{K_m\epsilon - K_m^* - \Pi}, \tilde{P}_3(t_0)\right\}$$

and then,

$$\limsup\{P_3(t)\} < \limsup\{\tilde{P}_3(t)\} \leq m.$$

Thus, we conclude that the solution of $P_3(t)$ in the NMT subsystem (4.10) is also bounded when $K_m\epsilon > K_m^* + \Pi$.

The proof of the boundedness of $P_4(t)$ and the same analysis as for Theorem 4.4 allows us to conclude on the asymptotical behaviour of System (4.10). Therefore, the same conclusion holds, the unique equilibrium (P_3^*, P_4^*) is GAS when $K_m\epsilon > K_m^* + \Pi$.

Finally, we can conclude that the unique equilibrium (P_2^*, P_3^*, P_4^*) of System (4.7) is globally asymptotically stable when the condition $K_m\epsilon > K_m^* + \Pi$ is satisfied, where $\epsilon = \min_t P_2(t)$. □

Now, returning to the full System (4.6), System (4.6) has a unique equilibrium

$$\left(M^*, P_2^*, P_3^*, P_4^*\right) = (c - P_2^*, P_2^*, \frac{DK_n}{K_m P_2^* - D}, \frac{\Pi}{r}),$$

where

$$0 < P_2^* = \begin{cases} \frac{-B-\sqrt{B^2-4AC}}{2A}, & \text{when } A \neq 0. \\ -\frac{C}{B}, & \text{when } A = 0. \end{cases}$$

The above notations A, B, C, D are defined in Equations (4.8).

1. When $K_m P_2^* > \frac{K_m^* \Pi}{r K_n^* + \Pi} + \Pi$, there exists a unique equilibrium that is locally asymptotically stable.

2. When $K_m \epsilon > K_m^* + \Pi$, the unique equilibrium point is globally asymptotically stable, where $\epsilon = \min_t P_2(t)$.

Note that the condition for global stability is more conservative, since $K_m P_2^* > K_m \epsilon > K_m^* + \Pi > \frac{K_m^* \Pi}{r K_n^* + \Pi} + \Pi$.

Theorems 4.5 and 4.6 hold for Version (b) of Model II. However, the condition for the existence, LAS and GAS simplifies to $\epsilon = \min_t P_2(t) > \Pi / K_m$. In summary, for Version (b) of Model II, when $\epsilon > \Pi / K_m$, there exists a unique equilibrium that is always GAS.

Biological Interpretation

When time is large, if the concentration of catalyst (pmTOR) is greater than the ratio of the producing rate over the consuming rate of NMT, the concentration of reactants will stabilize for any positive initial conditions.

4.4 Model III–Coupled mTOR-NMT Component–Irreversible drug reaction

In Model III, we add an irreversible drug reaction to the system. Recall equations for Model III (a):

$$\frac{dM}{dt} = - k_1 RM - \frac{\tilde{K_m} M}{\tilde{K_n} + M} + \frac{K_m^+ P_2}{K_n^+ + P_2}, \tag{4.11a}$$

$$\frac{dP_1}{dt} = k_1 RM, \tag{4.11b}$$

$$\frac{dP_2}{dt} = \frac{\tilde{K_m} M}{\tilde{K_n} + M} - \frac{K_m^+ P_2}{K_n^+ + P_2}, \tag{4.11c}$$

$$\frac{dP_3}{dt} = - \frac{K_m P_2 P_3}{K_n + P_3} + \frac{K_m^* P_4}{K_n^* + P_4} + \Pi, \tag{4.11d}$$

$$\frac{dP_4}{dt} = \frac{K_m P_2 P_3}{K_n + P_3} - \frac{K_m^* P_4}{K_n^* + P_4} - r P_4. \tag{4.11e}$$

Parameters are listed in Table 3.2.

To find equilibrium points $(M^*, P_1^*, P_2^*, P_3^*, P_4^*)$, we reduce the dimension of the system. Since $\frac{dM}{dt} + \frac{dP_1}{dt} + \frac{dP_2}{dt} = 0$, it follows that $M(t) + P_1(t) + P_2(t) = c$, where c is a constant, $c = M(t_0) + P_1(t_0) + P_2(t_0)$. Thus, System (4.11) can be reduced to a 4-dimensional system:

$$\begin{aligned}
\frac{dM}{dt} &= - k_1 RM - \frac{\tilde{K_m} M}{\tilde{K_n} + M} + \frac{K_m^+ P_2}{K_n^+ + P_2}, \\
\frac{dP_2}{dt} &= \frac{\tilde{K_m} M}{\tilde{K_n} + M} - \frac{K_m^+ P_2}{K_n^+ + P_2}, \\
\frac{dP_3}{dt} &= - \frac{K_m P_2 P_3}{K_n + P_3} + \frac{K_m^* P_4}{K_n^* + P_4} + \Pi, \\
\frac{dP_4}{dt} &= \frac{K_m P_2 P_3}{K_n + P_3} - \frac{K_m^* P_4}{K_n^* + P_4} - r P_4.
\end{aligned} \tag{4.12}$$

To calculate the equilibrium solutions, we have to solve the following equations:

$$- k_1 RM - \frac{\tilde{K_m} M}{\tilde{K_n} + M} + \frac{K_m^+ P_2}{K_n^+ + P_2} = 0, \tag{4.13a}$$

$$\frac{\tilde{K_m} M}{\tilde{K_n} + M} - \frac{K_m^+ P_2}{K_n^+ + P_2} = 0, \tag{4.13b}$$

$$- \frac{K_m P_2 P_3}{K_n + P_3} + \frac{K_m^* P_4}{K_n^* + P_4} + \Pi = 0, \tag{4.13c}$$

$$\frac{K_m P_2 P_3}{K_n + P_3} - \frac{K_m^* P_4}{K_n^* + P_4} - r P_4 = 0. \tag{4.13d}$$

Using (4.13a) - (4.13b), we can conclude that $M^* = 0$. Substituting $M^* = 0$ into (4.13b) gives $P_2^* = 0$ and since $M(t) + P_1(t) + P_2(t) = c$, $P_1^* = c$. Adding (4.13c) and (4.13d), we obtain $P_4^* = \Pi/r$. P_3^* cannot be explicitly calculated. We will have a theorem showing the nonexistence of equilibrium of System (4.11) later.

Observe that System (4.12) can be considered as 2 subsystems as follows:

$$\text{mTOR subsystem:} \quad \begin{cases} \frac{dM}{dt} = F_1(M, P_2) = -k_1 RM - \frac{\tilde{K_m} M}{\tilde{K_n} + M} + \frac{K_m^+ P_2}{K_n^+ + P_2}, \\ \frac{dP_2}{dt} = F_2(M, P_2) = \frac{\tilde{K_m} M}{\tilde{K_n} + M} - \frac{K_m^+ P_2}{K_n^+ + P_2}. \end{cases} \tag{4.14}$$

$$\text{NMT subsystem:} \quad \begin{cases} \frac{dP_3}{dt} = & -\frac{K_m P_2 P_3}{K_n + P_3} + \frac{K_m^* P_4}{K_n^* + P_4} + \Pi, \\ \frac{dP_4}{dt} = & \frac{K_m P_2 P_3}{K_n + P_3} - \frac{K_m^* P_4}{K_n^* + P_4} - rP_4. \end{cases} \tag{4.15}$$

The mTOR Subsystem (4.14) does not depend on P_3 and P_4, then the mTOR subsystem can be studied independently.

Theorem 4.7. *The mTOR Subsystem* (4.14) *has a unique equilibrium* $(M^*, P_2^*) = (0, 0)$*, which is globally asymptotically stable and the NMT Subsystem* (4.15) *is unbounded.*

Proof. In the mTOR subsystem, there is a unique equilibrium $(M^*,\ P_2^*) = (0,\ 0)$. The Jacobian matrix of the mTOR subsystem is

$$J_3 = \begin{pmatrix} -\frac{\tilde{K_m}\tilde{K_n}}{(\tilde{K_n}+M)^2} - k_1 R & \frac{K_m^+ K_n^+}{(K_n^+ + P_2)^2} \\ \frac{\tilde{K_m}\tilde{K_n}}{(\tilde{K_n}+M)^2} & -\frac{K_m^+ K_n^+}{(K_n^+ + P_2)^2} \end{pmatrix}.$$

The eigenvalues of matrix J_3 evaluated at $(M^*, P_2^*) = (0, 0)$ are:

$$\lambda_1 = -\frac{1}{2}\left[\sqrt{(\frac{\tilde{K_m}}{\tilde{K_n}} + k_1 R + \frac{K_m^+}{K_n^+})^2 - 4(k_1 R)(\frac{K_m^+}{K_n^+})} + \frac{\tilde{K_m}}{\tilde{K_n}} + k_1 R + \frac{K_m^+}{K_n^+}\right],$$

$$\lambda_2 = \frac{1}{2}\left[\sqrt{(\frac{\tilde{K_m}}{\tilde{K_n}} + k_1 R + \frac{K_m^+}{K_n^+})^2 - 4(k_1 R)(\frac{K_m^+}{K_n^+})} - \frac{\tilde{K_m}}{\tilde{K_n}} - k_1 R - \frac{K_m^+}{K_n^+}\right].$$

Therefore, the real part of the eigenvalue λ_1 is negative.

For the eigenvalue λ_2, we have the following:

If $\lambda_2 \in \mathbb{C}$, $Re(\lambda_2) < 0$.

If $\lambda_2 \in \mathbb{R}$,

$$\begin{aligned}\lambda_2 &= \frac{1}{2}\left[\sqrt{(\frac{\tilde{K_m}}{\tilde{K_n}} + k_1R + \frac{K_m^+}{K_n^+})^2 - 4(k_1R)(\frac{K_m^+}{K_n^+})} - (\frac{\tilde{K_m}}{\tilde{K_n}} + k_1R + \frac{K_m^+}{K_n^+})\right] \\ &= \frac{1}{2}\left[\sqrt{(\frac{\tilde{K_m}}{\tilde{K_n}} + k_1R + \frac{K_m^+}{K_n^+})^2 - 4(k_1R)(\frac{K_m^+}{K_n^+})} - \sqrt{(\frac{\tilde{K_m}}{\tilde{K_n}} + k_1R + \frac{K_m^+}{K_n^+})^2}\right].\end{aligned}$$

As $\sqrt{(\frac{\tilde{K_m}}{\tilde{K_n}} + k_1R + \frac{K_m^+}{K_n^+})^2 - 4(k_1R)(\frac{K_m^+}{K_n^+})} < \sqrt{(\frac{\tilde{K_m}}{\tilde{K_n}} + k_1R + \frac{K_m^+}{K_n^+})^2}$, the eigenvalue λ_2 is negative.

Consequently, the equilibrium point $(M^*,\ P_2^*)$ is locally asymptotically stable.

Furthermore, as previously shown, in the mTOR subsystem, $M(t)+P_2(t) \leq c$. This implies that the solutions of the mTOR subsystem are bounded in domain S_3 defined as $S_3 = \{M \geq 0, P_2 \geq 0,\ M + P_2 \leq c\}$. By the Poincaré-Bendixson Trichotomy, either the unique equilibrium (M^*, P_2^*) in mTOR subsystem is globally asymptotically stable (GAS) or periodic solutions or homoclinic orbits exist. However, the equilibrium point is unique and LAS, which rules out of the existence of homoclinic orbits. If there were periodic solutions, they would have to surround the unique equilibrium. In this case, the periodic orbit would run out of the positive quadrant as the equilibrium is a boundary equilibrium. However, we previously proved that solutions stay nonnegative. Hence, the presence of periodic solution is ruled out. Finally, under the Poincaré-Bendixson Trichotomy, the only possible situation is the global asymptotic stability of the boundary equilibrium $(M^*, P_2^*) = (0, 0)$.

The solution of $P_2(t)$ for the mTOR subsystem is approaching the equilibrium point $P_2^* = 0$ with any nonnegative initial conditions. Hence, for time t sufficiently large, the following differential equation for P_3 can be considered:

$$\frac{dP_3}{dt} = \frac{K_m^* P_4^*}{K_n^* + P_4^*} + \Pi.$$

It follows that

$$\Pi \leq \frac{dP_3}{dt}.$$

Integrating with respect to time t gives $\Pi t + P_3(t_0) \leq P_3(t)$. Consequently, the value of $P_3(t)$ will keep increasing to infinity, $P_3(t)$ is unbounded. Thus, there is no equilibrium point in the NMT Subsystem (4.11). □

Remark that Theorem 4.7 holds for Version (b) of Model III.

In summary, the mTOR Subsystem (4.14) has a unique equilibrium $(M^*, P_2^*) = (0, 0)$, which is

globally asymptotically stable and the NMT Subsystem (4.15) is unbounded.

Biological Interpretation

In the irreversible drug reaction case (Model III), the drug is very efficient and powerful enough to inhibit all the phosphorylation of mTOR, so that the concentration of catalyst or enzyme pmTOR will be absent in the long run. Because of the nonexistence of enzyme pmTOR, the system keeps producing NMT without allowing its phosphorylation, which makes the concentration of NMT increase without bounds. In reality, the unbounded increase of NMT will not occur.

4.5 Model IV–Coupled mTOR-NMT Components–Reversible drug reaction for Rapamycin-mTOR

The reaction of Rapamycin-mTOR is now assumed to be reversible. Mathematical equations of Model IV are expressed as follows:

$$\frac{dM}{dt} = - k_1 RM - \frac{\tilde{K_m} M}{\tilde{K_n} + M} + \frac{K_m^+ P_2}{K_n^+ + P_2} + kP_1, \tag{4.16a}$$

$$\frac{dP_1}{dt} = k_1 RM - kP_1 \tag{4.16b}$$

$$\frac{dP_2}{dt} = \frac{\tilde{K_m} M}{\tilde{K_n} + M} - \frac{K_m^+ P_2}{K_n^+ + P_2}, \tag{4.16c}$$

$$\frac{dP_3}{dt} = - \frac{K_m P_2 P_3}{K_n + P_3} + \frac{K_m^* P_4}{K_n^* + P_4} + \Pi, \tag{4.16d}$$

$$\frac{dP_4}{dt} = \frac{K_m P_2 P_3}{K_n + P_3} - \frac{K_m^* P_4}{K_n^* + P_4} - rP_4. \tag{4.16e}$$

Parameters are listed in Table (3.2).

Adding (4.16a)-(4.16c), gives $\frac{dM(t)}{dt} + \frac{dP_1(t)}{dt} + \frac{dP_2(t)}{dt} = 0$. Hence, $\forall t \geq 0, M(t) + P_1(t) + P_2(t) = c$ where c is a constant defined as $M(t_0) + P_1(t_0) + P_2(t_0) = c$. So, $P_2(t) = c - M(t) - P_1(t)$.

Therefore, the System (4.16) can be reduced to a 4-dimensional system:

$$\begin{aligned}
\frac{dM}{dt} &= -k_1 RM - \frac{\tilde{K_m} M}{\tilde{K_n} + M} + \frac{K_m^+(c - M - P_1)}{K_n^+ + (c - M - P_1)} + kP_1, \\
\frac{dP_1}{dt} &= k_1 RM - kP_1, \\
\frac{dP_3}{dt} &= -\frac{K_m(c - M - P_1)P_3}{K_n + P_3} + \frac{K_m^* P_4}{K_n^* + P_4} + \Pi, \\
\frac{dP_4}{dt} &= \frac{K_m(c - M - P_1)P_3}{K_n + P_3} - \frac{K_m^* P_4}{K_n^* + P_4} - rP_4.
\end{aligned} \tag{4.17}$$

Before stating the theorems, we introduce the following notations:

$$\begin{aligned}
A &= (\tilde{K_m} - K_m^+)(1 + n), \\
B &= -(\tilde{K_m} - K_m^+)c - \tilde{K_m} K_n^+ - (K_m^+ + nK_m^+)\tilde{K_n}, \\
C &= K_m^+ \tilde{K_n} c, \\
D &= \Pi(K_m^* + K_n^* r + \Pi), \\
E &= K_m(K_n^* r + \Pi), \\
n &= \frac{k_1 R}{k}.
\end{aligned}$$

Theorem 4.8. *System* (4.16) *has a unique equilibrium*

$$(M^*, P_1^*, P_2^*, P_3^*, P_4^*) = \left(M^*, nM^*, c - (1 + n)M^*, \frac{K_n D}{Ec - D - E(1 + n)M^*}, \frac{\Pi}{r} \right),$$

if and only if $P_2^* > \frac{D}{E} = \frac{\Pi(K_m^* + K_n^* r + \Pi)}{K_m(K_n^* r + \Pi)}$, *where*

$$0 < M^* = \begin{cases} \frac{-B - \sqrt{B^2 - 4AC}}{2A}, & \textit{when } A \neq 0. \\ -\frac{C}{B}, & \textit{when } A = 0. \end{cases}$$

When the equilibrium exists, it is locally asymptotically stable.

The proof of Theorem 4.8 is presented in Appendix C.

Theorem 4.9. *For any positive initial conditions, when* $K_m \epsilon > K_m^* + \Pi$ *with* $\epsilon = \min_t P_2(t)$, *System* (4.16) *has a unique positive equilibrium that is globally asymptotically stable.*

Proof. For positive initial conditions, $M(t_0), P_1(t_0), P_3(t_0), P_4(t_0) > 0$, the signs of differential equations of System (4.17) are: $\frac{dM}{dt} > 0$, $\frac{dP_1}{dt} > 0$, $\frac{dP_3}{dt} > 0$, $\frac{dP_4}{dt} > 0$, $\forall t \geq t_0$. That implies that $M(t)$, $P_1(t)$, $P_3(t)$, $P_4(t)$ cannot be equal to 0 with $M(t_0), P_1(t_0), P_3(t_0), P_4(t_0) > 0$. As $\frac{dM}{dt} + \frac{dP_1}{dt} + \frac{dP_2}{dt} = 0$, there is the conservation of total mTOR molecules, i.e. $M(t) + P_1(t) + P_2(t) = c$, $\forall t \geq t_0$, where c is a constant defined such as $c = M(t_0) + P_1(t_0) + P_2(t_0)$. Thus, a simply connected open domain S_4 is defined as $S_4 = \{M, P_1, P_3, P_4 |\, 0 < M < c,\ 0 < P_1 < c,\ 0 < P_3,\ 0 < P_4\}$. S_4 is invariant under the flow of System (4.17). Recall the mTOR subsystem,

$$\begin{aligned}
\frac{dM}{dt} &= -k_1 RM - \frac{\tilde{K_m} M}{\tilde{K_n} + M} + \frac{K_m^+ (c - M - P_1)}{K_n^+ + (c - M - P_1)} + kP_1 =: F_1(M, P_1), \\
\frac{dP_1}{dt} &= k_1 RM - kP_1 =: F_2(M, P_1).
\end{aligned}$$

We know that the solutions $M(t)$ and $P_1(t)$ are bounded. The Poincaré-Bendixson Trichotomy is applied to show that either the LAS unique interior equilibrium (M^*, P_1^*) is globally asymptotically stable or periodic solutions exist. The Bendixson negative Criterion is used to rule out the periodic solutions. Consider the divergence of the vector field defined in the mTOR subsystem:

$$\begin{aligned}
div(F_1, F_2) &= \frac{dF_1}{dM} + \frac{dF_2}{dP_1} \\
&= -\frac{\tilde{K_m}\tilde{K_n}}{(\tilde{K_n} + M)^2} - \frac{K_m^+ K_n^+}{(K_n^+ + c - M - P_1)^2} - k_1 R - k \\
&< 0 \text{ in } S_2.
\end{aligned}$$

The sign of $div(F_1, F_2)$ does not change on domain S_4. By Bendixson's negative Criterion, there does not exist any periodic solutions. Therefore, in the mTOR subsystem, there exists a unique equilibrium point (M^*, P_1^*) that is GAS.

Using the same method as in the proof of Theorem 4.4 and Theorem 4.6, the solutions P_3 and P_4 of system can be proved to be bounded by considering the following inequations:

$$\begin{aligned}
\frac{dP_3}{dt} &= -\frac{K_m P_2 P_3}{K_n + P_3} + \frac{K_m^* P_4}{K_n^* + P_4} + \Pi < -\frac{K_m \epsilon P_3}{K_n + P_3} + K_m^* + \Pi, \\
\frac{dP_4}{dt} &= \frac{K_m P_2 P_3}{K_n + P_3} - \frac{K_m^* P_4}{K_n^* + P_4} - rP_4 \leq K_m - rP_4.
\end{aligned}$$

Using a phase line analysis, Poincaré-Bendixson Trichotomy and Bendixson negative Criterion, we can also easily prove that the unique equilibrium of System (4.16) is globally asymptotically

stable when $K_m\epsilon > K_m^* + \Pi,$ where $\epsilon = \min\{P_2(t)\} > 0$. Combining the condition of existence and the condition of GAS, we have $\frac{\Pi(K_m^*+K_n^*r+\Pi)}{K_m(K_n^*r+\Pi)} < \frac{K_m^*+\Pi}{K_m} < \epsilon < P_2^*$. Thus, when $\frac{K_m^*+\Pi}{K_m} < \epsilon$, the unique equilibrium exists and is GAS. □

In summary, if $P_2^* > \frac{D}{E} = \frac{\Pi(K_m^*+K_n^*r+\Pi)}{K_m(K_n^*r+\Pi)}$, System (4.16) has a unique equilibrium

$$(M^*, P_1^*, P_2^*, P_3^*, P_4^*) = \left(M^*, nM^*, c-(1+n)M^*, \frac{K_nD}{Ec-D-E(1+n)M^*}, \frac{\Pi}{r}\right),$$

where

$$0 < M^* = \begin{cases} \frac{-B-\sqrt{B^2-4AC}}{2A}, & \text{when } A \neq 0, \\ -\frac{C}{B}, & \text{when } A = 0. \end{cases}$$

1. When $P_2^* > \frac{\Pi(K_m^*+K_n^*r+\Pi)}{K_m(K_n^*r+\Pi)}$ the equilibrium exists and it is locally asymptotically stable,
2. When $\epsilon > \frac{K_m^*+\Pi}{K_m}$, the unique equilibrium point is globally asymptotically stable, where $\epsilon = \min_t P_2(t)$.

A, B, C, D and E are defined in (C.3).

The condition for global asymptotic stability is more conservative, since $P_2^* > \epsilon > \frac{K_m^*+\Pi}{K_m} > \frac{\Pi(K_m^*+K_n^*r+\Pi)}{K_m(K_n^*r+\Pi)}$.

Theorems 4.8 and 4.9 hold for Version (b) of Model IV. However, the condition of existence and LAS simplifies to $P_2^* > \frac{\Pi}{K_m}$ and the condition for GAS simplifies to $\epsilon = \min_t P_2(t) > \frac{\Pi}{K_m}$.

Biological Interpretation

In the reversible drug reaction (Model IV), when the consumption rate of NMT ($K_m\epsilon$) is greater than the producing rate of NMT ($K_m^* + \Pi$), the concentration of reactants will stabilize for any positive initial conditions.

4.6 Mathematical summary of models

In order to interpret the biological implication of mathematical results, all mathematical conditions and conclusions are summarized into two different ways in Table 4.1 and Figure 4.1.

Table 4.1: Mathematical summary of asymptotic behaviour of models. Parameters used here are listed in Table 3.2. LAS means local asymptotic stability. GAS means global asymptotic stability. The mTOR subsystem is defined in System (4.14). The NMT subsystem is defined in System (4.15). In each model, the condition for LAS is only a condition for the existence of equilibrium; when the equilibrium exists, it is always LAS.

Models	Equilibria	Existence and LAS	Condition of GAS
Model I (a) Positive Initial Condition	Unique Interior Equilibrium	$1 > \frac{\Pi(K_m^*+K_n^* r+\Pi)}{K_m(K_n^* r+\Pi)}$	mTOR subsystem: GAS. When $1 > \frac{K_m^*+\Pi}{K_m}$, NMT subsystem: GAS.
Model I (b) Positive Initial Condition	Unique Interior Equilibrium	$1 > \frac{\Pi}{K_m}$	mTOR subsystem: GAS. When $1 > \frac{\Pi}{K_m}$, NMT subsystem: GAS.
Model II (a) Positive Initial Condition	Unique Interior Equilibrium	$P_2^* > \frac{\Pi(K_m^*+K_n^* r+\Pi)}{K_m(K_n^* r+\Pi)}$	mTOR subsystem: GAS. When $\epsilon > \frac{K_m^*+\Pi}{K_m}$, NMT subsystem: GAS.
Model II (b) Positive Initial Condition	Unique Interior Equilibrium	$P_2^* > \frac{\Pi}{K_m}$	mTOR subsystem: GAS. When $\epsilon > \frac{\Pi}{K_m}$, NMT subsystem: GAS.
Model III (a) Nonnegative Initial Condition	mTOR subsystem has a unique equilibrium. NMT subsystem is unbounded.	-	mTOR subsystem: GAS. NMT subsystem: unbounded.
Model III (b) Nonnegative Initial Condition	mTOR subsystem has a unique equilibrium. NMT subsystem is unbounded.	-	mTOR subsystem: GAS. NMT subsystem: unbounded.
Model IV (a) Positive Initial Condition	Unique Interior Equilibrium	$P_2^* > \frac{\Pi(K_m^*+K_n^* r+\Pi)}{K_m(K_n^* r+\Pi)}$	mTOR subsystem: GAS. When $\epsilon > \frac{K_m^*+\Pi}{K_m}$, NMT subsystem: GAS.
Model IV (b) Positive Initial Condition	Unique Interior Equilibrium	$P_2^* > \frac{\Pi}{K_m}$	mTOR subsystem: GAS. When $\epsilon > \frac{\Pi}{K_m}$, NMT subsystem: GAS.

In all models, the mTOR subsystem can be considered independently, and the equilibrium in the mTOR subsystem is always GAS. Furthermore, in Table 4.1, the values of P_2^* in Model II and Model IV are different, and ϵ is defined as the minimum values of $P_2(t)$ in the given models. The specific expressions of P_2^* can be found in Theorem 4.5 for Model II and Theorem 4.8 for Model IV, and the expressions of P_2^* are presented as follows:

Model II: $P_2^* = \dfrac{(\tilde{K_m} - K_m^+)c - \tilde{K_m}K_n^+ - K_m^+\tilde{K_n}}{2(\tilde{K_m} - K_m^+)}$

$$+ \frac{\sqrt{[(\tilde{K_m} - K_m^+)c + (\tilde{K_m}K_n^+) - (\tilde{K_n}K_m^+)]^2 + 4\tilde{K_m}K_m^+\tilde{K_n}K_n^+}}{2(\tilde{K_m} - K_m^+)},$$

Model III: $P_2^* = 0$,

Model IV: $P_2^* = \dfrac{(\tilde{K_m} - K_m^+)c - \tilde{K_m}K_n^+ - (1+n)K_m^+\tilde{K_n}}{2(\tilde{K_m} - K_m^+)}$

$$+ \frac{\sqrt{[(\tilde{K_m} - K_m^+)c + (\tilde{K_m}K_n^+) - (\tilde{K_n}K_m^+)(1+n)]^2 + 4\tilde{K_m}K_m^+\tilde{K_n}K_n^+(1+n)}}{2(\tilde{K_m} - K_m^+)}.$$

Note that $n = k_1 R/k$.

Table 4.1 shows that except Model III, all models have an unique interior equilibrium under some conditions. In Model III, the irreversible drug reaction results in the decrease of the concentration of pmTOR to 0. Consequently, the phosphorylation of NMT by pmTOR is inhibited. As NMT is synthesized, the concentration of NMT grows unbounded. In Table 4.1, the inequations which determine the existence of equilibrium, local asymptotic stability and global asymptotic stability show the connections between the mTOR subsystem and the NMT subsystem.

In Figure 4.1, a summary of the mathematical conditions is presented by taking K_m as a bifurcation parameter. Only Model I, Model II and Model IV are considered. In Model I, when the bifurcation parameter K_m is less than $\frac{\Pi(K_m^* + K_n^* r + \Pi)}{(K_n^* r + \Pi)}$, the concentration of NMT in Model I is unbounded. However, when parameter K_m is between $\frac{\Pi(K_m^* + K_n^* r + \Pi)}{(K_n^* r + \Pi)}$ and $K_m^* + \Pi$, Model I has a unique equilibrium that is locally asymptotically stable. Moreover, when K_m is greater than the bifurcation value $K_m^* + \Pi$, the unique equilibrium of Model I is not only locally asymptotically stable, but also globally asymptotically stable. For Model II and Model IV, when $K_m < \frac{\Pi(K_m^* + K_n^* r + \Pi)}{P_2^*(K_n^* r + \Pi)}$, both Model II and Model IV are unbounded. Furthermore, as for Model I, when K_m is between $\frac{\Pi(K_m^* + K_n^* r + \Pi)}{P_2^*(K_n^* r + \Pi)}$ and $\frac{K_m^* + \Pi}{\epsilon}$, Model II and Model IV have a unique equilibrium that is locally asymptotically stable. Finally, when K_m is greater than $\frac{K_m^* + \Pi}{\epsilon}$, the unique equilibrium in Model II and Model IV is globally asymptotically stable. The values of P_2^* in Model II and Model IV are distinct as well as $\epsilon = \min_t P_2(t)$.

Figure 4.1: Mathematical summary of models. Bifurcation values determine the asymptotical behaviour for Model I, Model II and Model IV.

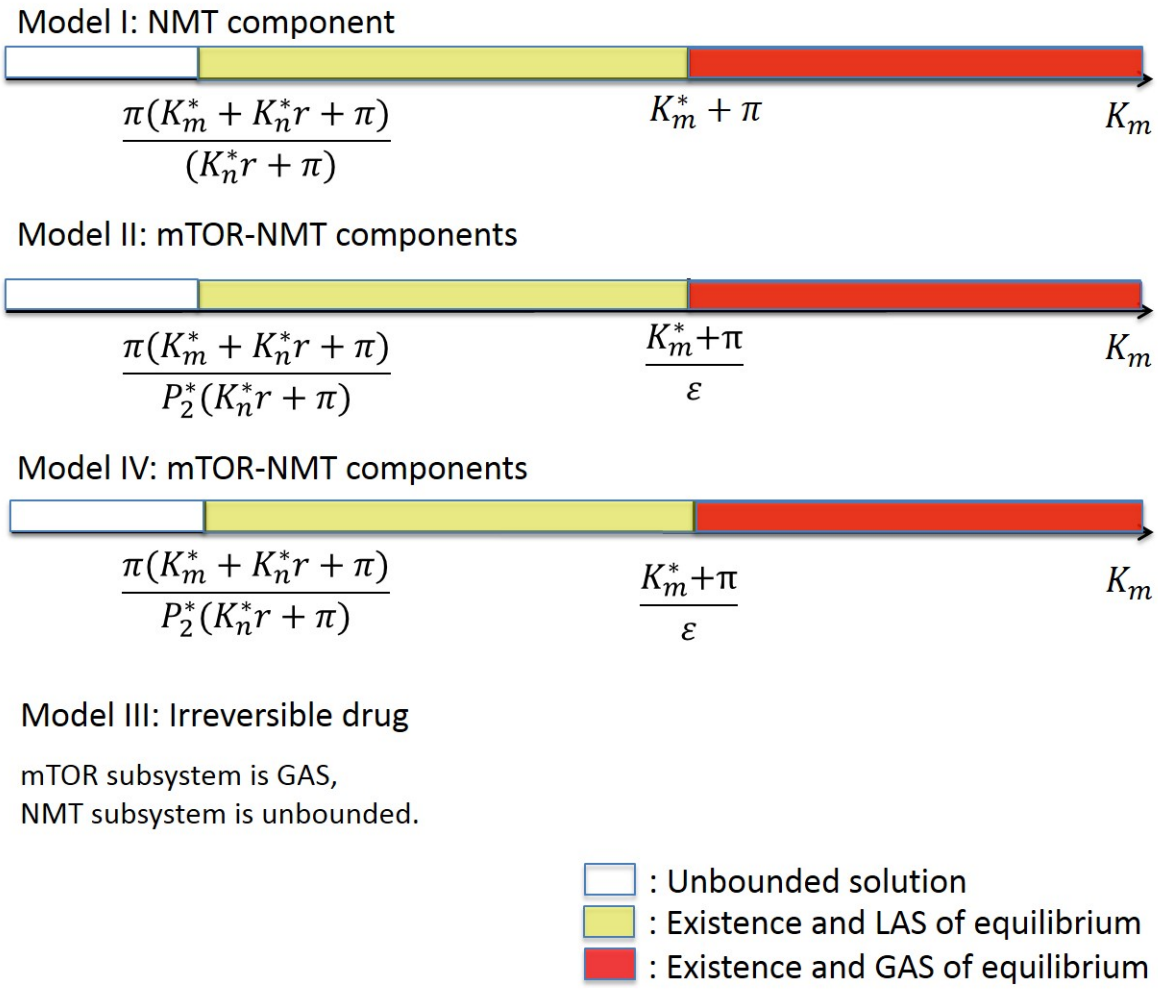

Chapter 5

Numerical analysis & results

5.1 Parameter Estimation

5.1.1 Data

Dr. Anuraag Shrivastav and Dr. Varma Shrivastav[1] provided the experimental data that are used for the calibration and validation of our mathematical models. The data represents the concentrations of total mTOR, pmTOR and NMT in cells treated or non-treated with the drug Rapamycin at 60 seconds, 300 seconds, 600 seconds and 1800 seconds. Recall that total mTOR refers to the sum of mTOR, Rapamycin-mTOR and pmTOR. Raw data from Dr. Shrivastav are shown in Table 5.1 and plotted in Figures 5.1– 5.3. The normalization of raw data is done by taking the data at a given time and dividing it by the data at 60 seconds.

Table 5.1: Raw data[2]. Units are listed in Table 3.2, these are concentration

Data	1 min	5 mins	10 mins	30 mins
total mTOR	8,431,024.00	8,551,756.00	7,905,224.00	6,393,388.00
pmTOR	8,479,170.07	7,021,670.96	6,516,744.89	4,299,069.68
NMT	350,262.92	1,442,335.56	2,660,528.56	3,122,983.96
total mTOR (no drug)	9,125,360,00	9,050,100.00	7,888,012.00	8,043,508.00
pmTOR (no drug)	8,831,683.41	7,458,227.31	9,080,854.17	8,211,956.25
NMT (no drug)	3,461,880.52	1,450,754.60	854,565.60	787,133.16

[1] Department of Biology, University of Winnipeg.
[2] Dr. Vasma Shrivastav et al unpublished data. 2015.

Figure 5.1: Experimental data without Rapamycin. Left column: (Raw data) concentrations of total mTOR, pmTOR and NMT. Right column: (Normalized data) total mTOR, pmTOR and NMT.

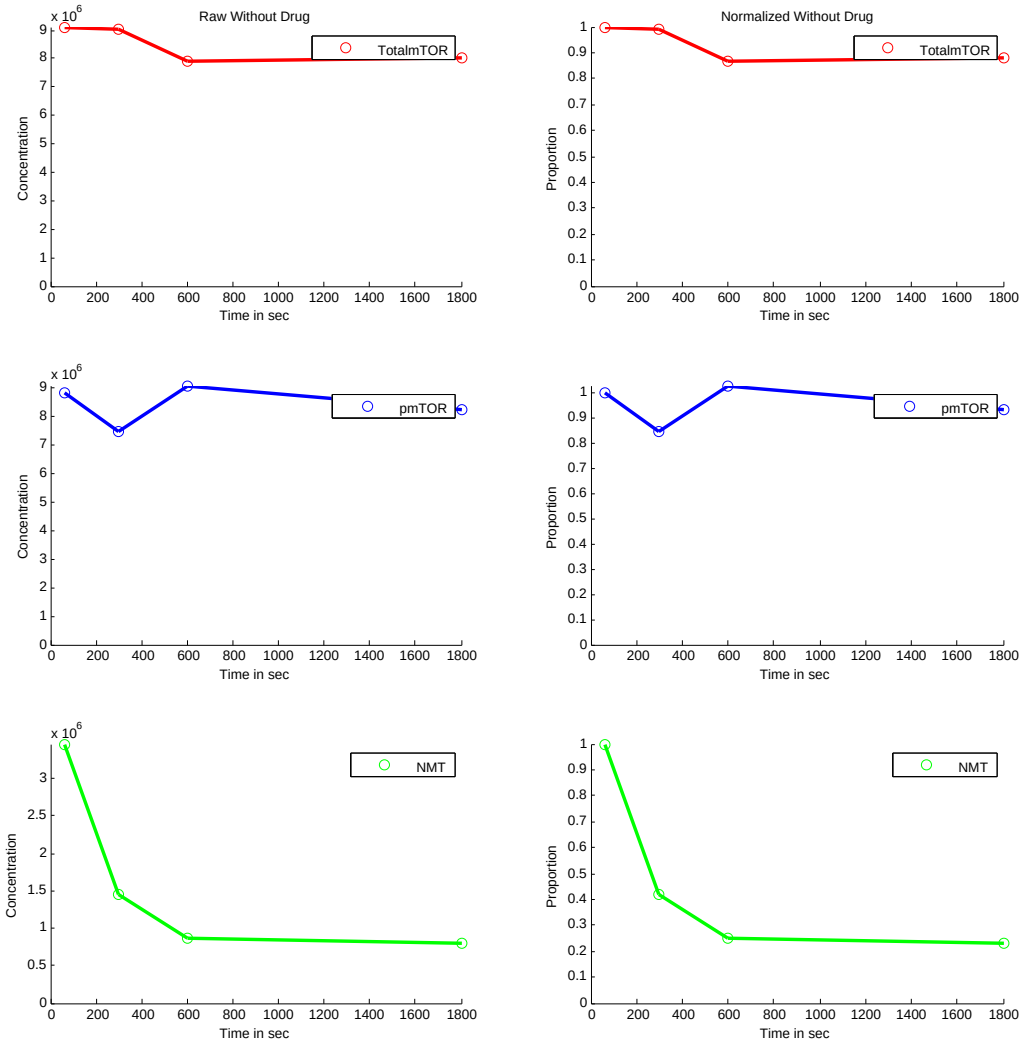

In absence of drug, Figure 5.1 depicts the fact that the concentrations of the total mTOR and pmTOR stay constant. However, the concentration of NMT decreases quickly from 60 seconds to 300 seconds and it stabilizes after 600 seconds.

Figure 5.2: Data with Rapamycin, Left column: (Raw data) concentrations of mTOR, pmTOR and NMT. Right column: (Normalized data) total mTOR, pmTOR and NMT.

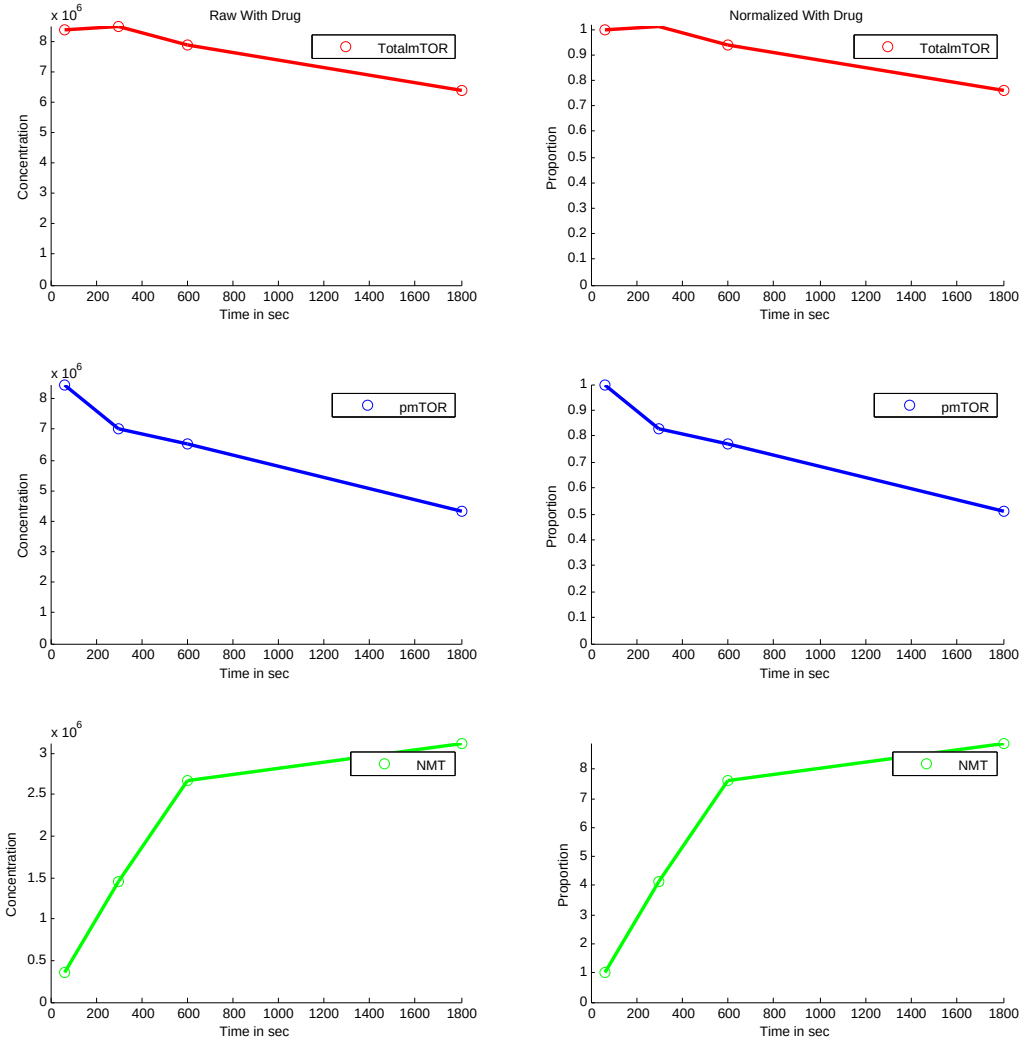

Under the effect of drug, the concentration of total mTOR stays constant, while the concentration of pmTOR decreases. Moreover, the concentration of NMT increase and then stabilize (Figure

5.2). In the presence of the drug, the concentration of NMT is increasing fast (Figure 5.2). This behaviour can be explained by the fact that the Rapamycin inhibits the phosphorylation of mTOR, which lowers the concentration of pmTOR and results in less phosphorylation of NMT, and an increase of the concentration of NMT.

Figure 5.3: Data with and without drug comparison, the dashed curves are the data without drug and the solid curves are the data with drug.

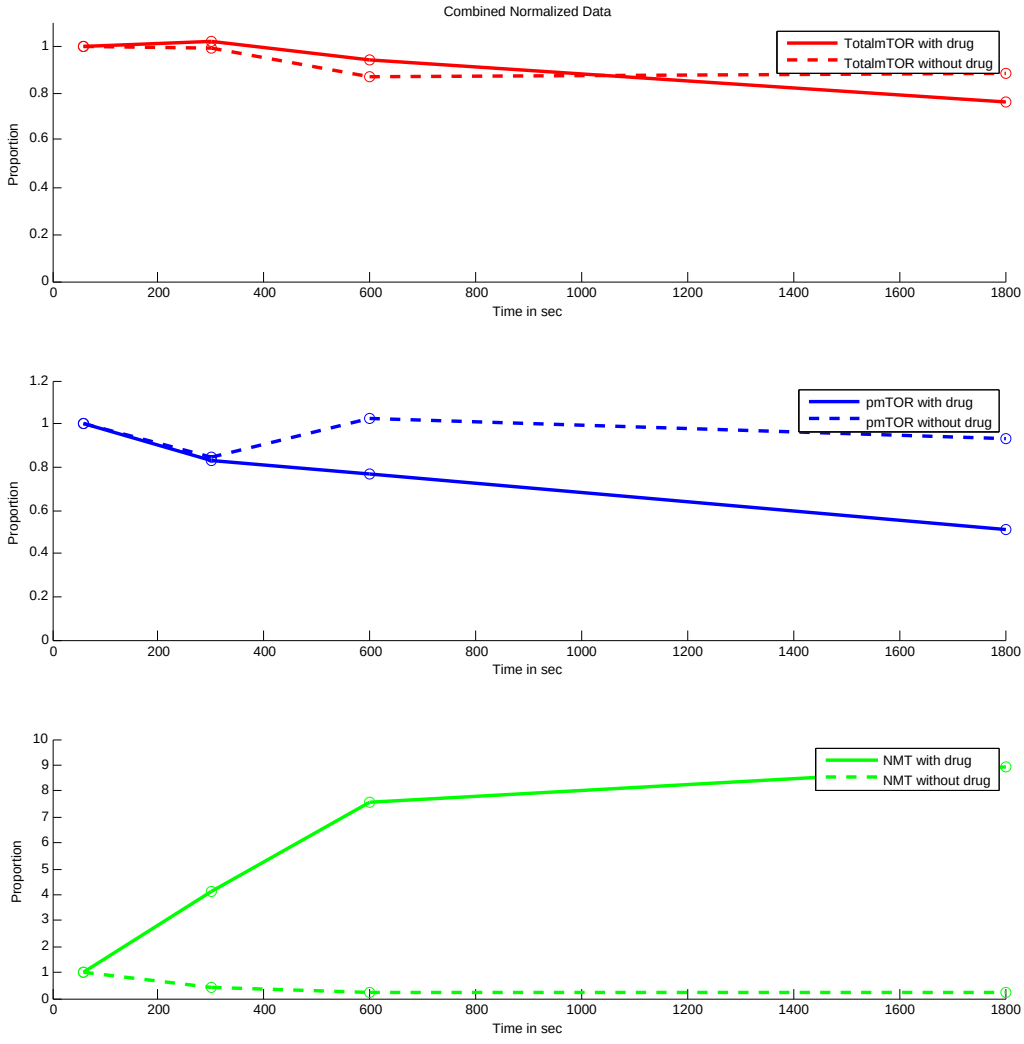

Figure 5.3 combines Figures 5.1 and 5.2 to highlight the effect of the drug. The concentration of pmTOR is decreasing with Rapamycin, while the concentration stays constant without it. In addition, the total mTOR molecules are conserved and concentration of total mTOR stays constant with or without Rapamycin. Moreover, under the drug effects, the concentration of NMT increases at the beginning and stabilizes at the end, while it decreases and stabilizes without the drug.

5.1.2 Parameter Values & Best Fit

Optimization method is applied to estimate the values of the parameter set for each model in order to obtain the best fit for the experimental data. The values of parameters P^* obtained by DE are presented in Table 5.2. Simulations of the model responses, using these parameter sets, are plotted in Figures 5.4 – 5.7.

Parameter values

Table 5.2: Best values of parameters. Assumptions of Model I (a)-Model IV (b) are presented in Table 3.1. Model-IanoD (Model-IbnoD) refers to Model I (a) (resp. Model I(b)) calibrated with no drug data. The last column presents the values of the cost function that is defined in the Equation (2.8).

	k1	r	$\tilde{K_m}$	K_m^+	K_m	K_m^*	k	cost
Model-IanoD	-	0.0676	-	-	0.0493	0.3269	-	0.0001
Model-IbnoD	-	0.0108	-	-	0.0089	-	-	1.9×10^{-7}
Model-Ia	-	0.0001	-	-	0.8322	0.3978	-	0.4386
Model-Ib	-	0.0108	-	-	0.4515	-	-	3.4355
Model-IIa	-	0.1046	0.1776	0.0533	0.0142	0.2504	-	0.0496
Model-IIb	-	0.0476	0.3557	0.1063	0.3025	-	-	0.0629
Model-IIIa	0.0099	0.0019	0.1231	0.0038	0.6439	0.2789	-	1.7784
Model-IIIb	0.0016	1.5099	0.0058	0.0048	1.5538	-	-	2.3723
Model-IVa	0.0203	0.0414	0.1146	0.0426	0.2953	0.0501	0.0507	0.6554
Model-IVb	0.0217	0.1218	0.5436	0.0471	0.3284	-	0.0055	0.7364

	Π	R	$\tilde{K_n}$	K_n^+	K_n	K_n^*	cost
Model-IanoD	0.0211	-	-	-	0.0508	4.8650	0.0001
Model-IbnoD	0.0019	-	-	-	0.6879	-	1.9×10^{-7}
Model-Ia	0.1122	-	-	-	49.5053	0.0278	0.4386
Model-I b	0.1370	-	-	-	211.1888	-	3.4355
Model-IIa	0.0039	-	20.0548	3.6884	0.2954	7.9222	0.0496
Model-IIb	0.5851	-	1.9313	31.1428	0.0091	-	0.0629
Model-IIIa	0.0995	24.9627	53.3736	146.1926	49.2085	0.1922	1.7784
Model-IIIb	0.2582	0.0081	32.6027	262.8448	943.2399	-	2.3723
Model-IVa	0.0377	16.2663	16.8634	3.1134	1.5272	25.2724	0.6554
Model-IVb	0.0337	7.6101	18.9901	3.0226	2.7272	-	0.7364

The parameter set P^* is defined in Equation (2.8) and values are given in Table 5.2. Depending on the models, the numbers and the definitions of parameter sets differs and are listed in Table 5.3.

Table 5.3: For each candidate model, the dimensions of the parameter set and the definitions of the components are given.

	Number of parameters	Definition of parameter set P
Model-IanoD	6	$P_1 = [r, K_m, K_m^*, \Pi, K_n, K_n^*]$
Model-IbnoD	4	$P_2 = [r, K_m, , \Pi, K_n]$
Model-Ia	6	$P_3 = [r, K_m, K_m^*, \Pi, K_n, K_n^*]$
Model-Ib	4	$P_4 = [r, K_m, , \Pi, K_n]$
Model-IIa	10	$P_5 = [r, \tilde{K_m}, K_m^+, K_m, K_m^*, \Pi, \tilde{K_n}, K_n^+, K_n, K_n^*]$
Model-IIb	8	$P_6 = [r, \tilde{K_m}, K_m^+, K_m, \Pi, \tilde{K_n}, K_n^+, K_n]$
Model-IIIa	12	$P_7 = [k_1, r, \tilde{K_m}, K_m^+, K_m, K_m^*, \Pi, R, \tilde{K_n}, K_n^+, K_n, K_n^*]$
Model-IIIb	10	$P_8 = [k_1, r, \tilde{K_m}, K_m^+, K_m, \Pi, R, \tilde{K_n}, K_n^+, K_n]$
Model-IVa	13	$P_9 = [k_1, r, \tilde{K_m}, K_m^+, K_m, K_m^*, k, \Pi, R, \tilde{K_n}, K_n^+, K_n, K_n^*]$
Model-IVb	11	$P_{10} = [k_1, r, \tilde{K_m}, K_m^+, K_m, k, \Pi, R, \tilde{K_n}, K_n^+, K_n]$

Best Fit

Figures 5.4 - 5.7 show the time evolution of the concentrations normalized to the initial condition for the total mTOR, pmTOR and NMT. In these figures, circles are the normalized experimental data and the curves represent the concentrations of model responses for the given model. Specifically, the total mTOR is plotted in red, pmTOR is plotted in blue and NMT is plotted in green.

In Figure 5.4, the upper graphs show that for Model I, the concentration of NMT decreases from 60 seconds to 600 seconds and then stabilize at the end without treatment. However, in the presence of drug, the lower graphs depict a quick increase of the concentration of NMT at the beginning and a stabilization the end. As we can see in the graphs, the simulated responses show a good fit to the experimental data. Moreover, the value of cost function in Table 5.2 for Model I in Version (a) without drug is smaller than its cost function values with drug (e.g. the value of cost function for Model I in Version (a) without drug is 0.0001, and the value of cost function for Model I in Version (a) with drug is 0.4386), and also the model responses in Figure 5.4 show that Model I has a better performance to fit the experimental data without treatment (upper graphs). However, we cannot determine whether Version (a) or Version (b) of Model I is more likely to occur, since Model I in Version (b) fits better data with no treatment and Version (a) performs better to represent experimental data with treatment. Therefore, we must consider the complexity

Figure 5.4: Best Fit for Model I-NMT component. Left column: Version (a). Right column: Version (b). Upper: Without drug. Lower: With drug.

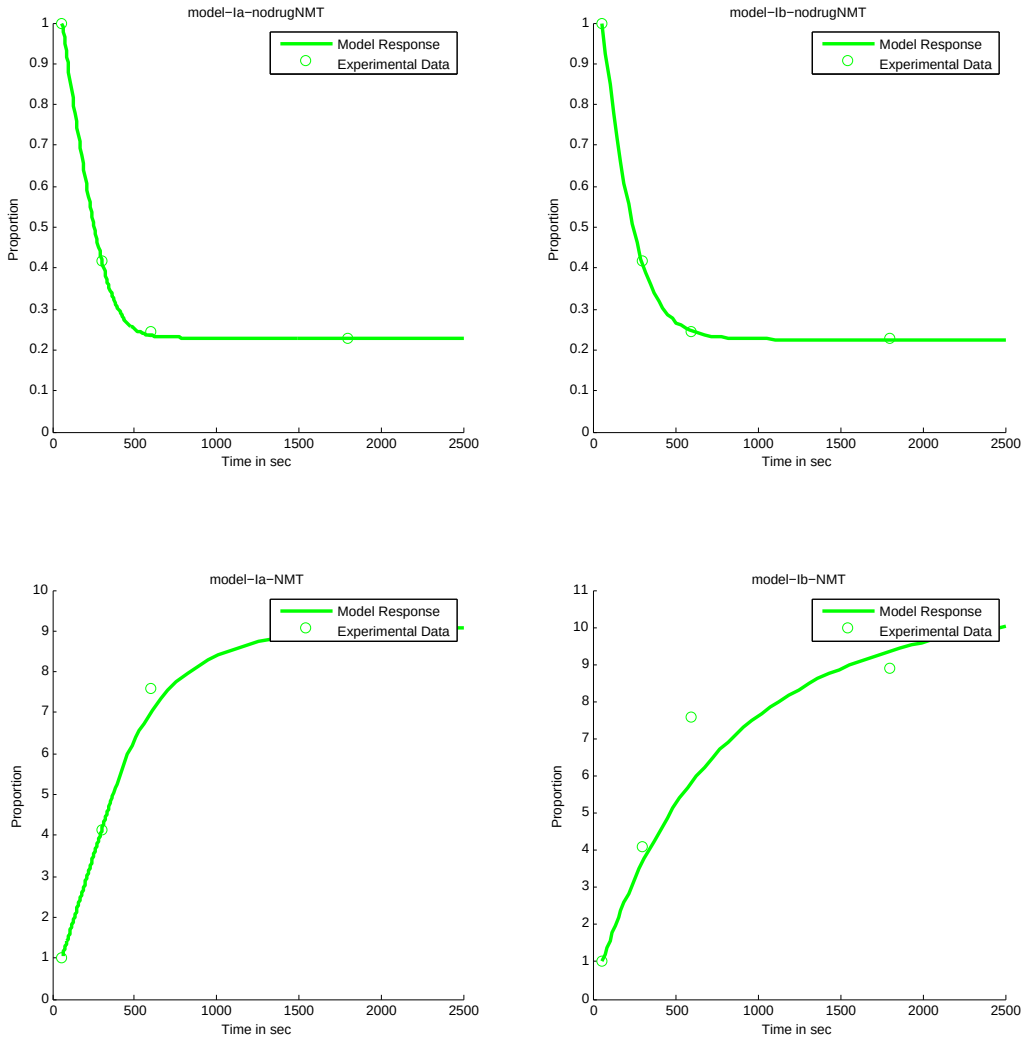

of models to determine the most suitable version. To achieve this, model selection is used in Section 5.2.

Models II–IV consider the both mTOR-NMT components, and the concentrations of total mTOR are always conserved as proved in the mathematical analysis in Chapter 4. The conservation of the total mTOR was introduced in models to mimic the experimental data (see Figures 5.1– 5.3).

As an illustration, Figures 5.4 - 5.7 show that the sum of the model responses related to mTOR always stay constant.

Figure 5.5: Best Fit for Model II, mTOR-NMT components with no treatment. Left column: Version (a). Right column: Version (b).

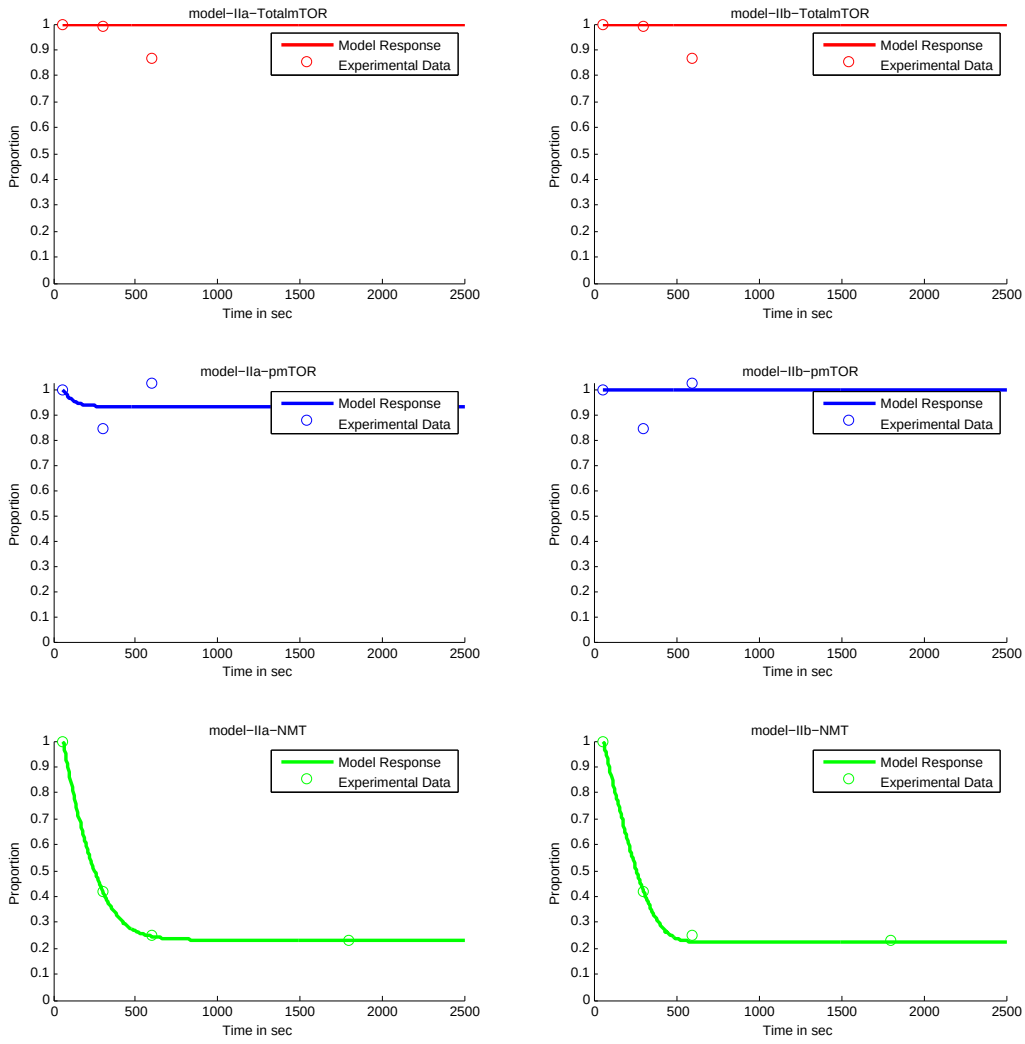

In Model II, Figure 5.5 depicts that in Version (a), the concentration of pmTOR begins by decreasing and stabilizes at the end, while it seems to stay constant in Version (b). Furthermore, the

concentration of NMT starts with a quick decrease and stabilizes at the value of 0.2 to the end. The graphs of the concentration of NMT in Version (a) and Version (b) are very similar.

Figure 5.6: Best Fit for Model III, mTOR-NMT components and irreversible drug reaction. Left column: Version (a). Right column: Version (b).

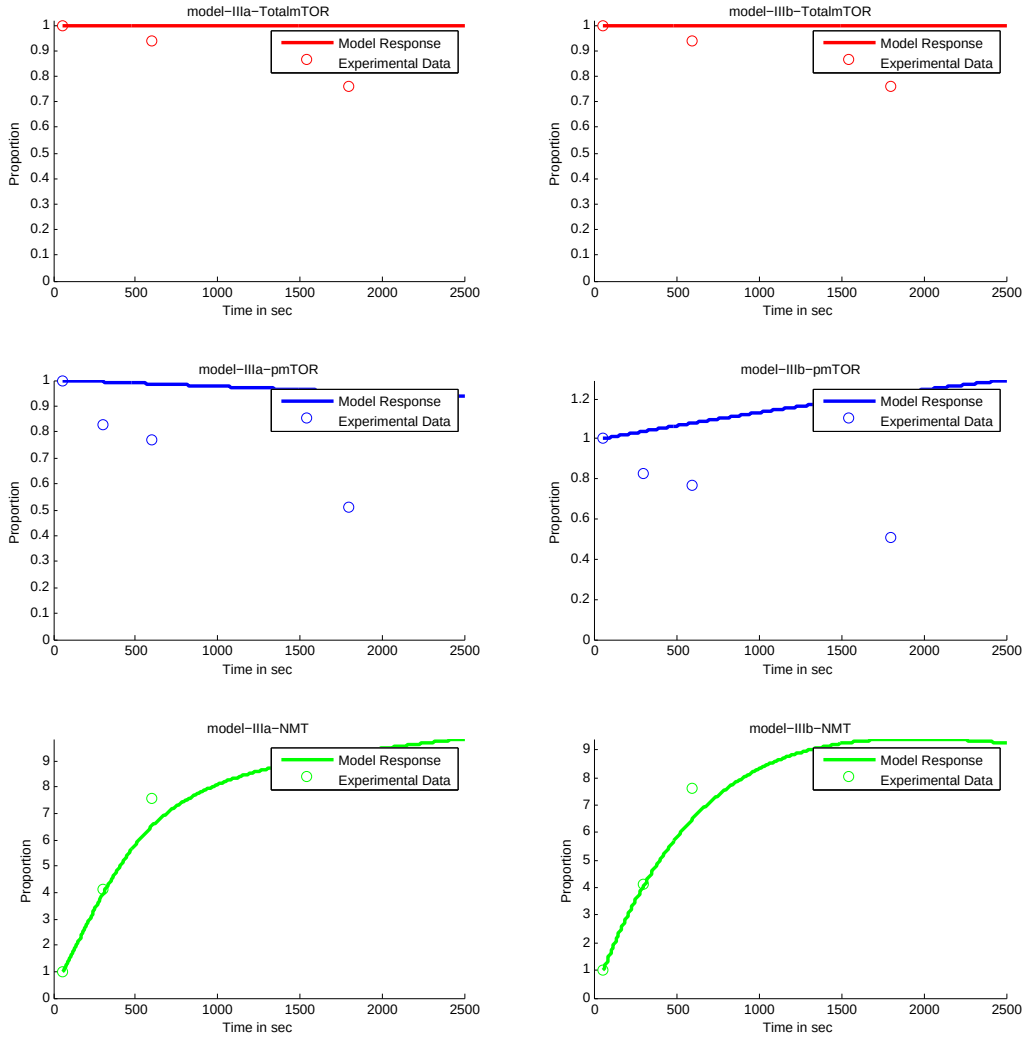

Figure 5.6 represents the different behaviour of the model responses of pmTOR in Version (a) and Version (b) for Model III. Both do not fit the experimental data well. The concentration of pmTOR in Version (a) is decreasing, while it is increasing slightly in Version (b). Furthermore,

model responses for NMT are slowly increasing in both versions similarly to experimental data. For Model III, pmTOR transient responses differ depending on the version of the model whereas their asymptotic responses match as shown in Figure 5.8. Theorem (4.7) states that in Model III, pmTOR component of equilibrium stabilizes at 0 and the NMT subsystem is unbounded. This statement is illustrated in Figure 5.8. As shown in Figure 5.8, in Version (a) of Model III, the model response for pmTOR decreases and then stabilizes at 0 to the end. However, in Version (b), it increases quickly at the beginning and then decreases to 0. Simultaneously, in Version (a) of this model, the concentration of NMT increases to the end, while in Version (b) it increases, decreases, and finally increases again.

In Figure 5.7, both Version (a) and (b) give the same transient behaviour of Model IV. The model responses of pmTOR decrease quickly at the beginning and become stable after. Simultaneously, the concentration of NMT is increasing and then stabilizes at the end.
In summary, Figures 5.4 - 5.7 show that model responses of NMT represents the experimental data (with or without drug), whereas the pmTOR model responses fit poorly.

In Chapter 4, mathematical analyses have been carried out to find the mathematical conditions that determine the asymptotic behaviour of models. All the mathematical conditions are related to the parameters. Here, the best parameter sets are obtained by fitting model responses to experimental data. Now, for each model, we check if the best values of the parameter set P^* given in Table 5.2 satisfy the mathematical conditions presented in Table 4.1. The mathematical conditions for the global asymptotic stability of the equilibrium are first investigated and then those for the local asymptotic stability. The results that fail to mathematical conditions are not presented, only positive results are shown. Moreover, in Model II and Model IV, the global asymptotic behaviour depends on the minimum values of pmTOR ϵ. We can see in Figures 5.5 and 5.7, the values of ϵ are equal to the equilibrium values in these simulations.

1. In Version (a) of Model I, Theorem 4.3 states that there exists a unique LAS equilibrium when $K_m > \frac{\Pi K_m^*}{\Pi + K_n^* r} + \Pi$. The best values of parameter, P_1 given in Table 5.2 are obtained by fitting Model I (a) to the no drug data. The best parameter set P_1 from Table 5.3 satisfies the condition of Theorem 4.3.

$$(0.0493) \qquad K_m > \frac{\Pi K_m^*}{\Pi + K_n^* r} + \Pi \qquad (0.0225 + 0.0211 = 0.0436).$$

Figure 5.7: Best fit for model IV, mTOR-NMT components and reversible drug reaction. Left column: Version (a). Right column: Version (b).

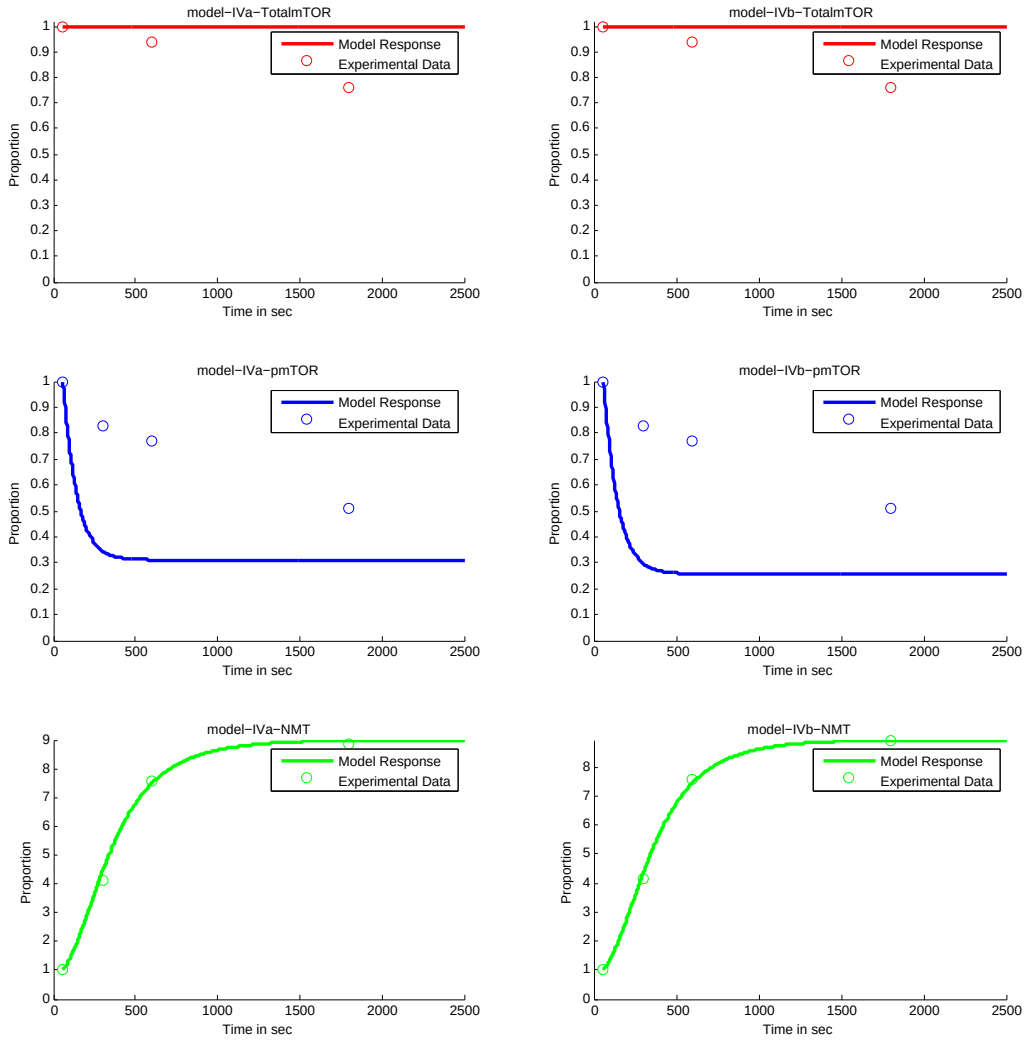

2. In Version (b) of Model I, Theorem 4.3 states that there exists a unique LAS equilibrium when $K_m > \Pi$. The best values of parameter, P_2 given in Table 5.2 are obtained by fitting Model I (b) to the no drug data. The best parameter set P_2 from Table 5.3 satisfies the condition of Theorem 4.3.

$$(0.0089) \qquad K_m > \Pi \qquad (0.0019).$$

3. In Version (a) of Model I, Theorem 4.4 states that there exists a unique GAS equilibrium when $K_m > K_m^* + \Pi$. The best values of parameter, P_3 given in Table 5.2 are obtained by fitting Model I (a) to the drug data. The best parameter set P_3 from Table 5.3 satisfies the condition of Theorem 4.4.

$$(0.8322) \qquad K_m > K_m^* + \Pi \qquad (0.3978 + 0.1122 = 0.51).$$

4. In Version (b) of Model I, Theorem 4.4 states that there exists a unique GAS equilibrium when $K_m > \Pi$. The best values of parameter, P_4 given in Table 5.2 are obtained by fitting Model I (b) to the drug data. The best parameter set P_4 from Table 5.3 satisfies the condition of Theorem 4.4.

$$(0.4515) \qquad K_m > \Pi \qquad (0.1370).$$

5. In Version (a) of Model II, Theorem 4.5 states that there exists a unique LAS equilibrium when $P_2^* > \frac{D}{K_m}$. The best values of parameter, P_5 given in Table 5.2 are obtained by fitting Model II (a) to the no drug data. The best parameter set P_5 from Table 5.3 satisfies the condition of Theorem 4.5.

$$(1.2992) \qquad P_2^* > \frac{D}{K_m} \qquad (0.0051).$$

6. In Version (b) of Model II, Theorem 4.6 states that there exists a unique GAS equilibrium when $\epsilon = P_2^* > \frac{\Pi}{K_m}$. The best values of parameter, P_6 given in Table 5.2 are obtained by fitting Model II (b) to the no drug data. The best parameter set P_6 from Table 5.3 satisfies the condition of Theorem 4.6.

$$(2.9488) \qquad \epsilon = P_2^* > \frac{\Pi}{K_m} \qquad (1.9342).$$

7. Theorem 4.14 for Model III for both Version (a) and (b) indicates that the equilibrium point of the mTOR subsystem is GAS and the NMT subsystem is unbounded without any conditions. At long run, the model responses illustrate the conclusions from Theorem 4.14 as shown in Figure 5.8.

8. In Version (a) of Model IV, Theorem 4.9 states that there exists a unique GAS equilibrium when $\epsilon = P_2^* > \frac{K_m^* + \Pi}{K_m}$. The best values of parameter, P_9 given in Table 5.2 are obtained by

fitting Model IV (a) to the drug data. The best parameter set P_9 from Table 5.3 satisfies the condition of Theorem 4.9.

$$(0.6566) \qquad \epsilon = P_2^* > \frac{K_m^* + \Pi}{K_m} \qquad (0.2973).$$

9. In Version (b) of Model IV, Theorem 4.9 states that there exists a unique GAS equilibrium when $\epsilon = P_2^* > \frac{\Pi}{K_m}$. The best values of parameter, P_{10} given in Table 5.2 are obtained by fitting Model IV (b) to the drug data. The best parameter set P_{10} from Table 5.3 satisfies the condition of Theorem 4.9.

$$(0.5818) \qquad \epsilon = P_2^* > \frac{\Pi}{K_m} \qquad (0.1026).$$

In summary, it is interesting to notice that the parameter values that best represent the data satisfy conditions that have systems in a stable regime. The best parameter values satisfy the mathematical conditions for the local asymptotic stability of the equilibrium of Model I considered without Rapamycin and Model II in Version (a). Furthermore, the mathematical conditions for the global asymptotic stability are satisfied for Model I with Rapamycin, Model II in Version (b), and Model IV.

5.2 Model Selection

Model selection is presented in Chapter 2, and is applied here to determine the "best" model among our candidates. Moreover, specific questions can be answered by using Akaike information weight.

Questions:

1. Is the drug reaction more likely to be reversible or irreversible?
2. Is the dephosphorylation of pNMT more likely to occur or not?
3. Do the reactions in mTOR subsystem and NMT subsystem have the same time scale under the non-treatment?

To answer the above questions, we need recall the best parameter values from Table 5.2, cost function (2.8) and its value from Table 5.2, as well as the AIC Equation (2.9). The number of parameters

Q is given in the 2nd-column in Table 5.3. RSS is the values of cost function given in the last column of Table 5.2. AICc is the value of Akaike information criterion. Δ is calculated using Equation (2.9). W is the Akaike weight calculated via Equation (2.10). SC is the value of Schwarz criterion.

Question 1. Is the drug reaction more likely to be reversible or irreversible?

Table 5.4: Model III vs Model IV.

	Q	RSS	AICc	Δ	W
Model-IIIa	12	1.7784	3.0897	12.5808	0.0014
Model-IIIb	10	2.3723	2.5475	12.0386	0.0019
Model-IVa	13	0.6544	-6.9079	2.5832	0.2149
Model-IVb	11	0.7364	-9.4911	0.0000	0.7818

Data with drug are used. Question 1 can be answered by comparing Model III against Model IV. In Table 5.4, the sum of Akaike weights for Model IV is (0.2149+0.7818)=0.9967, and the sum of Akaike weights for Model III is (0.0014+0.0019)=0.0033. This indicates that Model IV is 0.9967/0.0033 =302 times more likely to occur than Model III, which answers the above question: the drug reaction is more likely to be reversible.

Question 2. Is the dephosphorylation of pNMT more likely to occur?

Since our data is obtained from two types of experiments, experiments with and without Rapamycin can be subdivided into question 2a and question 2b. For question 2a we consider the data with Rapamycin, while for question 2b, data without it is used.

Question 2a. In the presence of treatment, is the dephosphorylation of pNMT more likely to occur?

Table 5.5: Model Version (a) vs Model Version (b).

	Q	RSS	AICc	Δ	W
Model-IIIa	12	1.7784	3.0897	28.7995	5.6×10^{-7}
Model-IIIb	10	2.3723	2.5475	28.2573	7.3×10^{-7}
Model-IVa	13	0.6544	-6.9079	18.8019	8.3×10^{-5}
Model-IVb	11	0.7364	-9.4911	16.2187	0.0003
Model-Ia	6	0.4386	-25.7098	0.0000	0.9996
Model-Ib	4	3.4355	-5.0091	20.7007	3.2×10^{-5}

To answer the question 2a, we consider all models (Model III and IV) with treatment of the group and Model I evaluated with parameter values estimated using with drug data. In Table 5.5, the sum of Akaike weights for the models in Version (a) is (5.6×10^{-7}+8.3×10^{-5}+0.9996)= 0.9997, and

the sum of Akaike weights for the models in Version (b) is (7.3×10^{-7}+0.0003+3.2×10^{-5})= 0.0003. The dephosphorylation of pNMT reactions are (0.9997/0.0003=)3332 times more likely to occur under the effect of drug. Moreover, for each model in Table 5.5, the Akaike weights of Version (a) and (b) can be compared. More specifically, the Akaike weight of Model-IV (b)/Model-IV (a) which is (0.0003/8.3×10^{-5})=3.6145, indicates that the reaction without dephosphorylation of pNMT is 3.6145 times more likely to occur in Model IV. Additionally, a similar calculation can be done for Model III and Model I. In Model III, the reactions without dephosphorylation of pNMT is $7.3\times10^{-7}/5.6\times10^{-7}$= 1.3036 times more likely to occur. In Model I, in the presence of Rapamycin, the reactions with dephosphorylation of pNMT is 0.9996/3.2×10^{-5} =31237.5 times more likely.

Question 2b. In the absence of treatment, is the dephosphorylation of pNMT more likely to occur or not?

Table 5.6: Model II vs Model I with no drug.

	Q	RSS	AICc	Δ	W
Model-IIa	10	0.0496	-43.8574	161.9625	6.8×10^{-36}
Model-IIb	8	0.0629	-45.0107	160.8092	1.2×10^{-35}
Model-Ianod	6	0.0001	-122.0226	83.7973	6.4×10^{-19}
Model-Ibnod	4	1.9×10^{-7}	-205.8199	0.0000	1.0000

All models without treatment are considered as a candidate group. As shown in Table 5.6, the value of Akaike weight for Model I (b) close to 1, which means in the case where drug is absent, the dephosphorylation of pNMT in reactions is more unlikely to occur.

Question 3. Do the reactions in mTOR subsystem and NMT subsystem have the same time scale in the absence of treatment?

Table 5.7: Model II vs Model I without the drug.

	Q	RSS	AICc	Δ	W
Model-IIa	10	0.0496	-43.8574	161.9625	6.8×10^{-36}
Model-IIb	8	0.0629	-45.0107	160.8092	1.2×10^{-35}
Model-Ianod	6	0.0001	-122.0226	83.7973	6.4×10^{-19}
Model-Ibnod	4	1.9×10^{-7}	-205.8199	0.0000	1.0000

From Table 5.7 which excludes Rapamycin, the sum of Akaike weights for Model I is greater than for Model II. This shows that in the absence of treatment, reactions in the mTOR subsystem are likely to be faster than reactions in the NMT subsystem.

Figure 5.8: Model III, mTOR-NMT components and reversible drug reaction in long run. Left column: Version (a). Right column: Version (b).

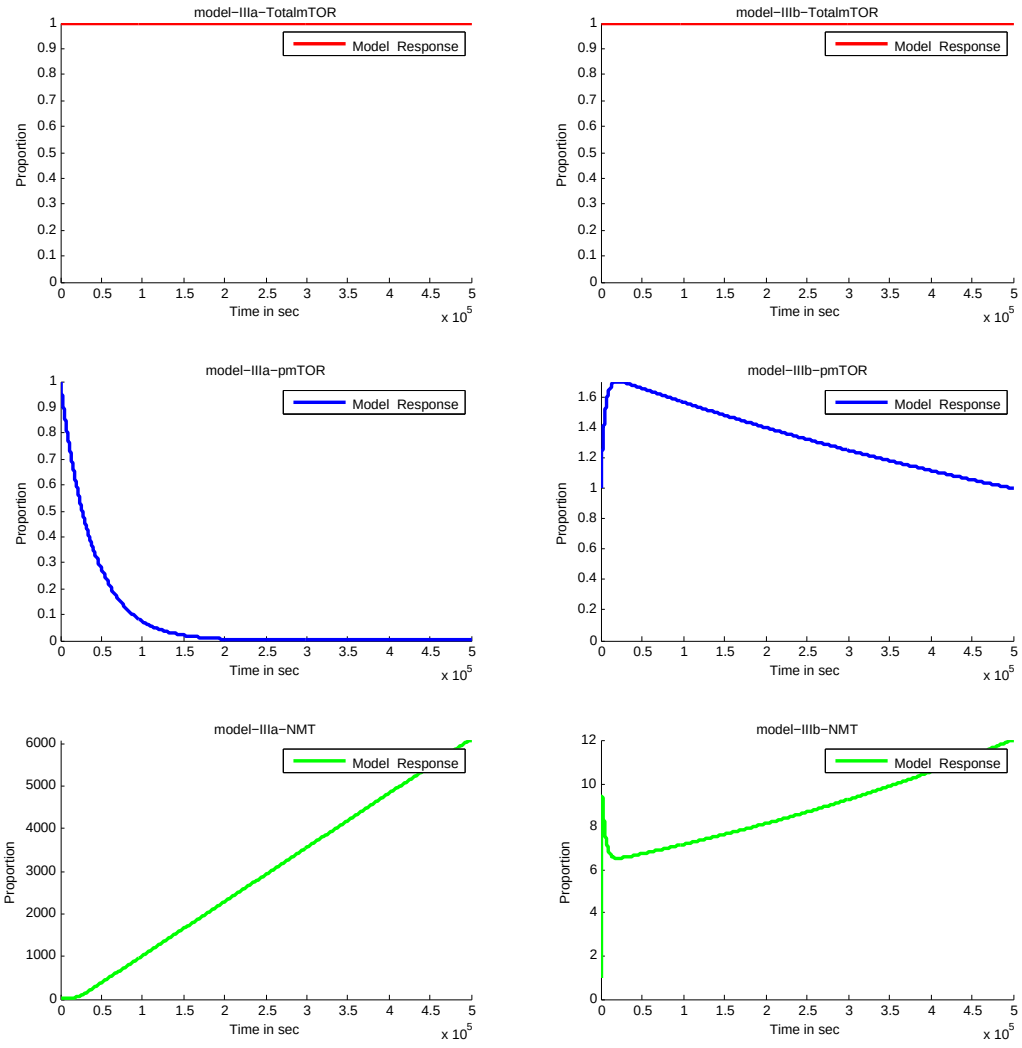

Chapter 6

Conclusion & Discussion

6.1 Summary

From the experimental data, we observe that in the presence of the drug, pmTOR decreases. Hence, less NMT will be converted into pNMT by pmTOR, resulting in an increase of NMT. Instead, due to the increase of pmTOR with absence of the drug, we observe the decrease of NMT (see in Figures 5.1-5.3).

Recall the question from Section 5.2: is the dephosphorylation of pNMT more likely to occur? As mentioned previously, depending on the data considered (with or without drug), the above question can be subdivided into question 2a and 2b. The answer to question 2a (related to the dynamics with drug) is that the dephosphorylation of pNMT is more likely to occur. Moreover, the answer to question 2b (related to the dynamics without drug) is that the dephosphorylation of pNMT is more unlikely to happen. Since the drug does not directly affect the dephosphorylation of pNMT, we expect that for all models considered with or without drug, the same conclusions should hold for the occurrence in the dephosphorylation of pNMT.

6.2 Discussion

Analyzing effects with the drug, we observe an increase of NMT, and the models selected include the dephosphorylation of pNMT. While no drug is involved, the decrease of NMT is observed and models without dephosphorylation of pNMT are preferred. As the dephosphorylation of pNMT contributes to the increase of NMT and the absence of dephosphorylation induces the decrease of NMT, the discrepancy in conclusions can be explained as a reinforcement of the dynamics of NMT.

However, we speculate the activity of one or more molecules controlling the dephosphorylation of pNMT could be directly or indirectly regulated by Rapamycin. This direction of research may be considered as very promising for breast cancer research.

Moreover, in this project, mathematical models were introduced to describe not only the targeted activities of mTOR- NMT signalling pathway, but also to analyze the response to treatment. Although the mathematical models and their numerical expectation have shown promising results, they can probably be improved. For example, if we increase the maximum running time, the estimation of parameters by a differential evolution algorithm may be improved to decrease the deviation between the model responses and the experimental data. Alternatively, since the convergence of solutions (parameter sets) in a differential evolution algorithm is not proven, the candidate solutions (parameter sets) may be stuck in a smaller interval or minima instead of the entire domain or minimum. Stronger results may be obtained from the differential evolution algorithm by re-running the algorithm. Additionally, if we increase the number of data points, the accuracy of the application of Akaike information criterion still can be improved.

Appendix A

MATLAB code for Differential Evolution algorithm

```
close all;
clear all;
%% mainloops
F = 0.2;          %differential weight
CR = .8;          %crossover constant
D  = 6;          %the number of parameters
NP = 20;          %population-the running times in one generation
maxgen = 1000;  %max generation
cost=1E6.*ones(NP*maxgen,1); %build initial cost funtion with random values
x1=zeros(NP,D);
trial=zeros(1,D);
x2=zeros(NP,D);

for i=1:1:NP    %build parameter searching space
   for j=1:1:3
        x1(i,k)=1E-3+(1E2-1E-3).*rand.*rand.*rand;
      end

end
```

```
for count=1:1:maxgen
    for i=1:1:NP
        a=floor(rand*(NP-1))+1;  %pick up three random numbers
        b=floor(rand*(NP-2))+2;
        c=floor(rand*(NP-3))+3;
        j=floor(rand*D)+1;       %pick up a random from [1,D]
        for k=1:1:D
            if(rand< CR || k==D)
                trial(j)=x1(c,j)+F.*(x1(a,j)-x1(b,j));  %the mutation happened
                if trial(j)<=0
                    trial(j)=x1(i,j);
                else
                    trial(j)=trial(j);
                end
            else
                 trial(j)=x1(i,j);
            end
        j=mod(j,D)+1;        %go to the next parameter in parameter space
        end
        score=costfunction(~,trial); %evaluate cost function
        if score<=cost(i+(count-1)*NP,1)
             x2(i,1:1:D)=trial(1:1:D);
             cost(i+1+(count-1)*NP,1)=score; %save the better cost function value
             trial0(1:1:D)=trial(1:1:D); % the best parameter is saved as trial 0
        else
                cost(i+1+(count-1)*NP,1)=cost(i+(count-1)*NP,1);

                x2(i,1:1:D)=x1(i,1:1:D);
```

```
        end
    end
 %update searching space x1 by getting better parameter space
        x1=x2;

end
```

Appendix B

Proof of Theorm 4.5

Proof. To find equilibia, we will need to solve the following 3-dimension system:

$$\frac{\tilde{K_m}(c-P_2)}{\tilde{K_n}+c-P_2} - \frac{K_m^+ P_2}{K_n^+ + P_2} = 0, \tag{B.1a}$$

$$-\frac{K_m P_2 P_3}{K_n + P_3} + \frac{K_m^* P_4}{K_n^* + P_4} + \Pi = 0, \tag{B.1b}$$

$$\frac{K_m P_2 P_3}{K_n + P_3} - \frac{K_m^* P_4}{K_n^* + P_4} - rP_4 = 0. \tag{B.1c}$$

From (B.1a), the following polynomial equation is obtained to find the equilibria of system:

$$f(P_2) = AP_2^2 + BP_2 + C = 0, \tag{B.2}$$

where

$$A = K_m^+ - \tilde{K_m},$$

$$B = -\tilde{K_m}K_n^+ - K_m^+\tilde{K_n} - (K_m^+ - \tilde{K_m})c,$$

$$C = \tilde{K_m}K_n^+ c.$$

We now solve polynomial Equation (B.2) for P_2. Note that $c > 0$.

I When $K_m^+ - \tilde{K_m} > 0$, then $A > 0$ and $B = -\tilde{K_m}K_n^+ - K_m^+\tilde{K_n} - (K_m^+ - \tilde{K_m})c < 0$.

To check the existence of a complex root pair, we need to determine the sign of $B^2 - 4AC$:

$$\begin{aligned}
B^2 - 4AC =& \tilde{K_m}^2 c^2 + K_m^{+2} c^2 + \tilde{K_m}^2 K_n^{+2} + K_m^{+2} \tilde{K_n}^2 + 2(\tilde{K_m}^2 K_n^+ c + K_m^{+2} \tilde{K_n} c + \tilde{K_m} K_m^+ \tilde{K_n} K_n^+) \\
& - 2(\tilde{K_m} K_m^+ c^2 + \tilde{K_m} \tilde{K_n} K_m^+ c + \tilde{K_m} K_m^+ K_n^+ c) \\
=& (\tilde{K_m} c - \tilde{K_n} K_m^+)^2 + (K_m^+ c - \tilde{K_m} K_n^+)^2 + (2\tilde{K_m}^2 K_n^+ c + 2K_m^{+2} \tilde{K_n} c - 2\tilde{K_m} K_m^+ c^2 + 2\tilde{K_m} K_m^+ \tilde{K_n} K_n^+) \\
=& (\tilde{K_m} c - \tilde{K_n} K_m^+)^2 + (K_m^+ c - \tilde{K_m} K_n^+)^2 - 2(\tilde{K_m} c - \tilde{K_n} K_m^+)(K_m^+ c - \tilde{K_m} K_n^+) + 4\tilde{K_m} K_m^+ \tilde{K_n} K_n^+ \\
=& [(\tilde{K_m} c - \tilde{K_n} K_m^+) - (K_m^+ c - \tilde{K_m} K_n^+)]^2 + 4\tilde{K_m} K_m^+ \tilde{K_n} K_n^+ \\
>& 0.
\end{aligned}$$

Thus, when $A = K_m^+ - \tilde{K_m} > 0$, $f(P_2)$ has only real roots.
The polynomial (B.2) has two sign changes in the coefficients (+ - +). By Descartes' rules of signs, we have 2 or 0 positive real roots. Considering the polynomial at $-P_2$, we obtain

$$f(-P_2) = AP_2^2 - BP_2 + C$$

that has no sign change (+ + +), which implies no negative real roots. Thus, when $A > 0$, $f(P_2)$ has 2 positive real roots which are such that

$$P_{2-}^* = \frac{-B - \sqrt{B^2 - 4AC}}{2A} < P_{2+}^* = \frac{-B + \sqrt{B^2 - 4AC}}{2A}.$$

However,

$$\begin{aligned}
f(c) &= (K_m^+ - \tilde{K_m}) c^2 - [(\tilde{K_m} K_n^+ + K_m^+ \tilde{K_n}) c + (K_m^+ - \tilde{K_m}) c^2] + \tilde{K_m} K_n^+ c \\
&= -(K_m^+ \tilde{K_n}) c < 0.
\end{aligned}$$

Since the leading coefficient of polynomial (B.2) is positive ($A > 0$), the graph of $f(P_2)$ is a concave up parabola that has 2 positive real roots P_{2-}^* and P_{2+}^* with $P_{2-}^* < P_{2+}^*$. As $f(c) < 0$, we can say $P_{2-}^* < c < P_{2+}^*$and $P_{2+}^* = \frac{-B+\sqrt{B^2-4AC}}{2A} \notin [0, c]$. Thus, the unique positive root of $f(P_2)$ in $[0, c]$ is $P_2^* = \frac{-B-\sqrt{-B^2-4AC}}{2A}$ when $A > 0$. The graph is shown in Figure B.1. **II** When $K_m^+ - \tilde{K_m} < 0$, then $A < 0$.
II a). If $\tilde{K_m} K_n^+ + K_m^+ \tilde{K_n} > -(K_m^+ - \tilde{K_m}) c$, we have $B > 0$.
The polynomial (B.2) has one sign change in the coefficients (- + +). By Descartes' rule of signs, the polynomial has exactly 1 positive real root.

Figure B.1: Graph of polynomial (B.2) in Model II (a) when $A > 0$.

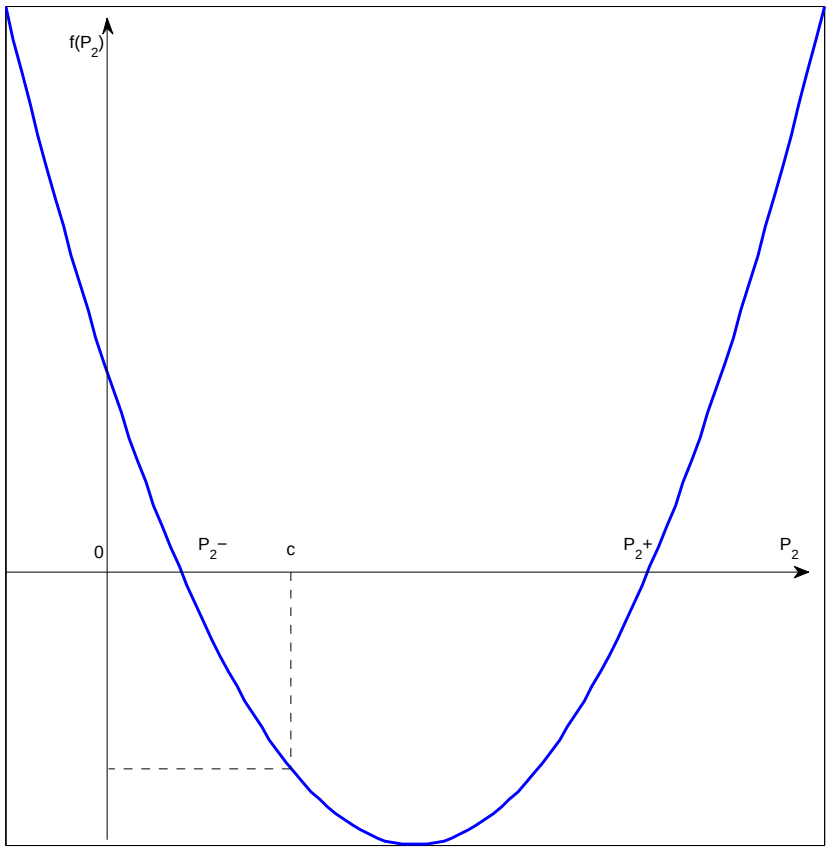

Hence, the greater value is chosen as the P_2-component of equilibrium between

$$\frac{-B+\sqrt{B^2-4AC}}{2A} \text{ and } \frac{-B-\sqrt{B^2-4AC}}{2A}.$$

Recalling that $B>0$ and $A<0$, then $-B<0$. We have $-B-\sqrt{B^2-4AC}<-B+\sqrt{B^2-4AC}$, and

$$P_{2+}^*=\frac{-B+\sqrt{B^2-4AC}}{2A}<P_{2-}^*=\frac{-B-\sqrt{B^2-4AC}}{2A}.$$

Therefore, the unique positive root is $P_{2-}^*=\frac{-B-\sqrt{B^2-4AC}}{2A}$. We will show that $P_2^*=\frac{-B-\sqrt{B^2-4AC}}{2A}\in[0,c]$ when $A<0$ and $B>0$ in the next part II b).

II b). If $\tilde{K_m}K_n^+ + K_m^+\tilde{K_n} < -(K_m^+ - \tilde{K_m})c$, then $B<0$.

The polynomial (B.2) has one sign change in the coefficients (- - +). By Descartes' rule of signs, the polynomial has exactly 1 positive real root. Hence, the greater value is chosen as the P_2-component of the equilibrium between

$$\frac{-B+\sqrt{B^2-4AC}}{2A} \text{ and } \frac{-B-\sqrt{B^2-4AC}}{2A}.$$

Recalling that $B<0$ and $A<0$, then $-B>0$. We have $-B-\sqrt{B^2-4AC}<-B+\sqrt{B^2-4AC}$ and

$$P_{2+}^*=\frac{-B+\sqrt{B^2-4AC}}{2A}<P_{2-}^*=\frac{-B-\sqrt{B^2-4AC}}{2A}.$$

Therefore, the unique positive root is $P_{2-}^*=\frac{-B-\sqrt{B^2-4AC}}{2A}$. When $A=K_m^+-\tilde{K_m}<0$, the leading coefficient of polynomial (B.2) is negative, then, the graph of $f(P_2)$ is a concave down parabola with one positive real root $P_{2-}^*=\frac{-B-\sqrt{B^2-4AC}}{2A}$ as shown in Figure B.2. As shown previously, $f(c)$ is always negative, then, we have $P_{2-}^*<c$. Thus, when $A<0$ and $B<0$, the P_2-component of the equilibrium is $P_2^*=\frac{-B-\sqrt{B^2-4AC}}{2A}\in[0,c]$. The same conclusion holds for part II a) when $A<0$ and $B>0$.

II c). If $\tilde{K_m}K_n^+ + K_m^+\tilde{K_n} = -(K_m^+ - \tilde{K_m})c$, then $B=0$.

The polynomial (B.2) reduces to

$$f(P_2)=AP_2^2+C.$$

When $A=K_m^+-\tilde{K_m}<0$, the leading coefficient of polynomial (B.2) is negative, thus, the graph of $f(P_2)$ is a concave down parabola with one positive real root $P_2^*=\frac{-B-\sqrt{B^2-4AC}}{2A}=\sqrt{-\frac{C}{A}}$ (similar

Figure B.2: Graph of polynomial (B.2) in Model II (a) when $A < 0$.

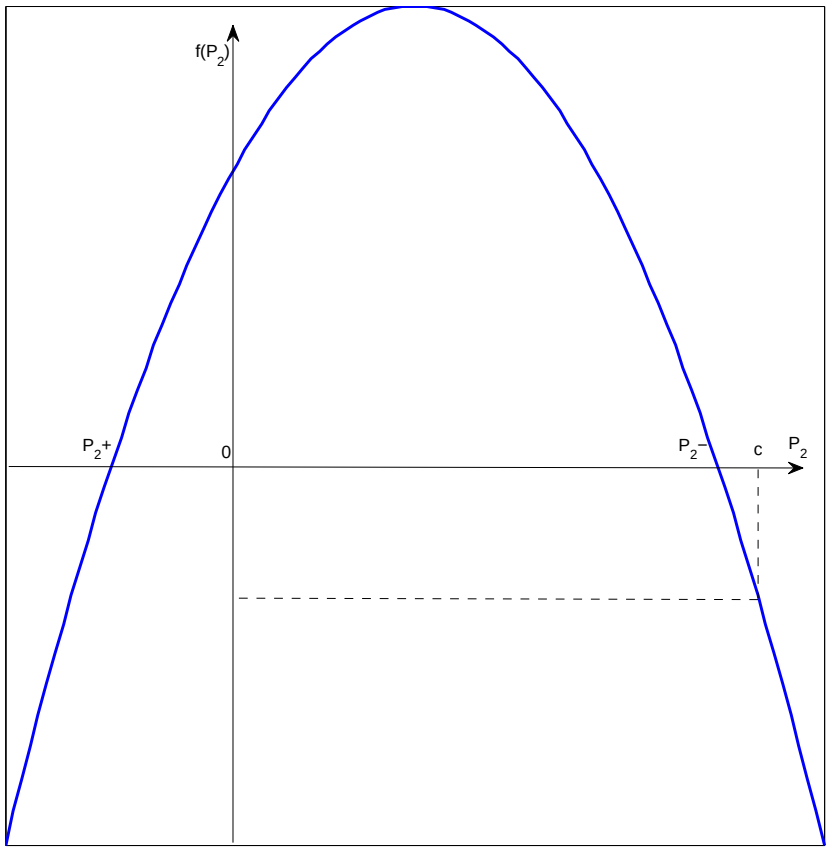

to Figure B.2). Since $f(c) < 0$, we have $P_{2-}^* < c$, thus, the P_2-component of the equilibrium is $P_2^* = \sqrt{-\frac{C}{A}} = \sqrt{\frac{\tilde{K_m} K_n^+ c}{-K_m^+ + \tilde{K_m}}} \in [0, c]$, when $A < 0$ and $B = 0$.
Therefore, the P_2-component of the equilibrium is $P_2^* = \frac{-B - \sqrt{B^2 - 4AC}}{2A} \in [0, c]$ when $A < 0$.

III When $K_m^+ = \tilde{K_m}$, then $A = 0$ and $B = -\tilde{K_m} K_n^+ - K_m^+ \tilde{K_n} < 0$. The polynomial can be rewritten as

$$f(P_2) = BP_2 + C = 0.$$

Thus, the graph of $f(P_2)$ is a straight line with a negative slope ($B < 0$). Then, the P_2-component of the equilibrium is $P_2^* = -\frac{C}{B} = \frac{\tilde{K_m} K_n^+ c}{\tilde{K_m} K_n^+ + K_m^+ \tilde{K_n}} \in [0, c]$ as $f(c) < 0$. The graph of f when $A = 0$ is shown in Figure B.3.

Figure B.3: Graph of polynomial (B.2) $f(P_2)$ in Model II (a) when $A = 0$.

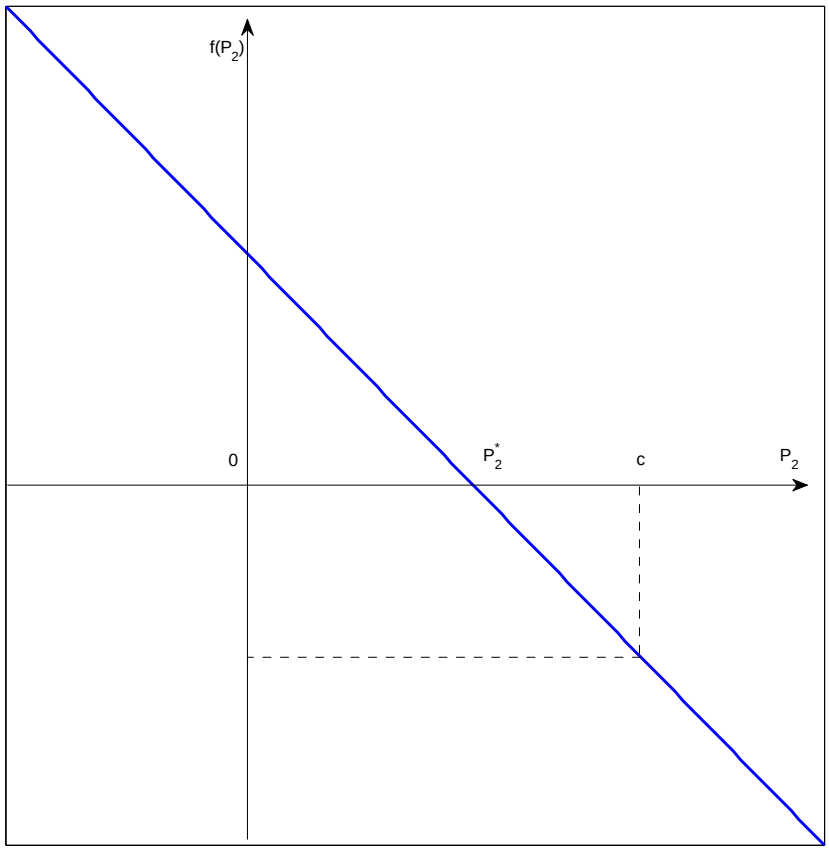

In summary, the polynomial function (B.2) has one positive real root

1. $P_2^* = \frac{-B-\sqrt{B^2-4AC}}{2A} \in [0, c]$, if $A = \tilde{K_m} - K_m^+ \neq 0$,
2. $P_2^* = -\frac{C}{B} \in [0, c]$, if $A = \tilde{K_m} - K_m^+ = 0$.

Adding (B.1b)-(B.1c), we obtain $P_4^* = \Pi/r$. Substituting P_2^* and P_4^* into Equation (B.1c), we get $\frac{K_m P_2^* P_3^*}{K_n+P_3^*} = \frac{K_m^* \Pi}{rK_n^*+\Pi} + \Pi$. We have

$$P_3^* = \frac{DK_n}{K_m P_2^* - D}, \tag{B.3}$$

where $D = \frac{K_m^* \Pi}{rK_n^*+\Pi} + \Pi$.

In order to make P_3^* positive, we require $K_m P_2^* - D > 0$.

Therefore, the unique positive equilibrium in System (4.7) is $(P_2^*, P_3^*, P_4^*) = (P_2^*, \frac{DK_n}{K_m P_2^* - D}, \frac{\Pi}{r})$ with the condition $P_2^* > D/K_m$.

The Jacobian matrix J_2 of System (4.7) takes the form:

$$J_2 = \begin{pmatrix} -\frac{\tilde{K_m}\tilde{K_n}}{(\tilde{K_n}+c-P_2)^2} - \frac{K_m^+ K_n^+}{(K_n^+ + P_2)^2} & 0 & 0 \\ -\frac{K_m P_3}{K_n+P_3} & -\frac{K_m K_n P_2}{(K_n+P_3)^2} & \frac{K_m^* K_n^*}{(K_n^*+P_4)^2} \\ \frac{K_m P_3}{K_n+P_3} & \frac{K_m K_n P_2}{(K_n+P_3)^2} & -\frac{K_m^* K_n^*}{(K_n^*+P_4)^2} - r \end{pmatrix}.$$

Note that $\tilde{K_n} + c - P_2 > 0$.

Hence, the eigenvalues of J_2 at an equilibrium point are,

$$\lambda_1 = -\frac{\tilde{K_m}\tilde{K_n}}{(\tilde{K_n} + c - P_2^*)^2} - \frac{K_m^+ K_n^+}{(K_n^+ + P_2^*)^2} < 0,$$

$$\lambda_2 = -\frac{1}{2}\left[\sqrt{(\frac{K_m K_n P_2^*}{(K_n+P_3^*)^2} + \frac{K_m^* K_n^*}{(K_n^*+P_4^*)^2} + r)^2 - 4\frac{K_m K_n P_2^*}{(K_n+P_3^*)^2} r} + (\frac{K_m K_n P_2^*}{(K_n+P_3^*)^2} + \frac{K_m^* K_n^*}{(K_n^*+P_4^*)^2} + r)\right],$$

then, we have $\lambda_2 < 0$ if $\lambda_2 \in \mathbb{R}$ or $Re(\lambda_2) < 0$ if $\lambda_2 \in \mathbb{C}$.

$$\lambda_3 = \frac{1}{2}\left[\sqrt{(\frac{K_m K_n P_2^*}{(K_n+P_3^*)^2} + \frac{K_m^* K_n^*}{(K_n^*+P_4^*)^2} + r)^2 - 4\frac{K_m K_n P_2^*}{(K_n+P_3^*)^2} r} - (\frac{K_m K_n P_2^*}{(K_n+P_3^*)^2} + \frac{K_m^* K_n^*}{(K_n^*+P_4^*)^2} + r)\right],$$

we conclude that $Re(\lambda_3) < 0$ if $\lambda_3 \in \mathbb{C}$.

If $\lambda_3 \in \mathbb{R}$, as $\sqrt{(\frac{K_m K_n P_2^*}{(K_n+P_3^*)^2} + \frac{K_m^* K_n^*}{(K_n^*+P_4^*)^2} + r)^2 - 4\frac{K_m K_n P_2^*}{(K_n+P_3^*)^2} r} < \sqrt{(\frac{K_m K_n P_2^*}{(K_n+P_3^*)^2} + \frac{K_m^* K_n^*}{(K_n^*+P_4^*)^2} + r)^2} = \frac{K_m K_n P_2^*}{(K_n+P_3^*)^2} + \frac{K_m^* K_n^*}{(K_n^*+P_4^*)^2} + r$, then, $\lambda_3 < 0$.

Therefore, all eigenvalues or their real part are negative for any equilibrium points. Then, any equilibria are LAS when they exist. □

Appendix C

Proof of Theorem 4.8

Proof. To find equilibria $(M^*, P_1^*, P_2^*, P_3^*, P_4^*)$ of System (4.16), the reduced System (4.17) at equilibrium point is considered.

$$-k_1RM^* - \frac{\tilde{K_m}M^*}{\tilde{K_n} + M^*} + \frac{K_m^+(c - M^* - P_1^*)}{K_n^+ + (c - M^* - P_1^*)} + kP_1^* = 0, \tag{C.1a}$$

$$k_1RM^* - kP_1^* = 0, \tag{C.1b}$$

$$-\frac{K_m(c - M^* - P_1^*)P_3^*}{K_n + P_3^*} + \frac{K_m^*P_4^*}{K_n^* + P_4^*} + \Pi = 0, \tag{C.1c}$$

$$\frac{K_m(c - M^* - P_1^*)P_3^*}{K_n + P_3^*} - \frac{K_m^*P_4^*}{K_n^* + P_4^*} - rP_4^* = 0, \tag{C.1d}$$

Note that $P_2^* = c - M^* - P_1^*$. Substituting (C.1b) into (C.1a), we have:

$$\frac{\tilde{K_m}M^*}{\tilde{K_n} + M^*} = \frac{K_m^+c - (K_m^+ + nK_m^+)M^*}{K_n^+ + c - (1+n)M^*}, \quad \text{with } n = \frac{k_1R}{k}.$$

Hence, the following polynomial is obtained to find the equilibrium point:

$$f(M) = AM^2 + BM + C = 0, \tag{C.2}$$

where

$$\begin{aligned} A &= (\tilde{K_m} - K_m^+)(1+n), \\ B &= -(\tilde{K_m} - K_m^+)c - \tilde{K_m}K_n^+ - (K_m^+ + nK_m^+)\tilde{K_n}, \\ C &= K_m^+\tilde{K_n}c > 0. \end{aligned} \tag{C.3}$$

The M-component of equilibria are the positive real roots of $f(M)$ taking the form:

$$M^* = \frac{-B \pm \sqrt{B^2 - 4AC}}{2A}.$$

Now, we investigate the number of positive real roots of $f(M)$.

I When $\tilde{K_m} - K_m^+ > 0$ then $A > 0$ and $B < 0$.

The polynomial Equation (C.2) has two sign changes in the coefficients (+-+). By Descartes' rule of signs, the polynomial has 2 or 0 positive real roots.

Considering the polynomial at $-M$, we obtain a second polynomial,

$$f(-M) = AM^2 - BM + C,$$

that has no sign change (+++), therefore, f has no negative real root. Checking the existence of a complex root pair, we compute

$$\begin{aligned}
B^2 - 4AC =& (\tilde{K_m} - K_m^+)^2 c^2 + (\tilde{K_m} K_n^+)^2 + (\tilde{K_n} K_m^+)^2 (1+n)^2 + 2(\tilde{K_m} - K_m^+) c (\tilde{K_n} K_m^+)(1+n) \\
&+ 2(\tilde{K_n} K_m^+) \tilde{K_m} K_n^+ (1+n) + 2(\tilde{K_m} - K_m^+) c \tilde{K_m} K_n^+ - 4(\tilde{K_m} - K_m^+) c (\tilde{K_n} K_m^+)(1+n) \\
=& (\tilde{K_m} - K_m^+)^2 c^2 + (\tilde{K_m} K_n^+)^2 + (\tilde{K_n} K_m^+)^2 (1+n)^2 - 2(\tilde{K_m} - K_m^+) c (\tilde{K_n} K_m^+)(1+n) \\
&+ 2(\tilde{K_n} K_m^+) \tilde{K_m} K_n^+ (1+n) + 2(\tilde{K_m} - K_m^+) c \tilde{K_m} K_n^+ \\
=& [(\tilde{K_m} - K_m^+) c + (\tilde{K_m} K_n^+) - (\tilde{K_n} K_m^+)(1+n)]^2 + 4(\tilde{K_n} K_m^+) \tilde{K_m} K_n^+ (1+n) \\
>& 0.
\end{aligned}$$

Hence, when $\tilde{K_m} - K_m^+ > 0$, $f(M)$ has 2 positive real roots.

II When $\tilde{K_m} - K_m^+ < 0$ then $A < 0$.

II a). If $-(\tilde{K_m} - K_m^+)c > \tilde{K_m} K_n^+ + (K_m^+ + nK_m^+)\tilde{K_n}$ then $B > 0$.

The polynomial (C.2) has one sign change in the coefficients (- ++). By Descartes' rule of signs, the polynomial has exactly 1 positive real root. Hence, the greater value is chosen between

$$\frac{-B + \sqrt{B^2 - 4AC}}{2A} \quad \text{and} \quad \frac{-B - \sqrt{B^2 - 4AC}}{2A}$$

as the M-component of the equilibrium.

Recalling that $B > 0$ and $A < 0$; thus, $-B < 0,$ we have $-B - \sqrt{B^2 - 4AC} < -B + \sqrt{B^2 - 4AC}$ and

$$M_1 = \frac{-B + \sqrt{B^2 - 4AC}}{2A} < M_2 = \frac{-B - \sqrt{B^2 - 4AC}}{2A}.$$

Therefore, the M-component of the equilibrium is $M^* = \frac{-B-\sqrt{B^2-4AC}}{2A}$ when $A = \tilde{K_m} - K_m^+ < 0$ and $B = -(\tilde{K_m} - K_m^+)c - \tilde{K_m}K_n^+ - (K_m^+ + nK_m^+)\tilde{K_n} > 0$.

II b). If $-(\tilde{K_m} - K_m^+)c < \tilde{K_m}K_n^+ + (K_m^+ + nK_m^+)\tilde{K_n}$ then $B < 0$.

The polynomial (C.2) has one sign change in the coefficients (- -+). By Descartes' rule of signs, the polynomial has exactly 1 positive real root. Hence, the greater value will be chosen between

$$\frac{-B + \sqrt{B^2 - 4AC}}{2A} \quad \text{and} \quad \frac{-B - \sqrt{B^2 - 4AC}}{2A}$$

as the M-component of the equilibrium.

Recalling that $B < 0$ and $A < 0$, then $-B > 0$. We will have $-B - \sqrt{B^2 - 4AC} < -B + \sqrt{B^2 - 4AC}$ and

$$\frac{-B + \sqrt{B^2 - 4AC}}{2A} < \frac{-B - \sqrt{B^2 - 4AC}}{2A}.$$

Therefore, under the above conditions, the M-component of the equilibrium is $M^* = \frac{-B-\sqrt{B^2-4AC}}{2A}$ when $A = \tilde{K_m} - K_m^+ < 0$ and $B = -(\tilde{K_m} - K_m^+)c - \tilde{K_m}K_n^+ - (K_m^+ + nK_m^+)\tilde{K_n} < 0$.

II c). If $B = 0$, the polynomial (C.2) reduces to

$$f(M) = AM^2 + C.$$

Therefore, the M-component of the equilibrium is

$$M^* = \frac{-B - \sqrt{B^2 - 4AC}}{2A} = \sqrt{\frac{K_m^+ \tilde{K_n} c}{(-\tilde{K_m} + K_m^+)(1+n)}} = \sqrt{-\frac{C}{A}},$$

when $A = \tilde{K_m} - K_m^+ < 0$ and $B = -(\tilde{K_m} - K_m^+)c - \tilde{K_m}K_n^+ - (K_m^+ + nK_m^+)\tilde{K_n} = 0$.

III Finally, when $\tilde{K_m} - K_m^+ = 0,$ then $A = 0$ and $B < 0$.

The polynomial equation (C.2) reduces to $f(M) = BM + C = 0$. Hence, the M-component of the equilibrium is $M^* = -\frac{C}{B} = \frac{K_m^+ \tilde{K_n} c}{\tilde{K_m} K_n^+ + (K_m^+ + n K_m^+)\tilde{K_n}}$ which is always positive.

In summary, the polynomial equation (C.2) has

1. two positive real roots $M^* = \frac{-B \pm \sqrt{B^2 - 4AC}}{2A}$, if $A = \tilde{K_m} - K_m^+ > 0$,
2. one positive real root $M^* = \frac{-B - \sqrt{B^2 - 4AC}}{2A}$, if $A = \tilde{K_m} - K_m^+ < 0$,
3. one positive real root $M^* = -\frac{C}{B}$, if $A = \tilde{K_m} - K_m^+ = 0$.

Next, we will seek for the existence of P_1^*, P_2^*, and then discuss the conditions of existence of M^*, P_1^*, P_2^*. Recall that $M^*, P_1^*, P_2^* \in [0, c]$.

We calculate the equilibrium of P_1^* by solving (C.1b), and we obtain $P_1^* = \frac{k_1 R M^*}{k} = nM^*$. As previously mentioned, $P_2^* = c - M^* - P_1^* = c - (1+n)M^*$. Furthermore, M^*, P_1^* and P_2^* have to satisfy the following conditions:

1. $0 \leq M^* \leq c$.
2. $0 \leq P_1^* \leq c$, which implies $0 \leq nM^* \leq c$, i.e. $0 \leq M^* \leq \frac{c}{n}$.
3. $0 \leq P_2^* \leq c$, which implies $0 \leq c - (1+n)M^* \leq c$, i.e. $0 \leq M^* \leq \frac{c}{n+1}$.

Combining all the above conditions, we have $M^* < \min\{c, \frac{c}{n}, \frac{c}{n+1}\}$. Consequently, we only need the condition $M^* \leq \frac{c}{1+n} = \frac{ck}{k + k_1 R}$ to satisfy $M^*, P_1^*, P_2^* \in [0, c]$.
The Intermediate Value Theorem will be applied to prove $M^*, P_1^*, P_2^* \in [0, c]$. Firstly, we calculate the value of the polynomial (C.2) at $\frac{c}{1+n}$.

$$\begin{aligned} f(\frac{c}{1+n}) &= (\tilde{K_m} - K_m^+)(1+n)(\frac{c}{1+n})^2 + (-(\tilde{K_m} - K_m^+)c - \tilde{K_m} K_n^+ - (K_m^+ + nK_m^+)\tilde{K_n})(\frac{c}{1+n}) \\ &\quad + K_m^+ \tilde{K_n} c \\ &= -\frac{\tilde{K_m} K_n^+ c}{1+n} \\ &< 0. \end{aligned}$$

When $A > 0$, the leading coefficient of polynomial (C.2) is positive, thus, the graph of $f(M)$ is a concave up parabola with 2 positive real roots as shown in Figure (C.1),

$$M_2^* = \frac{-B - \sqrt{B^2 - 4AC}}{2A} < M_1^* = \frac{-B + \sqrt{B^2 - 4AC}}{2A}.$$

Figure C.1: Diagram of polynomial (C.2) in Model IV (a) when $A > 0$.

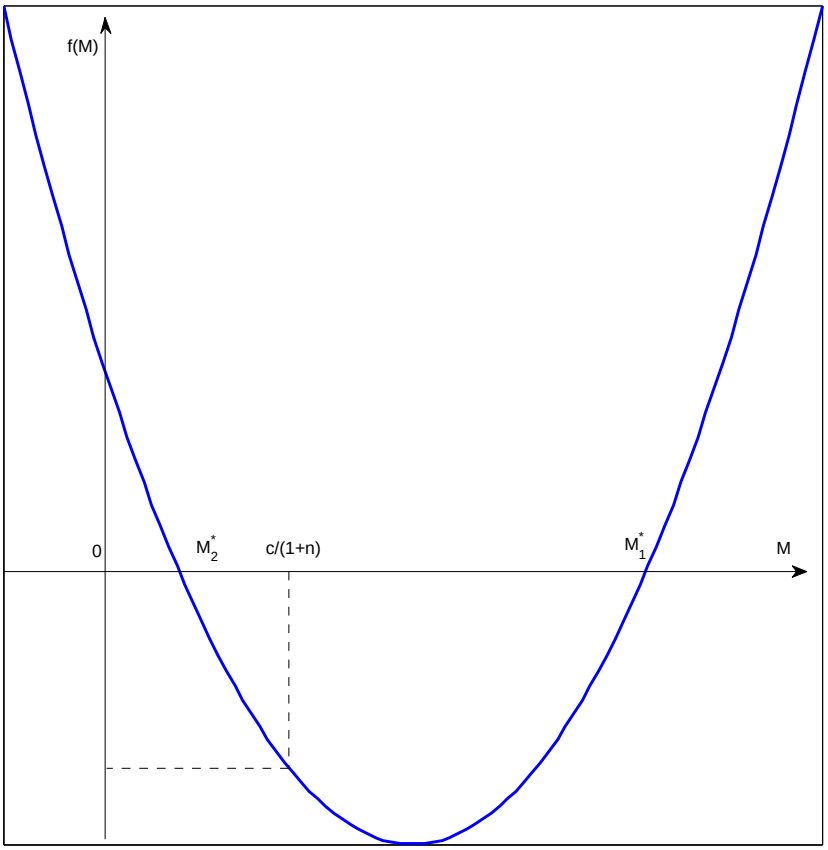

As $f(\frac{c}{1+n}) < 0$, we have $M_2^* < \frac{c}{1+n} < M_1^*$. Hence, there exists a unique value for M^*, $M^* = M_2^* \in [0, c]$, $P_1^* = nM_2^* \in [0, c]$, $P_2^* = c - (1 + n)M_2^* \in [0, c]$ when $A > 0$.

When $A < 0$ and $\forall B$, the leading coefficient of $f(M)$ is negative, then the graph of $f(M)$ is a concave down parabola with 1 positive real roots $M_2^* = \frac{-B-\sqrt{B^2-4AC}}{2A}$; see Figure (C.2).
Therefore, when $A < 0$ and for $\forall B$, as $f(\frac{c}{1+n}) < 0$, we have $M_2^* < \frac{c}{1+n} < c$. Hence, $M^* = M_2^* \in [0, c]$, $P_1^* = nM_2^* \in [0, c]$, $P_2^* = c - (1 + n)M_2^* \in [0, c]$ if $A < 0$.

Figure C.2: Diagram of polynomial (C.2) in Model IV (a) when $A < 0$.

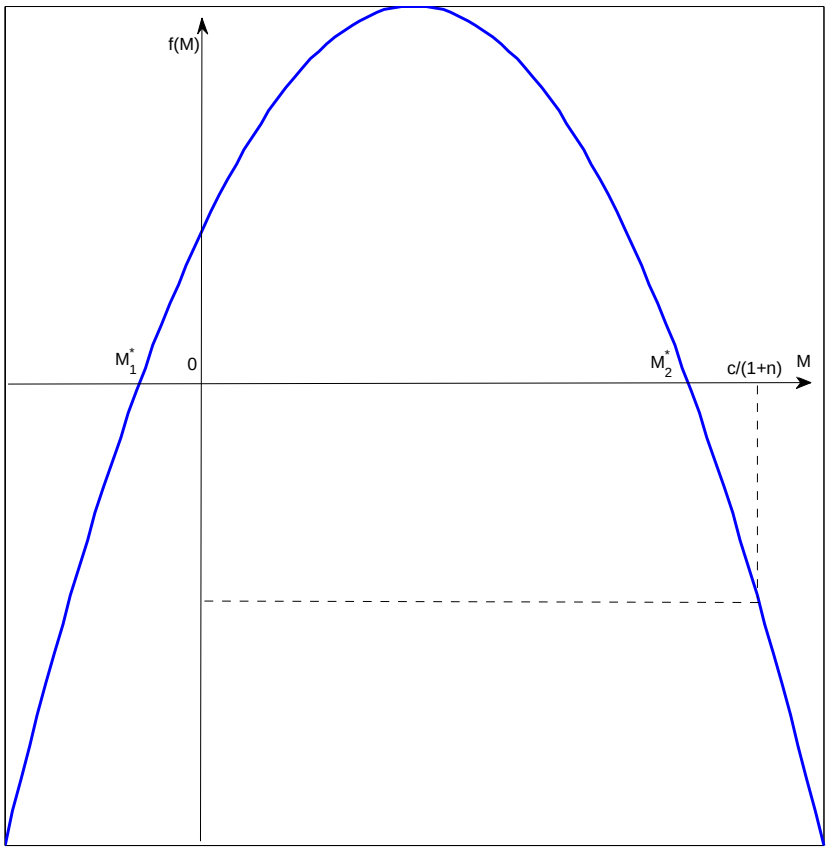

When $A = 0$, the graph of polynomial $f(M)$ (C.2) is a straight line with a negative slope. The positive root of $f(M)$ is $M^* = -\frac{C}{B}$ (Figure C.3). As $f(\frac{c}{1+n}) < 0$, we have $M^* = -\frac{C}{B} \in [0, c]$ when

Figure C.3: Diagram of polynomial (C.2) in Model IV (a) when $A = 0$.

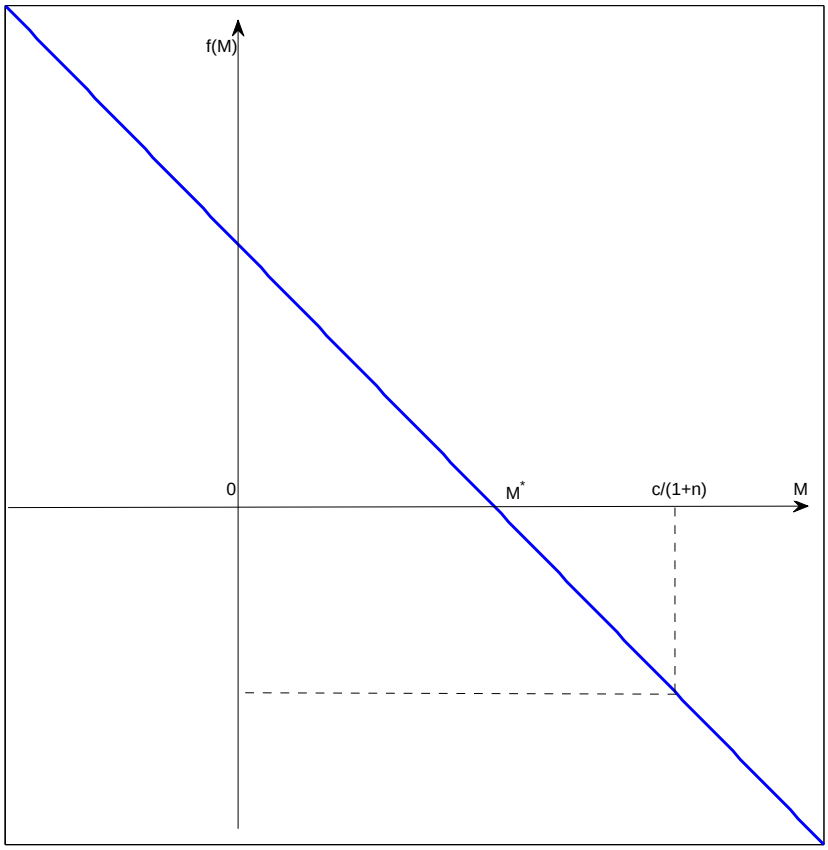

$A = 0$.

In conclusion, there is a unique value for M^*. When $A \neq 0$, $M^* = \frac{-B-\sqrt{B^2-4AC}}{2A}$ and when $A = 0$, $M^* = -\frac{C}{B}$.

Adding (C.1c) and (C.1d), we obtain $P_4^* = \Pi/r$ which is positive. Substituting M^*, P_1^*, P_4^* into

(C.1c), we get

$$\frac{K_m(c-M^*-P_1^*)P_3^*}{K_n+P_3^*}=\frac{K_m^*P_4^*}{K_n^*+P_4^*}+\Pi=\frac{K_m^*\Pi}{rK_n^*+\Pi}+\Pi=\frac{\Pi(K_m^*+K_n^*r+\Pi)}{rK_n^*+\Pi}.$$

Rewriting the above equation, we have

$$(rK_n^*+\Pi)K_m(c-(1+n)M^*)P_3^*=K_n\Pi(K_m^*+K_n^*r+\Pi)+\Pi(K_m^*+K_n^*r+\Pi)P_3^*.$$

Thus,

$$\begin{aligned}P_3^*&=\frac{K_n\Pi(K_m^*+K_n^*r+\Pi)}{K_mc(K_n^*r+\Pi)-\Pi(K_m^*+K_n^*r+\Pi)-K_m(K_n^*r+\Pi)(1+\frac{k_1R}{k})M^*}\\&=\frac{K_nD}{Ec-D-E(1+n)M^*},\end{aligned}$$

with $D=\Pi(K_m^*+K_n^*r+\Pi),$ and $E=K_m(K_n^*r+\Pi)$.
In order to make $P_3^*=\frac{K_nD}{Ec-D-E(1+n)M_2^*}$ positive, we need $Ec-D-E(1+n)M^*>0$, so that

$$M^*<\frac{Ec-D}{E(1+n)}=\frac{k}{k+k_1R}\left[c-\frac{\Pi(K_m^*+K_n^*r+\Pi)}{K_m(K_n^*r+\Pi)}\right]$$

with $c>\frac{D}{E}=\frac{\Pi(K_m^*+K_n^*r+\Pi)}{K_m(K_n^*r+\Pi)}$.

Therefore, when $M^*<\frac{Ec-D}{E(1+n)}$ and $c>\frac{D}{E}$, there exists a unique equilibrium point, which is $(M^*,P_1^*,P_2^*,P_3^*,P_4^*)=(M^*,nM^*,c-(1+n)M^*,\frac{K_nD}{Ec-D-E(1+n)M^*},\frac{\Pi}{r})$ where $M^*=\frac{-B-\sqrt{B^2-4AC}}{2A}$ if $A\neq 0$, and $M^*=-\frac{C}{B}$ if $A=0$.

The Jacobian matrix J_4 of System (4.17) is

$$J_4=\begin{pmatrix}-\frac{\tilde{K_m}\tilde{K_n}}{(\tilde{K_n}+M)^2}-\frac{K_m^+K_n^+}{(K_n^++c-M-P_1)^2}-k_1R & -\frac{K_m^+K_n^+}{(K_n^++c-M-P_1)^2}+k & 0 & 0\\ k_1R & -k & 0 & 0\\ \frac{K_mP_3}{K_n+P_3} & \frac{K_mP_3}{K_n+P_3} & -\frac{K_mK_n(c-M-P_1)}{(K_n+P_3)^2} & \frac{K_m^*K_n^*}{(K_n^*+P_4)^2}\\ -\frac{K_mP_3}{K_n+P_3} & -\frac{K_mP_3}{K_n+P_3} & \frac{K_mK_n(c-M-P_1)}{(K_n+P_3)^2} & -\frac{K_m^*K_n^*}{(K_n^*+P_4)^2}-r\end{pmatrix}.$$

The eigenvalues of matrix J_4 evaluated at any equilibrium point are:

$$\lambda_1 = \frac{1}{2}\left(-\frac{\tilde{K_m}\tilde{K_n}}{(\tilde{K_n}+M^*)^2} - \frac{K_m^+K_n^+}{(K_n^+ + c - M^* - P_1^*)^2} - k_1R - k + \sqrt{u}\right),$$
$$\lambda_2 = \frac{1}{2}\left(-\frac{\tilde{K_m}\tilde{K_n}}{(\tilde{K_n}+M^*)^2} - \frac{K_m^+K_n^+}{(K_n^+ + c - M^* - P_1^*)^2} - k_1R - k - \sqrt{u}\right),$$
$$\lambda_3 = \frac{1}{2}\left(-\frac{K_mK_n(c - M^* - P_1^*)}{(K_n+P_3^*)^2} - \frac{K_m^*K_n^*}{(K_n^*+P_4^*)^2} - r + \sqrt{v}\right),$$
$$\lambda_4 = \frac{1}{2}\left(-\frac{K_mK_n(c - M^* - P_1^*)}{(K_n+P_3^*)^2} - \frac{K_m^*K_n^*}{(K_n^*+P_4^*)^2} - r - \sqrt{v}\right),$$

with

$$u = \left(\frac{\tilde{K_m}\tilde{K_n}}{(\tilde{K_n}+M^*)^2} + \frac{K_m^+K_n^+}{(K_n^+ + c - M^* - P_1^*)^2} + k_1R - k\right)^2 - 4\left(-\frac{K_m^+K_n^+}{(K_n^+ + c - M^* - P_1^*)^2} + k\right)(k_1R)$$

and

$$v = \left(\frac{K_mK_n(c - M^* - P_1^*)}{(K_n+P_3^*)^2} - \frac{K_m^*K_n^*}{(K_n^*+P_4^*)^2} - r\right)^2 - 4\left(\frac{K_mK_n(c - M^* - P_1^*)}{(K_n+P_3^*)^2}\right)\left(\frac{K_m^*K_n^*}{(K_n^*+P_4^*)^2}\right).$$

To check the sign of the eigenvalues, we use the following notation,

$$a = \frac{\tilde{K_m}\tilde{K_n}}{(\tilde{K_n}+M^*)^2},$$
$$b = \frac{K_m^+K_n^+}{(K_n^+ + c - M^* - P_1^*)^2},$$
$$x = k_1R,$$
$$d = \frac{K_mK_n(c - M^* - P_1^*)}{(K_n+P_3^*)^2},$$
$$e = \frac{K_m^*K_n^*}{(K_n^*+P_4^*)^2},$$

where $a,\ b,\ x,\ d,\ e\ > 0$ at equilibrium points.

We also rewrite eigenvalues as follows:

$$\lambda_1 = \frac{1}{2}(-a-b-x-k+\sqrt{(a+b+x-k)^2-4bx}),$$
$$\lambda_2 = \frac{1}{2}(-a-b-x-k-\sqrt{(a+b+x-k)^2-4bx}),$$
$$\lambda_3 = \frac{1}{2}(-d-e-r+\sqrt{(d-e-r)^2-4de}),$$
$$\lambda_4 = \frac{1}{2}(-d-e-r-\sqrt{(d-e-r)^2-4de}).$$

As we can see, the eigenvalues $\lambda_{2,4}$ or $Re(\lambda_{2,4})$ are negative for any value of equilibrium points.

If $\lambda_3 \in \mathbb{C}$, $Re(\lambda_3) < 0$. If $\lambda_3 \in \mathbb{R}$, $\lambda_3 = \frac{1}{2}(-d-e-r+\sqrt{(d-e-r)^2-4de}) = \frac{1}{2}(-\sqrt{(d+e+r)^2}+\sqrt{(d-e-r)^2-4de})$.

As $(d+e+r)^2 = d^2+e^2+r^2+2er+2dr+2de > (d-e-r)^2-4de = d^2+e^2+r^2+2er-2dr-6de$, we will have $\sqrt{(d+e+r)^2} > \sqrt{(d-e-r)^2-4de}$, which gives $-\sqrt{(d+e+r)^2}+\sqrt{(d-e-r)^2-4de}) < 0$. Thus, $\lambda_3 = \frac{1}{2}(-d-e-r+\sqrt{(d-e-r)^2-4de})$ is negative.

If $\lambda_1 \in \mathbb{C}$, $Re(\lambda_1) < 0$. If $\lambda_1 \in \mathbb{R}$, $\lambda_1 = \frac{1}{2}(-a-b-x-k+\sqrt{(a+b+x-k)^2-4bx}) = \frac{1}{2}(-(a+b+x+k)+\sqrt{(a+b+x-k)^2-4bx}) = \frac{1}{2}(-\sqrt{(a+b+x+k)^2}+\sqrt{(a+b+x-k)^2-4bx})$. We will expand and compare $(a+b+x+k)^2$ and $(a+b+x-k)^2-4bx$ in order to investigate the sign of λ_1. We have

$$(a+b+x+k)^2 = (a+b+x)^2+k^2+2(a+b+x)k,$$
$$(a+b+x-k)^2-4bx = (a+b+x)^2+k^2-2(a+b+x)k-4bx.$$

Hence, we can say that $(a+b+x+k)^2 > (a+b+x-k)^2-4bx$, equivalently, $-\sqrt{(a+b+x+k)^2}+\sqrt{(a+b+x-k)^2-4bx} < 0$. Therefore, λ_1 is always negative.

Now, all eigenvalues or their real part of the Jacobian matrix evaluated at any equilibria are negative. Hence, the unique equilibrium of System (4.16) is locally asymptotically stable when it exists.

To make the conditions for each model consistent, we are going to use the same form of P_2^* to express the conditions. Referring that $P_2^* = c-(1+n)M^*$, then $M^* = \frac{c-P_2^*}{1+n}$. The condition for existence and LAS is $M^* < \frac{Ec-D}{E(1+n)} = \frac{k}{k+k_1R}(c-\frac{\Pi(K_m^*+K_n^*r+\Pi)}{K_m(K_n^*r+\Pi)})$. Substituting M^* into P_2^*, we have that $\frac{c-P_2^*}{1+n} < \frac{Ec-D}{E(1+n)}$, then the condition is $P_2^* > \frac{D}{E} = \frac{\Pi(K_m^*+K_n^*r+\Pi)}{K_m(K_n^*r+\Pi)}$. □

Bibliography

[1] **Bachar M, Batzel J** and **Ditlevsen S** "Stochastic Biomathematical Models with Applications to Neuronal Modeling". Springer. 2013.

[2] **Burnham K P** and **Anderson D R**. "Model Selection and Multi- model Inference: A Practical Information-Theoretic Approach". Springer. 2002.

[3] **Canadian Cancer Society's Advisory Committee on Cancer Statistics**. "Canadian Cancer Statistics 2015". Canadian Cancer Society, Statistics Canada. 2015.

[4] **Coddington E A** and **Levinson N**. "Theory of Ordinary Differential Equations". New York: McGraw-Hill. 1955.

[5] **Dennis G Z** and **Michael R Gullen**. "Advanced Engineering Mathematics". Fourth Edition. 2011.

[6] **Dobashi Y, Watanabe Y, Miwa C, Suzuki S** and **Koyama S**. "Mammalian target of rapamycin: a central node of complex signalling cascades". Int J Clin Exp Pathol. 4(5): 476-95. 2011.

[7] **Feng Z, Fan X, Jiao Y,** and **Ban K.** "Mammalian target of rapamycin regulates expression of beta-catenin in hepatocellular carcinoma". Hum Pathol. 42(5): 659-68. 2011.

[8] **Guertin D A** and **Sabatini D M**. "An expanding role for mTOR in cancer". Whitehead Institute for Biomedical Research, 9 Cambridge Center, Cambridge, MA 02141, USA. 2005.

[9] **Gillespie D T**. "Markov Processes:An introduction for physical Scientists". Academic Press; 1 edition. 1991.

[10] **Gillespie D T**. "A general method fro numerically simulating the stochastic time evolution of coupled chemical reactions". J.Comput.Phys. 22: 403-34. 1976.

[11] **Gillespie D T**. "Exact stochastic simulation of coupled chemical reactions". J.Phys.Chem.81:2340-61. 1977.

[12] **Givant S** and **Halmos P.** "Introduction to Boolean Algebras. Undergraduate Texts in Mathematics". Springer. 2009.

[13] **Haggag M**. "New Criteria of Model selection and model averaging in linear regression models". American Journal of Theoretical and Applied Statistics. 3(5): 148-166. 2014.

[14] **Hale J K**. "Ordinary differential equations". Dover Publications. 1969.

[15] **Johnson J B** and **Omland K S**. "Model selection in ecology and evolution". TRENDS in Ecology and Evolution. 2004.

[16] **Kittel C** and **H Kroemer**. "Thermal Physics, 2nd ed". W.H. Freeman and Company, San Fransisco. 1980.

[17] **Knowles JR**. "Enzyme-catalyzed phosphoryl transfer reactions". Annu. Rev. Biochem. 49: 877-919. 1980.

[18] **Laplante M** and **Sabatini D**. "mTOR signaling in growth control and disease". Cell. 149(2): 274-293. 2012.

[19] **Linda J S A**. "Mathematical Biology". PEARSON Prentice Hall. 2007.

[20] **McNabb A** and **Weir G**. "Comparison theorems for ordinary differential equations with general boundary conditions". Journal of Mathematical Analysis and Applications vol. 130 (1): 144-154. 1988.

[21] **Maynard Smith J** and **Price G R**. "The Logic of Animal Conflict". Nature 246 (5427): 15-18. 1973.

[22] **McQuarrie D**. "Stochastic approach to chemical kinetics". J.Appl.Probab. 4: 413-78. 1967.

[23] **Melanie M**. "An Introduction to Genetic Algorithms". Massachusetts Institute of Technology. 1996.

[24] **Michaelis L** and **Menten M L**. "Die Kinetik der Invertinwirkung". Biochem Z. 49: 333-369. 1913.

[25] **Petroulakis E, Mamane Y, Le Bacquer O, Shahbazian D** and **Sonenberg N**. "mTOR signaling: implications for cancer and anticancer therapy". Br J Cancer. 94(2): 195-199. 2006.

[26] **Price K, Storn R M** and **Lampinen J A**. "Differential Evolution: A Practical Approach to Global Optimization". Springer-Verlag New York, Inc. 2005.

[27] **Price K** and **Storn R M**. "Differential Evolution-A Simple and Efficient Heuristic for Global Optimization over Continuous Spaces". Kluwe Academic Pulishers. 1997.

[28] **Rajala RV, Datla RS, Moyana TN, Kakkar R, Carlsen SA,** and **Sharma RK.** "N-myristoyltransferase". Mol Cell Biochem. 204(1-2): 135-55. 2000.

[29] **Seghouane A K** and **Amari S**. "The AIC criterion and symmetrizing the Kullback-Leibler divergence". IEEE Trans Neural Netw. 18(1): 97-106. 2007.

[30] **Shrivastav Anuraag, Jaksic Danira, McQuiggin Andrew** and **Murphy Leigh**. "Identifying role of N-myristoyltransferase in the mTOR signalling cascade of ER-? positive breast cancer cells (MCF-7)". 4th International Conference on Biomarkers & Clinical Research. 10.4172/2155-9929.S1.018. 2013.

[31] **Shrivastav A** and **Murphy L**. "Interactions of PI3K/Akt/mTOR and estrogen receptor signalling in breast cancer". Breast Cancer Manage. 1(3): 235-249. 2012.

[32] **Sipido KR**. "Cardiovascular Research". Journal of European Society of Cardiology. 2015.

[33] **Storn J R** and **Price K** . "Differential evolution - a simple and efficient heuristic for global optimization over continuous spaces". Journal of Global Optimization. 11: 341-359. 1997.

[34] **Tea Tusar** and **Bogdan Filipic**. "Differential Evolution Versus Genetic Algorithms in Multi-objective Optimization". Springer Matsushima Japan. 4403: 257-271. 2007.

[35] **The MathWorks Inc**. "MATLAB: The language of technical computing, version 8.1.0.604 (R2013a)". The MathWorks Inc. 2013.

[36] **Vivanco L** and **Sawyers C L**. "The phosphatidylinositol 3-kinase AKT pathway in human cancer". Nat. Rev. Cancer 2: 489?501. 2002.

[37] **Victor H**. "Lois Generales de|Action des Diastases. Paris: Hermann". Google books (US only). 1903.

[38] **Vignot S, Faivre S, Aguirre D** and **Raymond E.** "mTOR-targeted therapy of cancer with rapamycin derivatives". Ann Oncol. 16(4): 525-37. 2005.

[39] **Wullschleger S, Loewith R** and **Hall MN**. "TOR signalling in growth and metabolism". Cell. 124(3): 471-84. 2006.

[40] **Zaytseva YY, Valentino JD, Gulhati P** and **Evers BM**. "mTOR inhibitors in cancer therapy". Cancer Letters. 319(1): 1-7. 2012.